Distribution Agreement

In presenting this thesis or dissertation as a partial fulfillment of the requirements for an advanced degree from Emory University, I hereby grant to Emory University and its agents the non-exclusive license to archive, make accessible, and display my thesis or dissertation in whole or in part in all forms of media, now or hereafter known, including display on the world wide web. I understand that I may select some access restrictions as part of the online submission of this thesis or dissertation. I retain all ownership rights to the copyright of the thesis or dissertation. I also retain the right to use in future works (such as articles or books) all or part of this thesis or dissertation.

Signature:

_____ _____

Maria Georgieva Georgieva Date

Immune modulation in tuberculosis:

Insights from the role of a *Mycobacterium tuberculosis*

protease Hip1 and its substrate

By

Maria Georgieva Georgieva
B.A.,Wesleyan College, 2009

Microbiology and Molecular Genetics

_____
Jyothi Rengarajan, Ph.D.
Advisor

_____
Daniel Kalman, Ph.D.
Committee Member

_____
Charles P. Moran, Ph.D.
Committee Member

_____
William M. Shafer, Ph.D.
Committee Member

_____
David S. Weiss, Ph.D.
Committee Member

Accepted:

_____
Lisa A. Tedesco, Ph.D.
Dean of the James T. Laney School of Graduate Studies

_____
Date

Immune modulation in tuberculosis:

Insights from the role of a *Mycobacterium tuberculosis*

protease Hip1 and its substrate

By

Maria Georgieva Georgieva

B.A., Wesleyan College, 2009

Advisor: Jyothi Rengarajan, Ph.D.

An abstract of

A dissertation submitted to the Faculty of the

James T. Laney School of Graduate Studies of Emory University

in partial fulfillment of the requirements for the degree of

Doctor of Philosophy

in Microbiology and Molecular Genetics

2015

Abstract

Immune modulation in tuberculosis:

Insights from the role of a *Mycobacterium tuberculosis*

protease Hip1 and its substrate

By Maria Georgieva Georgieva

Pathogenic microorganisms have evolved to respond rapidly during infection in order to evade host immunity and cause disease. *Mycobacterium tuberculosis* employs multiple strategies to evade host immune responses, persist within host phagocytic cells and promote pathogenesis. While substantial evidence points to the importance of hydrolytic enzymes in *M. tuberculosis* pathogenesis, the molecular and biochemical basis for their function remain largely uncharacterized. We have previously shown that the cell envelope-associated *M. tuberculosis* serine hydrolase, Hip1 (Hydrolase important for pathogenesis 1), prevents robust macrophage activation and interferes with dendritic cell functions, allowing *M. tuberculosis* to manipulate the host immune response and promote disease progression. However, the molecular basis for the immunomodulatory function of Hip1 remained unclear. In this dissertation work, we provide key mechanistic insights into the molecular and biochemical basis of Hip1 function. We establish that Hip1 is a serine protease with activity against protein and peptide substrates. Additionally, we show that the *M. tuberculosis* GroEL2 protein is a direct substrate of Hip1 protease activity. Further, enzymatic studies demonstrate that serine protease inhibitors specifically inhibit cleavage of GroEL2. We mapped the cleavage site within the N-terminus of GroEL2 and confirmed that this site is required for proteolysis of GroEL2 during *M. tuberculosis* growth. Interestingly, we discovered that Hip1-mediated cleavage of GroEL2 converts the protein from a multimeric to a monomeric form. Moreover, ectopic expression of cleaved GroEL2 monomers into the *hip1* mutant complemented the hyperinflammatory phenotype of the *hip1* mutant and restored wild type levels of cytokine responses in infected macrophages. Our investigations also reveal that *M. tuberculosis* modulates dendritic cell (DC) responses through Hip1-mediated proteolysis of GroEL2. Full length GroEL2 protein induced DC maturation, production of T helper 1 (Th1)-polarizing cytokines and promoted antigen presentation to $CD4^+$ T cells. In contrast, cleavage of GroEL2 abrogated these functions. In summary, our work has identified Hip1-dependent proteolysis of GroEL2 as a novel mechanism of immune modulation in *M. tuberculosis*. Importantly, our findings position Hip1 as an attractive target for inhibition for developing immunomodulatory therapeutics against *M. tuberculosis*.

Immune modulation in tuberculosis:

Insights from the role of a *Mycobacterium tuberculosis*

protease Hip1 and its substrate

By

Maria Georgieva Georgieva

B.A., Wesleyan College, 2009

Advisor: Jyothi Rengarajan, Ph.D.

A dissertation submitted to the Faculty of the

James T. Laney School of Graduate Studies of Emory University

in partial fulfillment of the requirements for the degree of

Doctor of Philosophy

in Microbiology and Molecular Genetics

2015

Acknowledgements

"We dance round in a ring and suppose,

But the Secret sits in the middle and knows."

Robert Frost, 1942

First, I would like to thank my parents Nonka and Georgi. Thank you for your unconditional and unreserved support. Thank you for allowing me to chart my own path all the while giving me insightful guidance. Thank you for being the most reasonable and wisest people I know – I have followed your valuable advice numerous times, never to be lead astray. I love you immeasurably, more than words can describe. My thoughts of you have given me great strength, calmness and motivation at hard times. I am immeasurably indebted to you for your enormous sacrifice to provide a better life for me. Thank you, mom, for always, unmistakably knowing when I needed a listening ear and never ceasing to support me in all that I have chosen to do. Thank you, dad, for always being unconditionally supportive, self-sacrificing and dedicated to my well-being. I look up to you both and admire your fortitude, integrity, compassion and selfless sacrifice.

To my extended family, here in the United States: Elena, Kosta, Plamena and Dimitar: Thank you for welcoming me into your home as one of your own – it has meant more to me than you will ever know! Thank you for being my anchor in a new, unknown country. Thank you for being my one stable, constant source of solace and comfort in this new

place. Thank you for making it possible to say, even so far away from home: “It’s alright. No matter what, I have family to lean on.”

I would also like to thank my mentor Jyothi. You are a truly inspiring and outstanding mentor. Thank you for ensuring I have the necessary skills and qualities for success both during and beyond graduate school. Thank you for setting the foundation and giving me a stepping-stone to realize my potential. Thank you for challenging me to seek higher achievement than I would have on my own. Thank you for leading by example and being a wonderful mentor and scientist I can only hope one day to become and humbly aspire to be. Thank you for knowingly and unknowingly (!) being my constant, unwavering support during these past years. Thank you for knowing when to let me stand on my own. Thank you for your uninhibited encouragement, unreserved trust and attention to my training. Thank you for your selfless dedication to mentoring me!

I would also like to thank my committee members David, Charlie, Dan and Bill. Each of you, many times, unknowingly and selflessly has encouraged me at moments when I needed it most. These moments were defining for me and I have leaned on your encouraging words at challenging times. Thank you for your fairness, patience and attention. Thank you for being wonderful teachers and role models!

Next, I would like to thank my labmates (past and present): Ameeta, Becky, Erica, Katia, Kevin, Marcos, Ranjna, and Toidi for brightening up each and every day. Thank you for all the laughs we have shared, your friendship, and your outstanding character! You

provided the warmest, most positive, and most inspiring work environment I have ever experienced. It has been a privilege to work side-by-side and BSL3 hood-by-BSL3 hood with you. Thank you for being hard workers, smart, rigorous scientists and great friends!

I would also like to thank Jackie, who inspired my love of biochemistry and graciously and unconditionally opened her home to me during all the trips to Boston. Thank you for all the biochemistry lessons and for accepting me as your peer. Thank you for being gracious in every respect!

To Silvia: Thank you for your understanding, your encouragement and support. Thank you for taking pride in knowing me. You are a caring person and a wonderful friend. I am forever indebted to you for your uninhibited and unreserved support and I can only hope to be at least half the friend you are to me in return!

Table of Contents

Chapter 1

Introduction

Part 1. Interactions between pathogenic microorganisms and their hosts

During infection, the pathogen and its human host interact in a dynamic and complex manner within the landscape of the immune system – a critical component of the host's defense against pathogens. The host employs a variety of immune defense mechanisms that recognize, protect against and neutralize or eliminate pathogens [1-4]. These mechanisms include both broad-spectrum, innate responses as well as antigen-specific adaptive immune responses.

Faced with host-derived stresses during the course of infection, pathogens respond rapidly. For a variety of microorganisms, these responses fall within common paradigms about immune evasion. One of these includes modulation of the nature and magnitude of the host immune response. For example, microorganisms produce a number of virulence factors that actively manipulate host immunity and contribute to disease progression and pathogenesis [1,5]. In the field of bacterial pathogenesis, several studies have illuminated the underlying mechanisms governing this process. For instance, *Salmonella* and *Chlamydia* species actively secrete effector molecules within infected cells thereby subverting the immune response and successfully persisting within a privileged niche in the host [1]. Similarly, *Mycobacteria* produce both cell-associated and secreted factors that contribute resistance to various host antimicrobial functions [6,7]. In addition to evading macrophage function, pathogenic *Mycobacteria* have also evolved to manipulate the host immune response during infection and interfere with responses to interferon gamma (IFN-γ), a key cytokine mediator of the adaptive immune response [5,8,9].

Though the mechanisms of *Mycobacterium tuberculosis* pathogenesis are actively investigated, we still do not have a good understanding of the molecular and biochemical basis of mechanisms of immune modulation. Immune evasion by *M. tuberculosis* stands out as a complex phenomenon – one that presents an outstanding interest in the field of tuberculosis research and certainly warrants detailed investigation.

Part 2. History and background of *Mycobacterium tuberculosis*

Part 2.1 History

Tuberculosis is caused by a bacterium called *Mycobacterium tuberculosis*. The bacilli usually attack the lungs, but can also infect any part of the body such as the kidney, brain and bones [10,11]. Tuberculosis is inarguably one of the most ancient diseases to plague humankind. Paleopathological data presents evidence of tuberculosis in bone remains from the Neolithic period in 5800 BCE and Egyptian mummies dating back to 2400 BCE. Pulmonary tuberculosis, most probably first described in ancient Greece by Hippocrates, was known as “phthisis” [12]. As evidenced from the descriptions in Hippocrates’ written aphorisms, physicians at the time were familiar with the clinical manifestations of tuberculosis and recognized the pulmonary form of the disease as the most prevalent one [12]. During the middle ages, the written records of tuberculosis become fewer but the disease remained one of the leading causes of death in Europe. The disease burden escalated substantially in the seventeenth and eighteenth century, when tuberculosis killed one in five adults in Europe and North America [12]. Nowadays, despite efforts to control the disease, 9 million cases of tuberculosis are reported worldwide each year and

1.5 million people die from the disease [13]. Currently, tuberculosis is second only to HIV/AIDS as the greatest killer worldwide due to a single infectious agent [13].

Part 2.2 Symptoms and treatment

The primary stage of the disease can be symptom-free or the patient may experience flu-like illness. The second stage of the disease, referred to as active disease, presents with slight fever, night sweats, weight loss and fatigue. Tuberculosis of the lung is usually associated with a dry cough that eventually leads to a productive cough with sputum. Also, chest pains and shortness of breath are common during this period. This is the contagious stage of tuberculosis disease, when the bacteria are spread to other individuals via the aerosol route [14].

To treat tuberculosis disease, antibiotic-based treatment is administered. Treatment of active disease involves taking several anti-tuberculosis drugs for six to nine months and possible confinement if the individual is considered infectious. Of the approved drugs, the first-line anti-tuberculosis agents that comprise the core of the treatment regimen include isoniazid (INH), rifampin (RIF), ethambutol (EMB) and pyrazinamide (PZA) [14]. Although antibiotics effectively decrease the numbers of *M. tuberculosis* bacilli within the host during the first two months of treatment, bacteria are not eradicated completely. *M. tuberculosis* persists at low levels and requires continuation of treatment of either four or seven months. Difficulties in adhering to this arduous treatment regimen have contributed to increased rates of multi- and extensively drug-resistant tuberculosis [15-17].

Bacillus Calmette-Guerin (BCG) is a vaccine for tuberculosis used in many countries with a high prevalence of tuberculosis to prevent childhood tuberculous meningitis and military disease. However, BCG has widely variable protection efficacy against adult pulmonary TB and is not administered to adults [18]. Overall, the challenges regarding treatment and the low efficacy of the BCG vaccine have motivated efforts to develop more efficacious treatment regimens. One idea that is actively explored is that adjunctive immunomodulatory therapies can be used in conjunction with antibiotics to shorten treatment regimen and improve outcome.

Part 2.3 Classification

Mycobacterium is a genus within the order *Actinomycetales,* comprising a number of species associated with the disease tuberculosis. Members of the *Mycobacterium* genus stand out with certain characteristic features including a complex cell wall structure and a high G + C genomic content [19].

M. tuberculosis is an aerobic, non-motile, acid-fast bacterium with a highly unusual cell wall. *Mycobacteria* have a cell wall consisting of an inner and outer layer surrounding the plasma membrane. The outer compartment of the mycobacterial cell wall consists of both lipids and proteins. These include a variety of complex species such as lipoarabinomannan (LAM), lipomannan, phthiocerol dimycocerosate, dimycolyl trehalose (cord factor), sulfolipids and phosphatidylinositol mannosides [20]. In slow-growing, pathogenic *Mycobacteria*, such as *M. tuberculosis*, the immunodominant LAMs are capped at the terminal β-Ara residues with mannose residues and are referred to as

ManLAMs. In contrast, the fast-growing, non-pathogenic *Mycobacteria*, such as *M. smegmatis* have phosphoinositol-capped LAMs [20]. Overall, the outer proteins and lipids are a rich source of signaling and effector molecules of *Mycobacteria* and are well known to have roles in interacting with the immune system.

The inner compartment of the cell wall consists of peptidoglycan (PG), arabinogalactan (AG), and mycolic acids (MA) covalently linked together to form a complex. This is the essential core of the mycobacterial cell wall. Arabinogalactan is the major polysaccharide of the mycobacterial cell wall and is important for cell wall integrity and for anchoring the MA layer to the PG layer. Mycolic acids are the primary determinant for cell wall permeability and consist of a variety of short α-alkyl and long β-hydroxyl fatty acids ranging from 60 to 90 carbons per chain. Regarding their PG structure, *Mycobacteria* are unique and possess muramic acid that has an N-glycolyl group rather than and N-acetyl group [20].

In summary, this unusual arrangement results in a cell structure of substantial thickness and low permeability that contributes to the low sensitivity of *Mycobacteria* to antibiotic agents and cell wall-directed stresses. Because of the nature of their cell wall, the genus *Mycobacterium* stains poorly with the Gram stain procedure. The presence of the highly abundant mycolic acids and other lipids contribute to low permeability and impede the entry of chemicals, thereby interfering with the traditional crystal violet staining. Instead, the basic dye carbol-fuchsin successfully binds to the mycobacterial cell wall and stains the bacilli bright red in the classic Ziehl-Neelsen method [21].

Besides its protective barrier function, the mycobacterial cell wall is an abundant source of immunogenic antigens [22,23]. A number of these have been identified as bioactive bacterial components with immunomodulatory roles during infection. A combination of genetic and molecular approaches has demonstrated that mycobacterial cell wall mannans, mannoproteins and arabinomannans have specific immunomodulatory functions and contribute to disease pathogenesis [22]. The demonstrated importance of cell wall factors in determining the trajectory of the immune response has motivated a number of studies to better understand molecular mechanisms underlying the function of bacterial cell surface-associated and released effectors during *M. tuberculosis* infection.

Part 2.4 *Mycobacterium tuberculosis* complex

The *M. tuberculosis* complex (MTBC) consists of the pathogenic *Mycobacteria*, namely, *M. tuberculosis, M. africanum, M. canettii, M. bovis,* and *M. microti [24]*. These are closely related organisms with 99 % identity at the whole-genome nucleotide level (with the exception of *M. canetti*). *M. tuberculosis* and *M. africanum* are the causative agents of human tuberculosis. Epidemiological studies demonstrate that the spread of *M. africanum* is restricted to West Africa where it causes about half of the cases of human TB in this region. Besides the human pathogenic strains, the MTBC includes animal-associated members such as *M. bovis,* the cause of bovine tuberculosis and *M. microti*, the agent of tuberculosis in voles. *M. canetti* is the most recently discovered mycobacterial strain (1969), and studies aimed at understanding its natural reservoirs and transmission characteristics are ongoing [24].

With the advent of sequencing techniques, the genome sequences of a number of *M. tuberculosis* strains became available and this substantially facilitated modern molecular and genetic studies in tuberculosis research. One of the most commonly used *M. tuberculosis* strains in the laboratory is H37Rv, a virulent strain originally isolated in 1905. Historically, it has been used as a reference strain to identify clinical isolates and has been extensively used in studies of mycobacteriology, mycobacterial molecular biology and in animal models of tuberculosis [21].

Part 2.5 Mouse model of tuberculosis

Various animal models have been used to study aspects of human *M. tuberculosis* pathogenesis. These include mice, rabbits, guinea pigs and non-human primates [25]. The mouse model of tuberculosis is the most widely used for studying *M. tuberculosis* pathogenesis and is particularly useful for studying disease susceptibility and disease progression. Despite some differences from human disease, the mouse model has been very informative in providing insights into tuberculosis pathogenesis, immunology and drug efficacy. Mice have been successfully infected by the aerosol route and acquire infection with relatively low doses of *M. tuberculosis [25]*. Importantly, the availability of a variety of mouse immunological reagents makes the mouse animal model an essential tool for studying the bacterial contributions to tuberculosis pathogenesis.

Various inbred strains of mice are used in tuberculosis research. Commonly used inbred strains include C57BL/6, BALB/c, DBA/2 and severe combined immunodeficient (SCID) strains [26]. C57BL/6 and BALB/c mice are relatively resistant to *M.*

tuberculosis infection. After inoculation, the bacilli replicate logarithmically in the lungs for 2-3 weeks, after which, the colony forming units (CFU) reach a plateau. Despite this apparent control of bacterial replication, lung disease eventually results in lethality. DBA/2 mice are highly susceptible to *M. tuberculosis*. In this genetic background, after infection, CFU numbers rise at a slow rate and pathology develops rapidly, resulting in host death. Similarly, SCID mice, which completely lack the ability to mount an acquired immune response, do not control bacterial numbers and are highly susceptible to *M. tuberculosis* infection [26].

Using genetically targeted mouse strains, various groups have investigated the contribution of host components to the response against *M. tuberculosis*. Using these models, investigators demonstrated the importance of cytokines IFN-γ and IL-12, as well as Myd88 adaptor protein and TNF receptor for control of *M. tuberculosis*. Also, $CD4^+$ and $CD8^+$ T cells were first demonstrated to be important for control of tuberculosis in the mouse model of infection [27]. Other studies using the mouse model include these with toll-like receptor (TLR) knockout mice. The TLR receptors known to be involved in recognition of *M. tuberculosis* are TLR2, TLR4, and TLR9. $TLR2^{-/-}$ mice infected with high doses of *M. tuberculosis* have a greatly enhanced susceptibility to infection compared to wild type mice. In addition, $TLR2^{-/-}$ mice display defects in controlling chronic infection with *M. tuberculosis*. *In vivo* murine studies on the role of TLR4 in the recognition of *M. tuberculosis* have shown conflicting results, likely due to a redundant role of TLRs for the host defense against *Mycobacteria*. When infected with a high dose

of *M. tuberculosis*, animals lacking TLR9 succumb earlier to infection than wild type animals [28].

Part 3. Life cycle of *M. tuberculosis* within the host

Part 3.1 Progression of the tuberculosis granuloma

Transmission of tuberculosis is primarily through the airborne route and infection with *M. tuberculosis* begins with inhalation of aerosol droplets containing bacteria (Figure 1). In the lung, resident macrophages recognize the bacilli through pattern recognition receptors (PRRs), engulf the bacilli via phagocytosis and sequester them within phagosomes [3,29]. Following internalization, the bacilli are trapped within the hostile environment of phagosomal compartments. *M. tuberculosis* actively prevents the formation of the phagolysosome and thereby avoids the activity of digestive enzymes that degrade intracellular microbes. In addition, *M. tuberculosis* successfully resists host antimicrobial functions and replicates within macrophages [29]. Studies to identify bacterial factors responsible for surviving the hostile environment of macrophages and for modulating phagolysosome formation have highlighted the contributing role of cell-wall factors and secreted bacterial effectors [30].

Within the lungs, the phagocytosed bacteria induce a proinflammatory cytokine response that results in the recruitment of mononuclear cells and lymphocytes from neighboring blood vessels (Figure 1) [11,31]. These cells become the building blocks of the granuloma, also referred to as a tubercle, which is a hallmark structure of tuberculosis.

While the precise mechanisms leading to the formation of granulomas are not well defined, we understand the overall composition of these structures. Granulomas are composed of *M. tuberculosis* infected macrophages in the center, surrounded by lipid-rich foamy macrophages, dendritic cells, neutrophils, and an outer periphery of lymphocytes associated with a fibrous cuff that defines the boundary of the structure [3]. The initial view of the tuberculosis granuloma as a static structure has been challenged by results from histological and molecular studies incorporating the use of animal models of tuberculosis. These studies show that the granuloma is dynamic in nature and that both host and bacterial factors play a role in its development and maintenance [29,31]. Primarily, studies in the field dating back to the 1960s have implicated cell wall lipid components in the formation of granulomas. More specifically, from studies with the rabbit and mouse model of infection, we know that biologically active components from mycobacterial cell walls, such as mycobacterial glycolipids and trehalose-6, 6'-dimycolate (TDM) promote granuloma formation [32,33].

Besides influencing the initial stages of granuloma formation, numerous bacterial components also modulate the cellular immune response that frames its development and maintenance. For example, phthiocerol dimycocerosate (PDIM), trehalose dimycocerosate (TDM) and phenolic lipids of *M. tuberculosis*, were also implicated in disease pathology and immune modulation during infection [22,34]. In addition, the *M. tuberculosis* cell wall components mannosylated lipoarabinomannan (ManLAM) and arabinomannan promote pathogenesis following their release from bacteria during infection [33]. These bacterial components are known to traffic both within the infected

cells as well as extracellularly via the exosomal release pathway [35,36]. Further, mycobacterial cell wall-associated proteins belonging to the Ag85 family are highly immunodominant and present in exosomes from infected macrophages. Other examples of actively secreted immunodominant bacterial components are the early secreted antigenic target 6 (ESAT-6) and culture filtrate protein 10 (CFP10) [37]. Following extracellular release during infection, these bacterial effectors are well positioned within host cells to drive an unfavorable host immune response culminating in granuloma formation. Overall, these findings underscore the dynamic and complex interaction between *M. tuberculosis* and the host and more specifically, the biological significance of cell wall-associated and secreted bacterial effectors.

Part 3.2 Phagosome maturation arrest by *Mycobacterium tuberculosis*

Within the host, the outcome of infection with *M. tuberculosis* is determined by a complex interplay between the host immune response and pathogen factors that promote virulence. In response to multiple host-derived stresses, *M. tuberculosis* employs a wide array of strategies to evade the first-line defenses mounted by host innate immune responses and successfully replicates intracellularly within macrophages. *M. tuberculosis* interferes with IFN-γ-mediated activation, hinders macrophage functions by inhibiting phagosome maturation and acidification, counters toxic reactive oxygen (ROI) and nitrogen intermediates (RNI) and resists antimicrobial agents that damage the mycobacterial cell envelope [5,8,38]. Within this array of immune evasion strategies, the most outstanding feature is the striking ability of *M. tuberculosis* to interfere with phagosome maturation, a key component of the host protective response.

Historically, the defective trafficking of *Mycobacteria* and the capability of *M. tuberculosis* to prevent phagosome-lysosome fusion became apparent during studies involving localization of labeled bacteria and lysosomal markers. *Mycobacteria* gain entry to macrophages through several cell-surface molecules, including members of the integrin family of receptors such as complement receptors, mannose receptors and Fcγ receptors. Following uptake within the phagosome, changes in the concentration of intracellular Ca^{2+} and phosphatidylinositol-3-kinase (PI3K) activity are essential for proper phagosomal maturation [39,40]. Pathogenic *Mycobacteria* have been shown to interfere with Ca^{2+} and PI3K signaling pathways to impair this process [5,41]. This process is mediated in part by the lipid effector molecule ManLAM, which is able to inhibit ionophore-induced increases in Ca^{2+} concentration [42]. Interestingly, ManLAM from *M. tuberculosis* but not from the non-pathogenic *Mycobacterium smegmatis (M. smegmatis)* is capable of this activity.

Features of the mycobacterial phagosome include retention of early endosomal markers (Rab5) that are usually cleared from the mature phagosome surface and absence of late endosomal/lysosomal markers (Rab7) [39]. These characteristics reflect failure of the phagosomes to fully acidify and acquire active lysosomal proteolytic enzymes. Several mycobacterial lipid and protein effectors modulate phagosomal maturation. Two secreted *M. tuberculosis* effectors, PtpA, a tyrosine phosphatase and NdkA, a guanosine triphosphatase impair Rab7 activation on phagosomes. The *M. tuberculosis* cell wall component ManLAM and secreted phosphatase SapM disrupt the generation of

phosphatidylinositol 3-phosphate (PI3P) on the phagosomal surface – an important requirement for proper phagosomal maturation [39,43]. In addition, the *M. tuberculosis* effectors PknG, LpdC, Zmp1 are involved in phagosome maturation blockade, although their mechanisms of action remain unclear [8]. Furthermore, recent experiments on *M. avium* indicate that the close physical association formed between the bacterial cell wall and the phagosomal membrane is crucial for maintaining the phagosome in its arrested state [7,44]. Specifically, disruption of this association by depleting cholesterol directs the bacterium to the lysosome [3,7]. Overall, these findings underscore the importance of *M. tuberculosis* cell wall-associated and secreted effectors for modulation of the host immune response.

Part 3.3. Host recognition of *Mycobacterium tuberculosis*

The interaction between *M. tuberculosis* and the host immune system is dependent on the recognition of *M. tuberculosis* by several receptors. Most of the studies on mycobacterial entry into host cells have focused on macrophages, although other phagocytic cell types recruited to the lung (neutrophils and dendritic cells) are also capable of ingesting *Mycobacteria* (Figure 2). Macrophages and dendritic cells (DCs) differ in their roles during the immune response [45]. The release of proinflammatory cytokines and chemokines from infected macrophages is crucial for the generation of an effector T cell response (Figure 2). Subsequently, IFN-γ, a T cell cytokine mediator, is released and further activates infected macrophages to increase their antimicrobial activity [3].

After aerosol infection with *M. tuberculosis*, phagocytic DCs also ingest and harbor bacteria (Figure 2). Infected DCs migrate to the draining lymph nodes where they present antigen to naïve T cells and drive their development to effector and memory cells [9]. Uptake of *M. tuberculosis* by DCs results in their maturation as characterized by elevated surface expression of major histocompatibility class II (MHC II), co-stimulatory markers such as CD40, CD86, CD80, and secretion of Th1 polarizing cytokines such as IL-12 [46,47]. Importantly, recent studies have demonstrated that *M. tuberculosis* impedes DC maturation and interferes with DC migration from lungs to the draining lymph nodes [9]. However, the *M. tuberculosis* factors that impair DC functions are not well understood.

Several families of pattern recognition receptors (PRRs) are involved in *M. tuberculosis* recognition – C-type lectin receptors (CLRs), scavenger receptors (SRs), complement receptors (CRs) and Toll-like receptors (TLRs) [48]. The process of bacterial uptake is a critical component of the host immune response and essential for control of the infection. Early papers in this specific field suggested that the fate of phagocytosed *M. tuberculosis* is determined by the identity of the uptake receptor. For example, uptake via mannose receptor is thought to allow the bacteria to resist phagosome maturation, whereas uptake by CLRs is thought to result in delivery to the lysosome [49]. The TLR family recognizes pathogen- associated molecular patterns (PAMP) and alerts the host to the presence of microbial pathogens. Studies using TLR deficient mice show that TLR2, TLR4 and TLR9 each are involved in the recognition of *M. tuberculosis* by the host immune system [50]. For example, a component of the mycobacterial cell envelope, mannosyl phosphatidylinositol is capable of inducing a complex signaling cascade after engaging

TLR2 and TLR4 [49]. In addition, signalling via TLR4 has been confirmed for mycobacterial components such as the HSP70 protein, phosphatidyl-myo-inositol mannoside, and the 38 kDa glycolipoprotein [30,51]. Various lipids such as the 19 kDa antigen of *M. tuberculosis*, lipoarabinomannan and the LprG, LprA, LpqH lipoproteins are recognized by TLR2 [52]. Early in infection, the 19 kDa antigen engages TLR2 to stimulate cytokine production and prime immune cells [49].

3.5 *Mycobacterium tuberculosis* and modulation of host immunity

In addition to the numerous cell surface factors recognized by PRRs, *M. tuberculosis* secreted factors also engage host receptors and exert immunomodulatory functions during infection. The *M. tuberculosis* genome encodes five separate type VII secretion systems, which are specialized in the delivery of virulence factors across the cell envelope [53]. Each of the five loci encodes for a secretion apparatus (annotated as ESX) as well as secreted effector proteins [37]. *M. tuberculosis* encodes for more than twenty such proteins, whose functions during infection are poorly defined. The best-studied type VII secretion system is ESX-1, which is deleted in the vaccine strain BCG and whose absence largely accounts for the attenuation of BCG [37]. Recent work suggests that ESX-1 mediates damage to the *Mycobacteria*-containing phagosome membrane and appears to enable escape of *M. tuberculosis* from the phagosome [54,55]. Two effectors secreted by the ESX-1 secretion system, ESAT-6 and CFP10 are implicated in this membrane damage [55,56]. By damaging the phagosomal membrane, these effectors also allow for innate immune sensing of *M. tuberculosis* components [37]. For example, the *M. tuberculosis* cell wall component N-glycolyl-muramyl dipeptide stimulates the cytosolic

sensor NOD2 to produce type I interferons only if the ESX-1 system is intact [57]. Also, the ESX-1 system is required for activation of the host cytoplasmic inflammasome during infection [6,58]. These findings underscore the critical role of secreted effectors in manipulating and exploiting the host immune response for the benefit of the pathogen.

Part 4. Hydrolases in bacterial pathogenesis and immune modulation

Under adverse environmental conditions encountered in the host, bacteria launch stress responses that improve their chances of survival [8]. While the role of transcriptional responses to immune-mediated stress is well established, it is becoming increasingly clear that post-transcriptional regulation is also critical for pathogen survival in the host [59-61]. Regulating protein activity in response to stress would allow rapid adaptation to changing host environments and promote immune evasion. In this context, in multiple bacterial pathogens, hydrolases have been shown to play critical roles in virulence by enzymatically regulating the fate and activity of a wide range of critical bioactive proteins and lipids. For example, *Chlamydia* species secrete a number of proteolytic effectors into host cells to successfully establish infection and modulate the host response [62]. The chlamydial proteasome activity factor (CPAF) is a serine protease that acts on a variety of host cell targets during infection to alter the expression of cell surface molecules, evade immune recognition, and inhibit apoptosis [63,64]. The pathogenic *Yersinia* species also encode proteolytic effectors, namely the Yop effectors, which deregulate immune signaling pathways [59,65,66].

However, relatively little is known about how hydrolases function in *M. tuberculosis* pathogenesis [67,68]. It is widely appreciated that the lipid-rich *M. tuberculosis* cell envelope effectively protects the pathogen from antimicrobial agents, immune toxins and provides a potent hydrophobic barrier against several antibiotics [22]. In accordance with this concept, several groups have demonstrated that integrity of the cell envelope during infection is critical for *M. tuberculosis* resistance to antimicrobial activity encountered within the host [23,69-72]. Regulation of cell wall integrity, cell surface remodelling and release of secreted factors are processes controlled by the activity of hydrolytic enzymes. These cell surface-associated modifications occur in response to stress, thereby allowing *M. tuberculosis* to adapt to the rapidly changing immune milieu and to successfully persist within the host. In *M. tuberculosis,* two hydrolases, resuscitation promoting factor B (RpfB) and RpfE, directly interact with rpf-interacting protein A (RipA), a peptidoglycan peptidase and synergize to regulate cell division and remodeling under stress. Another *M. tuberculosis* peptidoglycan hydrolase, Rv2719c is similarly involved in cell division and response to DNA damage.

Hydrolytic enzymes are well known to control the fate of bioactive proteins and lipids in eukaryotes and prokaryotes, but the identity of their substrates can vary widely. Depending on the nature of their substrates, hydrolytic enzymes can include proteases, esterases, and lipases [73]. Proteases are critical for the virulence of multiple pathogens and hydrolysis of proteins is certainly an important regulatory mechanism in pathogenesis [74]. In tuberculosis, too, several predicted proteases have been implicated

in pathogenesis [74]. These findings have inspired studies to define in detail the molecular basis for their activity and to identify their physiological targets.

Despite considerable effort, for the majority of *M. tuberculosis* proteases, their molecular and biochemical functions remain undefined and their physiological substrates remain largely unknown. For example, MarP (Rv3671) is a periplasmic protease that is required for *M. tuberculosis* resistance to acid and oxidative stress and exhibits protease activity against synthetic peptide substrates, but its target during infection remains unclear [75]. In another study, PepD, a secreted serine protease that promotes *M. tuberculosis* virulence was shown to hydrolyze the general protease substrate casein but its physiological substrate was undefined [76,77]. Yet another study focused on the serine protease MycP1, which cleaves the ESX-1 substrate EspB and is required for secretion of ESX-1 substrates, well known to be important for *M. tuberculosis* virulence [70,78]. The intramembrane protease Rip1 (Rv2869c) is one of the very few proteases with known substrates. Rip1 is involved in regulating cell envelope mycolic acids by cleaving *M. tuberculosis* anti-sigma factors leading to release of the sigma factors SigK and SigL which in turn regulate cell envelope composition [78]. Rip1 also cleaves a penicillin-binding protein, PBP3 under conditions of oxidative stress [78].

The capacity of proteases to mediate quick responses at the protein level offers a unique mechanism for *M. tuberculosis* to respond to changing environmental conditions. In this manner, *M. tuberculosis* can rapidly orchestrate immune evasion strategies that promote disease progression and facilitate adaptation to the host immune milieu [2,5].

Part 5. Hydrolase important for pathogenesis 1 (Hip1)

Using functional genomics, we previously identified the cell envelope-associated serine hydrolase, Hip1 (Hydrolase important for pathogenesis 1; Rv2224c), as a key immunomodulatory protein, critical for *M. tuberculosis* virulence and survival in macrophages (Figure 3) [79,80]. We showed that mice infected with a *hip1* mutant survive significantly longer than wild type infected mice and show reduced lung pathology. Our studies also indicated that Hip1 prevents robust activation of macrophages following *M. tuberculosis* infection and controls the onset and magnitude of proinflammatory responses induced by *M. tuberculosis [79-81]*. This strategy of dampening early proinflammatory responses is likely to be advantageous to the pathogen by allowing it to escape immune detection. In addition, ours and other groups showed that *M. tuberculosis* Hip1 and its *M. smegmatis* ortholog are important for maintaining cell envelope integrity and resistance to cell envelope-directed stresses [75,80,82]. Specifically, the *hip1* mutant is more susceptible to stresses that are indicative of a compromised cell envelope (lysozyme, acidic pH, SDS, lipophilic antibiotics) [80,82,83].

Part 5.1 Molecular and biochemical characteristics of Hip1

In the *M. tuberculosis* genome, Hip1 is present in a predicted operon with Rv2223c. Rv2223c, unlike Hip1 is secreted extracellularly of *M. tuberculosis* (unpublished data, Erica Bizzell, Jyothi Rengarajan). The sequences of both Hip1 and Rv2223c possess features traditionally associated with serine proteases [84]. Hip1 is a 520 amino acid protein with molecular weight of 55 kDa. The closest orthologs to Hip1 are the

Streptomyces lividans mycelium associated tripeptidyl-peptidases TPP A (Tap; 30% seq ID), TPP B (SlpD; 36% seq ID) and TPP C (SlpE; 36% seq ID) [84-86]. These enzymes are all serine proteases and are categorized in clan SC, family S33 according to the MEROPS Peptidase database [84]. Characteristics of this clan include a catalytic triad comprised of Serine, Aspartic acid and Histidine residues, with the Ser residue as part of a GXSXG consensus sequence. All members of clan SC possess an α/β hydrolase fold, found in hydrolases, esterases, lipases and proteases. The S33 family consists of exopeptidases that have a preference for N-terminal Pro residues. Specifically, Hip1 possesses a predicted catalytic triad consisting of Serine (S_{228}), Aspartic acid (D_{463}), and Histidine (H_{490}) residues [84]. Also, Hip1 possesses a type II signal sequence typically present in prokaryotic lipoproteins. Within this N-terminal signal sequence, a cysteine residue is crucial for the processing and maturation of the lipopeptide. The steps involved in the formation of the mature protein are two-fold. First, a diglyceride unit is added to the cysteine residue via thioester linkage, followed by cleavage immediately after the lipidated cysteine. This cysteine becomes the first residue of the N-terminus of the mature lipoprotein [80].

Around the time we initiated our biochemical studies on Hip1, another group published a report on recombinant Hip1 expressed in *Escherichia coli (E. coli)* and its ability to hydrolyze synthetic ester substrates *in vitro* [87]. Because soluble esters are readily hydrolyzed by esterases, lipases and proteases, these findings did not permit confident annotation of the specific enzymatic activity of Hip1, thereby leaving this important question open-ended. The clearly meaningful biological role of Hip1 during infection

motivated our group to investigate the true enzymatic activity of Hip1 and establish it with confidence. Furthermore, because of our insight about the role of Hip1 in virulence, we appreciated the likely involvement of the physiological targets of Hip1 in pathogenesis, too. Therefore, we also set out to identify and characterize the interaction between Hip1 and its substrates during *M. tuberculosis* infection.

Part 5.2 Hip1 modulates host immunity

At the time that we initiated these studies, our group had demonstrated that Hip1 suppresses the macrophage innate immune response by limiting the production of proinflammatory cytokines and chemokines [80,81]. Our findings indicated that a *hip1* mutant induced earlier and more robust proinflammatory responses in macrophages via enhanced activation of TLR2- and inflammasome-dependent pathways [81]. Based on the immunomodulatory function of Hip1 as well as its predicted enzymatic activity, we hypothesized that one mechanism for Hip1 modulation of innate immunity is likely to be through cleavage of physiological substrates. Specifically, we proposed that Hip1 modifies cell envelope factors to modulate innate immunity. In our search for physiological substrates of Hip1, we employed a proteomics approach and identified a candidate substrate, the *M. tuberculosis* protein GroEL2 [80]. Although annotated as a member of the chaperone family of heat shock proteins, in many respects GroEL2 does not resemble canonical chaperones. Overall, GroEL2 differs greatly in structure from other chaperones, and exhibits minimal levels of ATP hydrolysis activity (a well established and accepted readout for chaperone function) [88]. At the time, several published studies on GroEL2 inspired a curious hypothesis about a likely involvement of

GroEL2 in some of the Hip1-associated phenotypes we previously reported on. Interestingly, these findings demonstrated that GroEL2 is highly induced in response to environmental cues during infection such as heat shock, oxidative stress, growth in macrophages and hypoxia [89-92]. Furthermore, various groups showed that GroEL2 is immunostimulatory as it induces a robust cytokine-mediated innate immune response [93]. Overall, these findings suggested a likely connection between GroEL2 and the Hip1-dependent immune modulation and motivated our subsequent investigations on the molecular basis of Hip1 function and the interplay between Hip1 and its candidate substrate GroEL2.

Part 6. Thesis overview

Mycobacterium tuberculosis employs a variety of mechanisms to evade host immunity and cause disease. In the tuberculosis field, a substantial body of work has implicated hydrolytic enzymes in pathogenesis, but the molecular and biochemical basis for their function have remained largely uncharacterized. Recently, several genome-wide screens have provided direct evidence for the contribution of proteolytic enzymes to *M. tuberculosis* pathogenesis and have spurred efforts to gain a better understanding of the mechanisms regulating the activity of these enzymes. For example, our own studies contributed to this knowledge with the identification of the immunomodulatory *M. tuberculosis* cell wall-associated protease Hip1. Motivated by these initial findings, we investigated in detail the molecular basis for the immunomodulatory function of Hip1. In this dissertation work, we provide key mechanistic insights into the enzymatic activity of

Hip1. We also contribute a rare insight - the identity of the physiological target of a protease; Hip1 cleaves the *M. tuberculosis* protein GroEL2. Subsequently, building upon these mechanistic insights, we discovered a role for GroEL2 in modulating the host macrophage response during infection with *M. tuberculosis* (Chapter 2). Furthermore, in Chapter 3, we report that GroEL2 also modulates the innate-adaptive axis at the DC-T cell interface. In summary, our dissertation work identifies and provides insight on a novel and mechanistically intriguing approach to immune modulation by *M. tuberculosis.*

Identifying the full range of mechanisms and strategies employed my *M. tuberculosis* to evade and subvert host immunity continues to be a long-standing goal in the tuberculosis field. In these aspirations, focused investigations (such as the ones outlined here) of the immunomodulatory activities of *M. tuberculosis*-derived factors can be particularly valuable. Such efforts are certainly necessary and will continue to provide invaluable insight into how *M. tuberculosis* modulates host immunity and inform the design of more efficacious vaccines and immunotherapies for tuberculosis.

Figure 1. Transmission and life cycle of *Mycobacterium tuberculosis* within the host

In the lung, recognition of the bacteria by macrophages and dendritic cells is mediated by pattern recognition receptors (PRRs). Following phagocytosis, a localized proinflammatory response is initiated that leads to the recruitment of other uninfected phagocytes and lymphocytes. These cells then become the building blocks for the granuloma. The granuloma consists of a kernel of infected macrophages, foamy macrophages, and dendritic cells surrounded by a mantle of lymphocytes. This tissue response reflects the containment phase of the infection, in which there are no overt signs of disease and the host does not transmit the infection to others. Containment usually fails when the immune status of the host changes. Following such a change in the immune status, the granuloma decays into a less structured mass, ruptures and spills infectious bacilli into the airway.

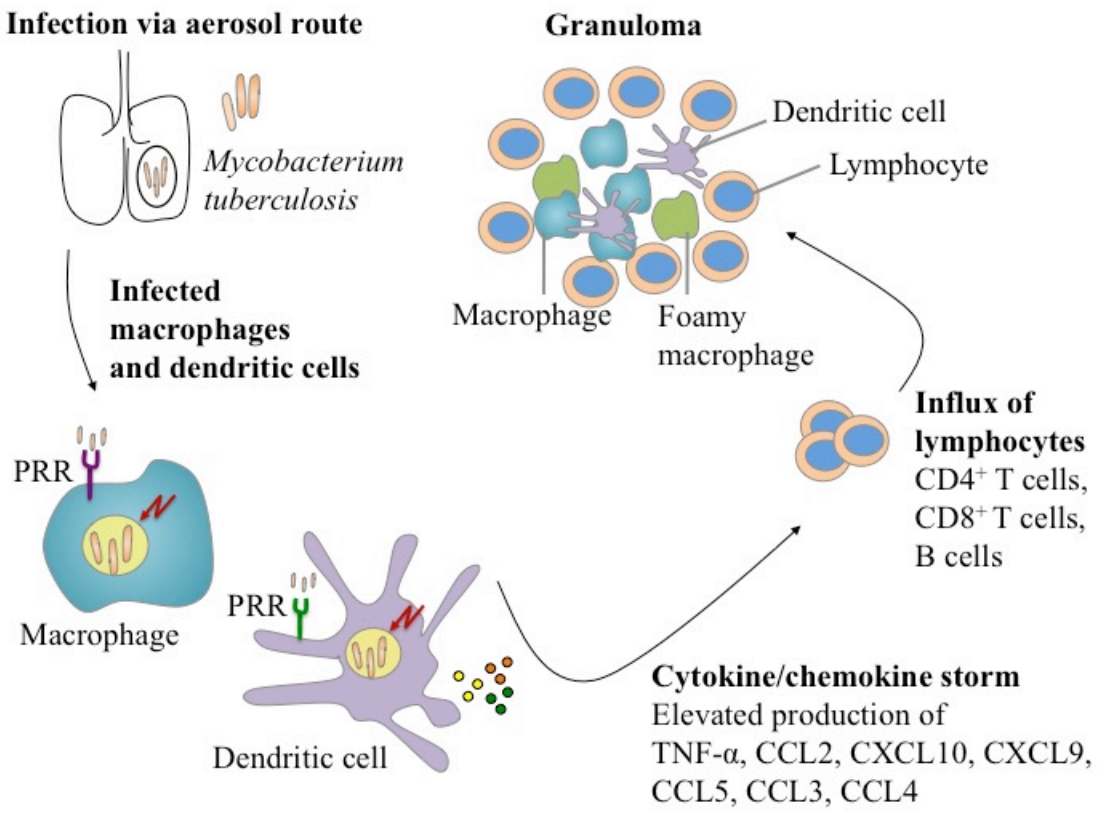
Infection via aerosol route
Mycobacterium tuberculosis
Infected macrophages and dendritic cells
PRR
Macrophage
PRR
Dendritic cell
Granuloma
Dendritic cell
Lymphocyte
Macrophage
Foamy macrophage
Influx of lymphocytes
CD4+ T cells,
CD8+ T cells,
B cells
Cytokine/chemokine storm
Elevated production of
TNF-α, CCL2, CXCL10, CXCL9,
CCL5, CCL3, CCL4

Figure 2. *Mycobacterium tuberculosis* and modulation of host immunity

Alveolar macrophages and lung dendritic cells are among the major cell types that become infected with *M. tuberculosis.* Following infection, macrophages respond by secreting a number of proinflammatory cytokines and chemokines. These secreted factors mediate activation of T cells, which produce IFN-γ capable of increasing the antimicrobial function of macrophages. The pathogen responds to the host phagocytic environment during infection in a rapid fashion. An important component of this response is modification of the *M. tuberculosis* cell envelope composition which is coupled with release into the extrabacterial space of bacterial effector molecules. Uptake of *M. tuberculosis* by DCs results in presentation of antigen to T cells and subsequent T cell activation. Successful T cell stimulation requires three DC-derived signals: high surface expression of major histocompatibility class II (MHC II), co-stimulatory markers such as CD40, CD86, CD80, and secretion of polarizing cytokines. Recent studies have demonstrated that *M. tuberculosis* interferes with DC functions and inhibits antigen presentation to T cells.

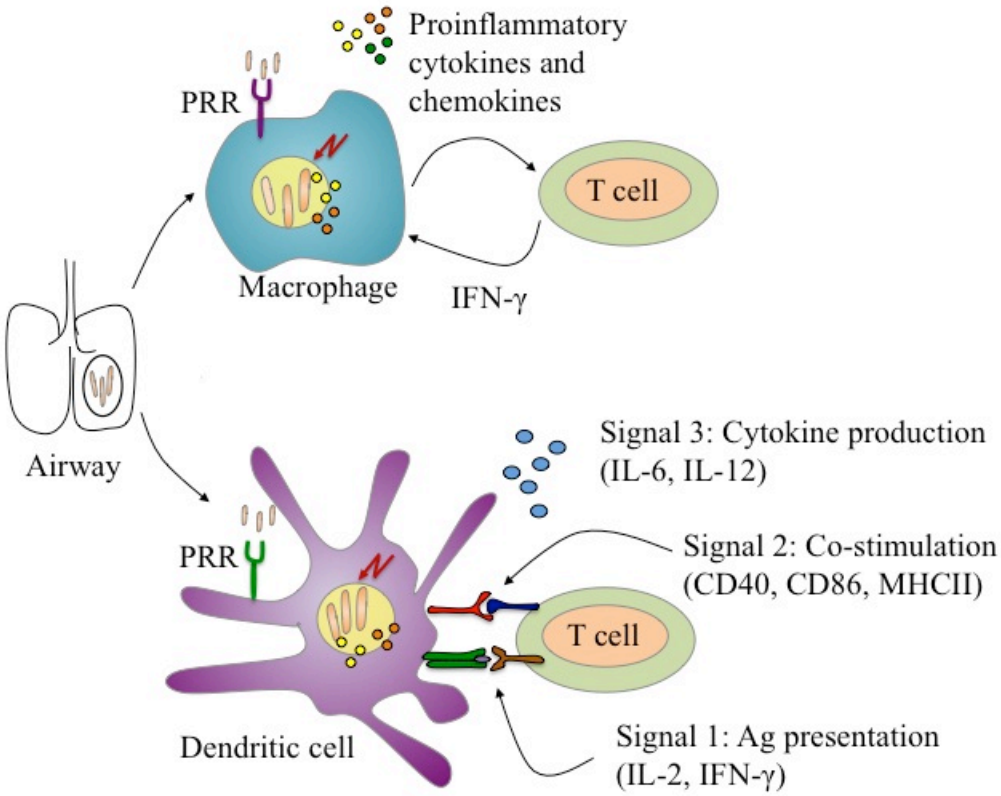
Proinflammatory
cytokines and
chemokines
PRR
T cell
Macrophage
IFN-γ
Airway
Signal 3: Cytokine production
(IL-6, IL-12)
Signal 2: Co-stimulation
(CD40, CD86, MHCII)
PRR
T cell
Dendritic cell
Signal 1: Ag presentation
(IL-2, IFN-γ)

Figure 3. Our previously published work demonstrates that *Mycobacterium tuberculosis* Hip1 as a cell wall-associated immunomodulatory protease that manipulates the innate-adaptive immune axis by dampening macrophage responses and impairing DC functions. *M. tuberculosis hip1* mutant induces earlier and more robust proinflammatory responses in macrophages via enhanced activation of TLR2- and inflammasome-dependent pathways. Furthermore, the *hip1* mutant also induces robust DC maturation and improves antigen presentation capacity to antigen-specific T cells.

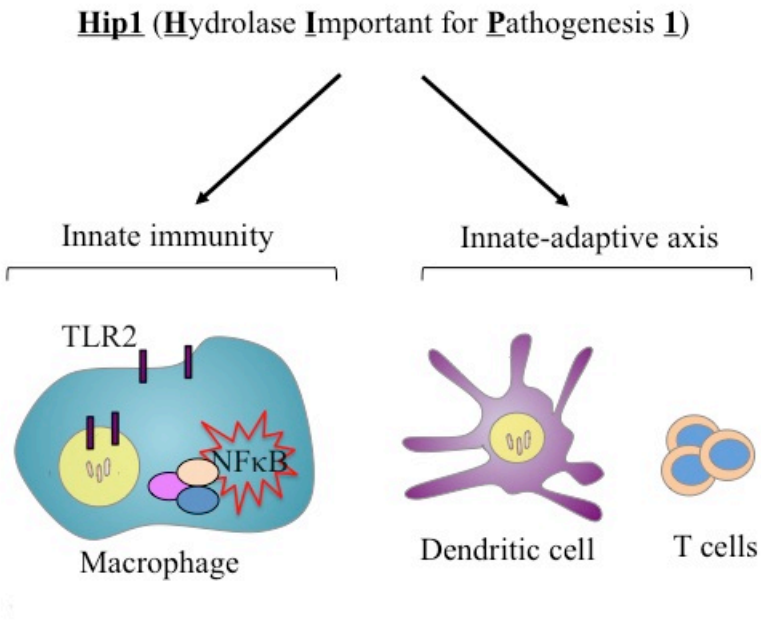

Chapter 2

Mycobacterium tuberculosis Hip1 modulates macrophage responses through proteolysis of GroEL2

Chapter adapted from:

Naffin-Olivos JL[*], **Georgieva M**[*], Goldfarb N[*] *et al*. (2014)

Mycobacterium tuberculosis Hip1 modulates macrophage responses through proteolysis of GroEL2. PLoS Pathog 10(5): e1004132. doi:10.1371/journal.ppat.1004132

[*]These authors contributed equally

Abstract

Mycobacterium tuberculosis (*M. tuberculosis)* employs multiple strategies to evade host immune responses and persist within macrophages. We have previously shown that the cell envelope-associated *M. tuberculosis* serine hydrolase, Hip1, prevents robust macrophage activation and dampens host proinflammatory responses, allowing *M. tuberculosis* to delay immune detection and accelerate disease progression. We now provide key mechanistic insights into the molecular and biochemical basis of Hip1 function. We establish that Hip1 is a serine protease with activity against protein and peptide substrates. Further, we show that the *M. tuberculosis* GroEL2 protein is a direct substrate of Hip1 protease activity. Cleavage of GroEL2 is specifically inhibited by serine protease inhibitors. We mapped the cleavage site within the N-terminus of GroEL2 and confirmed that this site is required for proteolysis of GroEL2 during *M. tuberculosis* growth. Interestingly, we discovered that Hip1-mediated cleavage of GroEL2 converts the protein from a multimeric to a monomeric form. Moreover, ectopic expression of cleaved GroEL2 monomers into the *hip1* mutant complemented the hyperinflammatory phenotype of the *hip1* mutant and restored wild type levels of cytokine responses in infected macrophages. Our studies point to Hip1-dependent proteolysis as a novel regulatory mechanism that helps *M. tuberculosis* respond rapidly to changing host immune environments during infection. These findings position Hip1 as an attractive target for inhibition for developing immunomodulatory therapeutics against *M. tuberculosis*.

Introduction

The outcome of infection with *Mycobacterium tuberculosis* (*M. tuberculosis*), the causative agent of tuberculosis (TB), is determined by a complex interplay between the host immune response and pathogen factors that promote virulence. In response to multiple stresses encountered during infection, *M. tuberculosis* employs a wide array of strategies to evade the first-line defenses mounted by host innate immune responses and successfully replicates intracellularly within host macrophages [9]. *M. tuberculosis* hinders macrophage functions by inhibiting phagosome maturation and acidification, interferes with IFN-γ-mediated activation, counters toxic reactive oxygen (ROI) and nitrogen intermediates (RNI) and resists antimicrobial agents that damage the mycobacterial cell envelope [8,94]. The lipid-rich *M. tuberculosis* cell envelope effectively protects the pathogen from antimicrobial agents and immune toxins and provides a potent hydrophobic barrier against several antibiotics [15]. Remodeling of its cell envelope in response to the rapidly changing immune milieu allows *M. tuberculosis* to adapt to intracellular macrophage environments and to persist within granulomatous lesions in the lung. *M. tuberculosis* also secretes a number of gene products extracellularly, many of which can serve as effector molecules to modulate host cells and promote disease progression [69]. Delineating the molecular functions of cell envelope-associated and extracellular *M. tuberculosis* factors that are required for evading host immunity is therefore critical for understanding *M. tuberculosis* pathogenesis.

We have recently identified the cell envelope-associated serine hydrolase, Hip1 (Hydrolase important for pathogenesis 1; Rv2224c), as a key immunomodulatory protein that prevents robust activation of macrophages following *M. tuberculosis* infection and controls the onset and magnitude of proinflammatory responses induced by *M. tuberculosis* [79-81]. This strategy of dampening early proinflammatory responses is likely to be advantageous to the pathogen by allowing it to escape immune detection. In addition, *M. tuberculosis* Hip1 and its *Mycobacterium smegmatis* (*M. smegmatis)* ortholog are important for maintaining *M. tuberculosis* cell envelope integrity and confer resistance to cell envelope-directed stresses [80,82,83]. In this study, we provide key insights into the molecular and biochemical mechanisms underlying Hip1 enzymatic activity and its immunomodulatory functions. Hip1 is predicted to encode a serine protease based on its similarity to the tripeptidyl-peptidases TPP B (SlpD) and TPP C (SlpE) from *Streptomyces lividans*, which are mycelium-associated proteases involved in cell growth [86]. Hip1 possesses the catalytic triad S_{228}, D_{463}, H_{490}, present in α/β hydrolase family members, including esterases, lipases and proteases, but the presence of 11 cysteine residues and 5 predicted disulfide bonds within the protein, complicated previous efforts to purify this protein and, thus, the true enzymatic activity of Hip1 has remained unclear [95,96]. We now conclusively demonstrate that Hip1 is a serine protease with activity against protein and peptide substrates. Further, we show that the *M. tuberculosis* GroEL2 protein is a substrate of Hip1 protease activity. While several proteases have been implicated in promoting *M. tuberculosis* virulence, identification of their physiological substrates has been largely lacking and the interplay between proteases and their substrates during *M. tuberculosis* infection is poorly understood [6,75-

77,97-102]. Here, we show that Hip1 proteolytically cleaves GroEL2 in the N-terminus of the protein and we have mapped the cleavage site within GroEL2. Interestingly, cleavage of GroEL2, which encodes a chaperone-like immunomodulatory protein, converts the protein from a multimeric form to a monomeric form. Remarkably, while GroEL2 remains uncleaved in the *hip1* mutant, ectopic expression of cleaved GroEL2 monomers within the *hip1* mutant strain restores wild type levels of cytokine responses in infected macrophages. Our studies implicate Hip1-dependent proteolysis of its substrate as a novel regulatory mechanism in *M. tuberculosis* that helps the pathogen respond rapidly to changing host immune environments during infection.

Results

Purification of recombinant Hip1 protein

Hip1 is a cell envelope-associated α/β hydrolase that is predicted to have serine protease activity. Multiple attempts to overexpress full length or truncated Hip1 proteins in *Escherichia coli* (*E. coli)* yielded insoluble protein (data not shown) and we suspected that the presence of 11 cysteine residues and 5 predicted disulfide bridges within the protein hindered our initial efforts at refolding the protein *in vitro* [95]. To overcome these challenges, we developed a method to successfully refold Hip1 under anaerobic conditions, which resulted in correctly folded, active protein (described in detail in Methods). Hip1 (minus the first 49 amino acid segment which contains within it a Type II signal sequence) with an in-frame N-terminal polyhistidine tag was expressed in *E. coli*, immobilized on nickel (Ni^{2+}) beads and allowed to completely refold under reducing conditions in an anaerobic chamber. To promote refolding of Hip1 into its native conformation, the protein was refolded on the beads in a step-wise procedure using buffers containing varying concentrations of denaturant as well as reducing and oxidizing agents. The protein rich elution fraction was further purified on an anion exchange column (Figure 1A). Since the different peaks in the elution spectrum likely represent differently refolded species, protein fractions corresponding to each peak were tested for activity and only the fraction that showed the highest level of enzyme activity (indicated by the arrow in Figure 1) was used for subsequent experiments. Similar methods were used to express and purify a Hip1 protein containing a serine to alanine mutation in the predicted active site at Ser_{228} (Figure 1B). Purity of Hip1 and Hip1(S228A) proteins was

confirmed by SDS-PAGE (Figure 1A, B). Circular dichroism (CD) analysis (Figure 1C) showed that both proteins contain alpha-helical structures as indicated by the negative bands at 222 and 208 nm. CD spectra for wild-type Hip1 and Hip1(S228A) were identical, indicating that mutating the serine at residue 228 does not affect the overall folding of the protein.

Hip1 exhibits serine protease activity

Hip1 shares 30%, 38% and 32% identity with the TPP A, TPP B and TPP C serine proteases from *Streptomyces lividans* and contains a catalytic triad (Ser_{228}, Asp_{463}, His_{490}) that is typically present in serine proteases [86,96]. Thus, while Hip1 is predicted to encode a serine protease, previous reports were unable to detect protease activity and the enzymatic activity of Hip1 has not been conclusively established [84,87]. To determine the enzymatic activity of purified recombinant Hip1, we first tested its activity against general protease and esterase substrates (Figure 2A, B). We found that Hip1 exhibited esterase activity against the ester substrate *p*-nitrophenylbutyrate (Figure 2A), indicating that the purified protein was active. Importantly, Hip1 exhibited protease activity against the general protease substrate azocasein (Figure 2B). In contrast, Hip1(S228A), carrying a mutation of the serine residue in the active site of the protein, was unable to hydrolyze azocasein (Figure 2B), indicating that Hip1 catalytic activity was necessary for its protease activity. To further investigate the enzymatic activity of Hip1 against peptide substrates, we used the peptides Ala-Pro-Ala and Gly-Pro-Leu, which are substrates for TPP A and TPP B, as well as Ala-Pro-Ala-Arg, which is a substrate for TPP C. We also included Ac-Ala-Pro-Ala-Arg to test if blocking the N-terminus prevents enzymatic

cleavage of the peptide substrate [86]. These peptides were synthesized with the addition of a C-terminal *p*-nitroanilide (*p*Na) chromophore, and Hip1 enzyme activity against these peptides was assessed first in an endpoint spectrophotometric assay. Figure 2C shows that Hip1 shows the best activity against the Ala-Pro-Ala-*p*Na and Gly-pro-Leu-*p*Na substrates. Taken together, these data show that Hip1 is a serine protease that is capable of hydrolyzing ester and peptide substrates.

We used a continuous spectrophotometric assay using the chromogenic substrate Ala-Pro-Ala-*p*Na to test inhibition of Hip1 protease activity with inhibitors for the major classes of proteases (Figure 2D). Hip1 proteolytic activity is abolished in the presence of 4-(2-Aminomethyl) benzenesulfonyl fluoride (AEBSF). AEBSF is a serine protease-specific active site inhibitor that sulfonylates only the active site serine to inhibit catalysis [103]. Hip1 activity was abolished by leupeptin and significantly reduced by chymostatin and antipain, all three of which block both serine and cysteine proteases [104,105]. However, the cysteine protease inhibitor E-64, the aspartyl protease inhibitor pepstatin, and EDTA, which chelates the essential metal ion of metalloproteases [84,103] do not inhibit Hip1 indicating that Hip1 is a serine protease. These results demonstrate that Hip1 is a serine protease and support our mutagenesis studies showing that Ser_{228} is required for Hip1 activity *in vitro* (Figure 2).

M. tuberculosis GroEL2 is a Hip1 substrate

To determine the mechanism for Hip1 function in *M. tuberculosis* pathogenesis, we sought to identify physiological substrates of Hip1 protease activity. We previously reported that full length *M. tuberculosis* GroEL2 protein (Rv0440, hsp65) was present in

mycobacterial cell wall fractions, while a smaller cleaved form was secreted extracellularly into culture supernatants [80]. This cleaved form of GroEL2 was absent in the *hip1* mutant, suggesting that Hip1 was necessary for GroEL2 processing. To test whether GroEL2 is a direct target of Hip1 protease activity, we incubated purified recombinant GroEL2 protein with recombinant Hip1 and assayed for GroEL2 cleavage by Western blotting. The GroEL2 contains a His6X-tag at the N-terminus and a C-terminal S-tag for ease of purification as well as visualizing on Western blot. The presence of the two different tags also allowed us to verify which end of the protein is being cleaved. In the presence of Hip1, full length GroEL2 protein was cleaved to a smaller form, GroEL2(cl), which was detected by Western blotting using anti S-tag antibodies (Figure 3A). Cleavage of GroEL2 was entirely dependent on the catalytic serine active site as no cleavage was observed with the Hip1(S228A) protein (Figure 3A) and GroEL2 processing was inhibited by the serine protease inhibitor AEBSF (Figure 3B). Further, incubation of Hip1 and GroEL2 under varying pH conditions showed that Hip1 protease activity against GroEL2 was optimal between pH 5.37 and 7.67 (Figure 3C). Thus, GroEL2 is a substrate of Hip1 serine protease activity.

To examine protein-protein interactions between Hip1 and its substrate GroEL2 within mycobacteria, we used the Mycobacterium Protein Fragment Complementation (M-PFC) assay. This assay is based on functional reconstitution of two small murine dihydrofolate reductase (DHFR) domains that are independently fused to two interacting proteins of interest. Interaction between candidate proteins *in vivo*, i.e. within *M. smegmatis*, leads to reconstitution of the DHFR domains and results in resistance to trimethoprim. Figure 3D

shows that Hip1 and GroEL2 interact with each other, as seen by growth on plates containing trimethoprim. This interaction appears to be more robust in the presence of Hip1(S228A), suggesting as expected that interaction of GroEL2 with catalytically inactive Hip1 may be stronger. These interactions appear to be specific, as GroEL2 does not interact with *M. tuberculosis* KdpE, InhA or SigA proteins. These results are consistent with the formation of an enzyme-substrate complex between Hip1 and GroEL2.

Hip1 proteolytically cleaves GroEL2 between Arg_{12} and Gly_{13}

To identify the site at which Hip1 cleaves GroEL2, we electrophoretically separated *M. tuberculosis* cell-free culture supernatants, and excised the bands corresponding to full length and cleaved GroEL2 from SDS-PAGE. The eluted proteins were subjected to LC/MS mass spectrometry, which indicated that cleavage occurred within the first 18 amino acids at the N-terminus of GroEL2 (data not shown). To further delineate the cleavage site, we synthesized a peptide corresponding to amino acids 1-19 of GroEL2 (AKTIAYDEEARRGLERGLN; m/z = 2163) and subjected this to proteolysis by Hip1 (Figure 4B). LC/MS analysis showed that the peptide was cleaved at two positions. Based upon the masses of the most abundant cleavage products (IAYDEEARR; m/z = 1122) and (GLERGLN; m/z = 757) the positions of the cleavage sites were determined using the FindPept tool on the Expasy server. The small polar fragment, AKT, was not detected due to its lack of retention on the reverse phase column. The cleavages sites were determined to be between the $Thre_3$ and Ile_4, as well as between Arg_{12} and Gly_{13} (Figure 4B). Hip1 mediated processing at the $Thre_3$/Ile_4 and Arg_{12}/Gly_{13} cleavage sites was completely inhibited by the serine protease inhibitor, AEBSF (Figure 4C).

To test whether the cleavage site predicted by experiments with the GroEL2 peptide corresponds to the cleavage site within the intact *M. tuberculosis* GroEL2 protein, we developed an assay system in *M. smegmatis* (Figure 4E). We first expressed *M. tuberculosis* GroEL2 containing a C-terminal FLAG tag in *M. smegmatis.* Figure 4E shows that while full length, uncleaved, GroEL2-FLAG is present in the culture supernatant fraction of *M. smegmatis*, the cleaved form is absent. *M. tuberculosis* GroEL2-FLAG is effectively cleaved in the presence of recombinant Hip1 provided *in trans* (Figure 4E), thus providing a convenient assay for testing *M. tuberculosis* GroEL2 harboring mutations in the predicted cleavage sites. Although two cleavage sites were predicted by the *in vitro* LC/MS study, we chose to focus the mutational studies on the Arg_{12}/Gly_{13} cleavage site, since this is the only cleavage site that could have resulted in the GroEL2 mass shift observed in our earlier studies. We expressed FLAG-tagged *M. tuberculosis* GroEL2 containing mutations in the predicted Arg_{12} and Gly_{13} cleavage sites by replacing Arg_{12} with proline (R12P), or both Arg_{12} and Gly_{13} with prolines (R12P/G13P). *M. smegmatis* supernatants containing each of the GroEL2 cleavage site mutants were incubated with Hip1 and assayed for full length and cleaved GroEL2 by Western blot using anti-FLAG antibodies. GroEL2 R12P showed reduced cleavage while cleavage was completely abolished in GroEL2 R12P/G13P. These results indicate that GroEL2 is cleaved between Arg_{12} and Gly_{13} within the N-terminus of GroEL2. To test whether Arg_{12} and Gly_{13} within GroEL2 are required for cleavage within *M. tuberculosis*, we expressed intact FLAG-tagged GroEL2 and the cleavage site mutant R12P/G13P in wild type *M. tuberculosis* and prepared protein extracts from pellet (P) and supernatant (S) fractions to detect GroEL2 cleavage by Western blot using anti-FLAG antibodies

(Figure 4F). As predicted, the R12P/G13P mutant was unable to be cleaved, thus demonstrating that cleavage of GroEL2 occurs between Arg_{12} and Gly_{13} within *M. tuberculosis*.

Hip1-dependent proteolytic cleavage converts multimeric GroEL2 to a monomeric form

The oligomeric state of a protein is intrinsically linked to its biological function and many chaperones have been shown to form higher order oligomers [106] [107]. While the precise function of GroEL2 in *M. tuberculosis* remains unclear, GroEL2 shows sequence similarity to members of the heat shock protein (Hsp) family of molecular chaperones [107]. To investigate the oligomeric state of full length, uncleaved GroEL2 protein, we used analytical size exclusion chromatography to determine its molecular weight. We found that GroEL2 eluted as a multimer with the molecular weight ranging from 198 to 321 kDa across 4 independent experiments (i.e. 198, 219, 258, 312 kDa), with the average molecular weight corresponding to 245 kDa. Figure 5A shows a representative experiment where the molecular weight of the multimer is 312 kDa. We next asked whether cleavage of GroEL2 by Hip1 would alter its multimeric state. Full length GroEL2 was incubated with Hip1 for 24 hours for complete cleavage to occur. Nickel beads were used to remove Hip1 protein and the small N-terminal fragment of GroEL2 (amino acids 1-12), leaving behind the cleaved GroEL2 protein. The presence of cleaved GroEL2 was confirmed using anti-S-tag antibodies as seen in the Western blot in supplementary Figure S1A. Cleaved GroEL2 was then applied to the size exclusion column and interestingly, eluted from the size exclusion column as a monomer of

approximately 54 kDa (Figure 5A). To show that Ni^{2+}-bead depletion removed the majority of the Hip1, we performed a Western blot using anti-His antibodies and showed that Hip1 protein was absent from depleted fraction (Supplementary Figure S1B). Thus the predominant protein eluting from the size exclusion column is cleaved GroEL2. These results show that proteolytic cleavage by Hip1 converts GroEL2 from a multimer to a monomer (Figure 5A and 5B).

The cleaved form of GroEL2 complements the *hip1* mutant hyperinflammatory phenotype

We have previously shown that Hip1 modulates macrophage responses by limiting macrophage activation and dampening the production of TLR2-dependent proinflammatory responses [79-81]. Thus the *hip1* mutant strain induces significantly higher levels of proinflammatory cytokines compared to wild type *M. tuberculosis*. While several studies have reported that purified GroEL2 protein is capable of inducing cytokine production in macrophages *in vitro*, insights into the contribution of cleaved GroEL2, which accumulates in wild type, but not in *hip1* mutant supernatants, are lacking [90,108]. To investigate the role of Hip1-dependent proteolytic cleavage of GroEL2 in infection of macrophages and its contribution to the hyperinflammatory phenotype of the *hip1* mutant, we generated a *hip1* mutant strain complemented with a secreted, cleaved form of GroEL2. This strain was constructed by cloning GroEL2(cl) (starting at amino acid G13) downstream of a signal sequence derived from the secreted *M. tuberculosis* Ag85B protein and containing a C-terminal Myc tag. We confirmed that this protein was present in the supernatant fraction by Western blotting with anti-Myc antibody

(Supplementary Figure S2A). We also compared levels of endogenous GroEL2 in each of the *M. tuberculosis* strains used for infection of macrophages (Supplementary Figure S2B). To determine the effect of introducing cleaved GroEL2 into the *hip1* mutant, we infected macrophages derived from the bone marrow of C57BL/6 mice with wild type, *hip1* mutant, *hip1* mutant complemented with Hip1, or *hip1* mutant complemented with cleaved GroEL2, and assayed for the production of the proinflammatory cytokines IL-6, IL-1β, and TNF-α in macrophage supernatants, 24 hours post-infection. As shown previously, the levels of IL-6, IL-1β, and TNF-α were significantly increased in the absence of Hip1 (Figure 6) [81]. This enhanced cytokine production was complemented by ectopic expression of Hip1 protein, which restored wild type levels of IL-6, IL-1β, and TNF-α (Figure 6). Interestingly, expression of cleaved GroEL2 in the *hip1* mutant strain significantly abrogated the hyperinflammatory response induced by the *hip1* mutant (Figure 6). This finding suggests that the enhanced cytokine responses induced in *hip1* mutant-infected macrophages are directly linked to defective GroEL2 cleavage and that Hip1-dependent proteolytic processing of GroEL2 contributes to dampening early macrophage responses.

To provide further mechanistic insights into GroEL2 cleavage, we tested whether full length and cleaved GroEL2 proteins exhibit differences in eliciting cytokine production by macrophages. We purified recombinant full length GroEL2 and cleaved GroEL2 and compared the ability of purified GroEL2 and GroEL2(cl) to induce cytokine production from macrophages. As shown in Figure 7A, GroEL2 induced significantly higher levels of IL-6 and IL-1β compared to GroEL2(cl), and this was partially dependent on TLR2

(Figure 7B). These results suggest that cleavage of GroEL2 reduces its ability to induce proinflammatory cytokine responses and that Hip1-dependent proteolysis of GroEL2 modulates macrophage responses. The presence of GroEL2(cl) dampens these proinflammatory responses since the levels of cytokines induced by a 1:1 molar ratio of GroEL2 and GroEL2(cl) in combination is less than the additive effect of each individual protein (Figure 7C). Together, these studies reveal proteolysis of effector proteins as a novel immune evasion mechanism employed by *M. tuberculosis* to modulate host immunity.

We propose a model in which Hip1-dependent cleavage of multimeric GroEL2 results in release of cleaved monomeric GroEL2 into the extracellular milieu (Figure 8). Within macrophages, this is likely to occur upon contact with the macrophage cell surface and continue within the phagosomal compartment. In contrast, in the *hip1* mutant, in the absence of cleavage, GroEL2 is present as a multimer. Thus, conversion of multimeric GroEL2 into monomeric GroEL2 via Hip1 proteolysis is likely to be a mechanism for regulating GroEL2 functions during *M. tuberculosis* pathogenesis.

Discussion

Establishing the true enzymatic activity of Hip1 is critical for understanding the mechanistic basis for how Hip1 modulates host innate immune responses during *M. tuberculosis* infection. While *hip1* was predicted to encode a protease, the true enzymatic activity of Hip1 has remained unclear [84,87]. In this study, we demonstrate that *M. tuberculosis* Hip1 is a protease with a serine-based active site and report the identification of a physiological substrate, *M. tuberculosis* protein GroEL2 (Figure 3). Hip1 contains highly conserved α/β hydrolase fold sequences and GxSxG consensus motifs that are typically present in serine proteases, esterases and lipases. Also typical is the catalytic triad consisting of the catalytic nucleophile serine active site (Ser_{228}), which associates with the proton carrier histidine (His_{490}), and a charge relaying aspartic acid (Asp_{463}). The closest structural orthologs of Hip1, which is localized to the cell envelope of *M. tuberculosis*, are the serine proteases TPP A, TPP B and TPP C from *Streptomyces lividans*, which are mycelium-associated proteases involved in cell growth [86]. Previous work from our group showed that GroEL2 is present as both a full length and a smaller processed form in wild type *M. tuberculosis* and that this processing was defective in the absence of *hip1*, suggesting that GroEL2 may be a substrate for Hip1 protease activity [80]. However, our initial efforts to characterize the enzymatic activity of Hip1 were hindered by difficulties in producing soluble recombinant protein in *E.coli*, and refolding of denatured protein from insoluble fractions using standard refolding procedures did not result in correctly folded protein as determined by 1-dimensional NMR (JN, unpublished results) and circular dichroism (CD) analyses. While refolded Hip1 protein was reported

to hydrolyze synthetic ester substrates *in vitro* [87], this study was unable to detect protease activity against general protease substrates and concluded that Hip1 encoded a carboxyesterase. However, since serine proteases are capable of hydrolyzing both ester and amide bonds, these data did not exclude the possibility that Hip1 was a protease [109]. Thus the true enzymatic activity of Hip1 remained unknown. We were able to overcome the difficulties inherent in refolding a protein containing multiple disulfide bonds by developing a method to successfully refold Hip1 and Hip1(S228A) (Figure 1), under reducing conditions in an anaerobic chamber, which resulted in correctly folded, active protein. This allowed us to demonstrate that Hip1 exhibits proteolytic activity against a general protease substrate azocasein, synthetic peptides and against the GroEL2 protein. This protease activity requires catalytically active enzyme and is inhibited by serine protease inhibitors (Figure 2) but not by cysteine protease inhibitors. Interestingly, while Hip1 was inhibited by AEBSF, this activity was not inhibited by PMSF. We suspect this is due to the fact that PMSF lacks the longer, positively charged amino group present in AEBSF, which binds in the S1 pocket of the enzyme's active site. Overall, our findings conclusively establish that Hip1 is a novel serine protease family member and studies are underway to determine its 3-dimensional structure by X-ray crystallography.

M. tuberculosis encodes over one hundred predicted proteases and it is increasingly appreciated that proteases play an important role in *M. tuberculosis* pathogenesis [110]. However, very few proteases have been characterized with respect to their enzymatic activities and even fewer have known physiological substrates. Moreover, many of these proteases, including Hip1, belong to novel protease families and therefore detailed

biochemical characterization of these enzymes and their substrates is an important goal [68,84,111]. In this study we demonstrate that Hip1 is a serine protease and have identified a key physiological substrate. We show that Hip1 cleaves *M. tuberculosis* protein GroEL2 *in vitro* and have mapped this cleavage site to the N-terminus of the GroEL2, between amino acid residues Arg_{12} and Gly_{13}. Interestingly, the optimal pH range that we determined for cleavage of GroEL2 *in vitro* (pH 5.65 to 7.39) overlaps with the intraphagosomal pH of the *M. tuberculosis*-arrested phagosome (estimated to be ~ 6.3), and that of the macrophage cell surface (~7.0) [43,112-114]. Since the pH of the lysosomal compartment is ~ 4.5 to 5.0, we speculate that, within macrophages, GroEL2 cleavage occurs upon contact with the macrophage cell surface and continues within the phagosomal compartment but is unlikely to occur within the acidic environment of the lysosome [113].

Additional insights into the relationship between Hip1 and GroEL2 are provided by our data showing that Hip1 not only directly cleaves GroEL2 but also impacts its oligomeric state. Size exclusion chromatography using recombinant full length GroEL2 indicates the presence of a single species of multimeric GroEL2, which is converted to a monomeric state after cleavage by Hip1. The apparent molecular weight of the GroEL2 multimer is consistent with a tetrameric or pentameric complex consisting of four or five monomer subunits. Our observations are consistent with previously reported data that GroEL2 is capable of forming higher order oligomers under certain conditions [91]. To test for concentration-dependent effects that may affect the oligomeric state of the protein, we tested the oligomeric state of recombinant GroEL2 over a range of concentrations and

identified that GroEL2 is a multimer even at the lowest concentration at which it is detectable on the size exclusion column (unpublished results). Thus, the conversion of multimeric GroEL2 to monomers in the presence of Hip1 is not a result of dilution of protein during the experimental procedures. The 3-dimensional structure of GroEL2 has been investigated by two separate X-ray crystallographic studies at 2.2 and 2.8 angstroms resolution. In both studies, GroEL2 was found to be a dimer in the asymmetric unit [115]. Our studies show that full length GroEL2 forms a multimer with an average molecular weight that predicts a tetrameric structure. Experimental studies in solution do not always agree with structural studies in determining the oligomeric state of proteins, since packing in the crystal can adversely impact oligomerization. While our analytical size exclusion studies are consistent with a multimeric structure for GroEL2, it is possible that GroEL2 consists of a dimer of dimers. Interestingly, a closer look at the crystal structure of GroEL2 revelas that the first 60 amino acids are absent from the crystal subunits [115]. This suggests that the N-terminal portion is most likely part of a flexible region of the protein and any modification in that segment of the protein will result in major structural changes. Based on our size exclusion data, we propose a model in which Hip1-dependent cleavage of multimeric GroEL2 results in release of cleaved monomeric GroEL2 into the extracellular milieu. In contrast, in the *hip1* mutant, in the absence of cleavage, GroEL2 is present as a multimer. Studies on *E. coli* chaperonin, GroEL, have demonstrated that the N terminus of the protein is a crucial element for its structure and that specific mutations at the N terminus lead to disruption of the formation of higher order GroEL oligomers [116]. While it is unclear whether *M. tuberculosis* GroEL2 functions as a canonical chaperonin, we show that removal of the N-terminal peptide of GroEL2

following cleavage by Hip1 clearly promotes GroEL2 monomer formation, which may be advantageous to the pathogen. Thus conversion of multimeric GroEL2 into monomeric GroEL2 via Hip1 proteolysis is likely to be a mechanism for regulating GroEL2 functions during *M. tuberculosis* pathogenesis.

To investigate the role of cleaved, monomeric GroEL2 in Hip1-dependent innate immune responses to *M. tuberculosis*, we examined a key phenotype of *hip1* mutant-infected macrophages. We have previously shown that the cell envelope in the *hip1* mutant is altered such that infection of macrophages with this mutant induces a more rapid onset and significantly higher levels of proinflammatory cytokines compared to wild type *M. tuberculosis* infection [79-81]. Thus Hip1 dampens proinflammatory responses in *M. tuberculosis*-infected macrophages. Our data supported a model in which contact between the *hip1* mutant and macrophage cell surfaces, early in infection, triggered a more rapid and robust activation of TLR and inflammasome pathways in macrophages, which in turn ameliorated TB disease progression and immunopathology at later stages [81]. Since purified full length GroEL2 protein has been implicated in modulating cytokine responses in murine and human macrophages *in vitro*, we sought to investigate the role of Hip1-mediated GroEL2 cleavage in modulating these cytokines by asking whether there was a connection between the defective processing of GroEL2 in the *hip1* mutant strain and its hyperinflammatory phenotype [85]. When we ectopically expressed the monomeric, cleaved form of GroEL2 into the *hip1* mutant strain, we found that the cytokine levels induced by this engineered strain were comparable to the low levels induced by wild type *M. tuberculosis* and the *hip1* mutant complemented with Hip1

(Figure 6). Thus provision of monomeric GroEL2 to the *hip1* mutant almost completely restored wild type cytokine levels, indicating that the cleaved, monomeric GroEL2 is biologically relevant and significantly contributes to Hip1-mediated dampening of innate immunity. Interestingly, we found that purified recombinant GroEL2(cl) protein is less stimulatory than full length GroEL2 when exposed to macrophages (Figure 7A, B) and is capable of dampening the stimulatory effect of full length GroEL2 (Figure 7C). These data suggest that Hip1-mediated proteolysis of GroEL2 contributes to the ability of *M. tuberculosis* to dampen macrophage proinflammatory responses during infection [81].

GroEL2 has been implicated in a wide variety of processes, ranging from modulating immune responses and conferring resistance to stress, to chaperone-like functions. GroEL2 is highly induced in response to environmental cues during infection like heat shock, oxidative stress, growth in macrophages and hypoxia [117-119]. GroEL2 is an abundant *M. tuberculosis* protein and is a dominant contributor to the potent immune response elicited by *M. tuberculosis* Purified Protein Derivative (PPD) [120]. Purified GroEL2 protein has also been shown to induce cytokine responses when exposed to macrophages, and have adhesion-like properties when localized to the *M. tuberculosis* cell wall. *M. tuberculosis* is unusual among bacteria in possessing two GroEL proteins, the cytoplasmic protein GroEL1, which is highly homologous to the *E. coli* GroEL chaperonin, and GroEL2, which is localized to the cell envelope and whose functions appear to be more diverse. While GroEL2 exhibited only weak ATPase activity *in vitro*, the crystal structures of GroEL2 suggest that it has chaperone-like qualities and may assist in protein folding or antigen presentation [115]. All the studies described here were

conducted with full length GroEL2. In light of our finding that Hip1 cleavage of GroEL2 impacts macrophage functions, it is interesting to speculate that multimeric and monomeric GroEL2 may have distinct functions. Further studies with the two oligomeric forms of GroEL2 will allow us to dissect their potential differential functions at the host-pathogen interface, along with the identification of additional pathogen-derived or host substrates of Hip1 proteolysis.

It is important to consider the studies presented here within the larger context of the role of proteases in *M. tuberculosis* pathogenesis. Compared to other bacterial pathogens like *Yersinia* and *Chlamydia*, relatively little was known about proteases in *M. tuberculosis*. However, in the past decade, several proteases have been implicated as virulence factors. For example, MarP (Rv3671) is a periplasmic protease that was shown to be required for *M. tuberculosis* resistance to acid and oxidative stress and exhibited protease activity against synthetic peptide substrates [75,98,99]. PepD, a secreted serine protease that promotes *M. tuberculosis* virulence was shown to hydrolyze the general protease substrate casein [19, [77]. Both these proteases also exhibited autoproteolytic activity but their physiological substrates remain unknown. As examples of proteases with known substrates, the intramembrane protease Rip1 (Rv2869c) was shown to be involved in regulating cell envelope mycolic acids by cleaving *M. tuberculosis* anti-sigma factors leading to release of the sigma factors SigK and SigL which in turn regulate cell envelope composition [69,78]. Further, Rip1 cleaves a penicillin-binding protein, PBP3 under conditions of oxidative stress [121]. The serine protease MycP1 is required for secretion of ESX-1 substrates, which are known to be important for *M. tuberculosis* virulence [70].

The authors demonstrated that MycP1 directly cleaved its substrate EspB and mapped the cleavage sites within the EspB protein [70]. Our studies on Hip1 and the examples of proteases described here underscore the idea that, as enzymes that allow for quick responses to changing environmental conditions, proteases offer a unique mechanism for regulating *M. tuberculosis* responses at the protein level. This allows *M. tuberculosis* to rapidly orchestrate immune evasion strategies that promote disease progression and facilitate adaptation to the host immune milieu.

As a cell surface protease involved in modulating host immune responses [79-81] and conferring resistance to cell envelope-directed stresses, Hip1 is an attractive target for inhibition [110]. *Hip1*-deficient *M. tuberculosis* is more susceptible to cell wall directed stresses [80,82], induces robust innate immune responses and causes mild immunopathology and significantly prolonged survival in infected mice, despite high bacterial burdens [79-82,87]. We speculate that Hip1 inhibitors have the potential to synergize with antibiotics to increase susceptibility to drugs and/or serve as adjunctive immunomodulatory therapeutics that elicit beneficial immune responses and thus improve or shorten anti-TB regimens. Using the information gained through our detailed analyses of Hip1 enzymatic activity and its molecular interaction with its substrate GroEL2, studies are underway to determine the 3-dimensional structure of Hip1 and develop inhibitors of the enzyme-substrate complex.

Materials and Methods

Ethics Statement

All experiments using tissue derived from animals were approved by the Institutional Animal Care and Use Committee at the Emory University. Experiments were carried out in strict accordance with the recommendations in the Guide for the Care and Use of Laboratory Animals of the National Institutes of Health. C57BL/6 mice were purchased from The Jackson Laboratory, and handled according to IACUC protocol yer-2002233-052816GN to obtain macrophages.

Cloning of recombinant proteins for expression in *E.coli*

Hip1 (Rv2224c) and Hip1(S228A): *M. tuberculosis hip1* lacking the first 49 amino acids of the protein (which removes the N-terminal signal sequence) was amplified from H37Rv genomic DNA using primers 5'-CATATGGTGGAGTGGACACCGTGCCGGTCG -3' and 5'-CTCGAGCTAGCACTTGGCGCCGCTGGG-3' and ligated into the TA cloning vector, pCR2.1 (Invitrogen, Carlsbad, CA). The fragment containing *hip1* was excised from the TA vector using the restriction enzymes *Nde*I and *Xho*I and then ligated into pET28a (EMD Chemicals, Darmstadt, Germany) yielding a construct carrying an in-frame polyhistidine affinity tag (6XHis-tag) at the N-terminus, yielding pET28Hip1Δ49. To generate Hip1 with a mutation in the serine active site (S228A), the serine at amino acid 228 of the Hip1 protein was mutated to alanine by site-directed mutagenesis using primer

5’-CTACCTGGGCTACGCGTACGGCACC-3’ and 5’-GTGCCGTACGCGTAGCCCAGGTAG-3’, yielding pET28Hip1Δ49 (S228A).

GroEL2: *M. tuberculosis groEL2* was cloned into pACYCDuet-1 (Merck Millipore, Darmstadt, Germany) via the restriction sites *Eco*RI and *Kpn*I using the In Fusion cloning system following the manufacturer’s protocol. *M. tuberculosis groEL2* was amplified using the primers 5’-GCCAGGATCCGAATTCGATGGCCAAGACAATTGCGTACGAC-3’ and 5’-TTACCAGACTCGAGGGTACCGAAATCCATGCCACCCATGTCGCC-3’, yielding a construct bearing an in-frame N-terminal 6XHis-tag and a C-terminal S-tag, yielding pACYCDuet-1 GroEL2. Site directed mutagenesis was used to introduce mutations at the GroEL2 cleavage site that changed Arg_{12} to Pro (R12P) and Glu_{13} to Pro (G13P) using primer 5’-GAGGCCCGTCCACCACTCGAGCGGGGC-3’ and 5’-GCCCCGCTCGAGTGGTGGACGGGCCTC-3’. Mutations were confirmed by sequencing.

Expression and purification of recombinant proteins in *E. coli*

Hip1 and Hip1(S228A)*:* The plasmids pET28Hip1Δ49 and pET28Hip1Δ49 (S228A) were transformed into *E. coli* BL21 Star (DE3) (Invitrogen, Carlsbad, CA) for protein expression. Luria-Bertani (LB) broth (1L) containing 50 µg/mL kanamycin was inoculated with 5 mL of overnight culture and incubated at 37°C to an OD_{600} of 0.6 to 1.0. The cells were cooled to room temperature for 15-30 minutes after which 1 mM IPTG (isopropyl β-D-thiogalactopyranoside, Gold Biotechnology, St. Louis, MO) was added and the cells were allowed to incubate overnight at 25°C. The cells were then centrifuged

at 10,000 rpm for 1 hour. The pellet containing Hip1 or Hip1(S228A) was resuspended in 1× PBS (Boston Bioproducts, Ashland, MA), sonicated and centrifuged at 10,000 rpm to separate the soluble and insoluble fractions. No protease inhibitors were used for this purification. Using a dounce homogenizer, the pellet containing the inclusion bodies was washed by resuspending in 50 mM Tris-HCl pH 8.0, 100 mM NaCl, and 0.5% Triton-X followed by centrifugation at 10,000 rpm for 1 hour. After washing twice, the inclusion bodies were resuspended in 50 mM Tris-HCl pH 8.0, 100 mM NaCl, 5 mM β−mercaptoethanol (BME) and 8 M urea and incubated overnight at 4°C while gently stirring to allow for complete solubilization of the proteins within the inclusion bodies. Nickel (Ni^{2+}) resin (Qiagen, Hilden, Germany) was added to the solubilized protein and allowed to equilibrate for 1 hour at 4°C before adding the suspension into a gravity column. The next steps were carried out in an anaerobic chamber at 4°C as follows. The proteins immobilized on the Ni^{2+}-charged beads were allowed to slowly refold into native conformation by stepwise decreasing the amount of urea in the wash buffer in the presence of a redox pair, reduced (Fisher Scientific, Fair Lawn, NJ) and oxidized glutathione (Calibiochem/EMD Millipore, Billerica, MA), within the anaerobic chamber. The beads were washed with 10 column volumes of buffer containing 50 mM Tris-HCl pH 8.0, 100 mM NaCl, 10 mM imidazole, 5% glycerol, 1mM reduced glutathione, 0.2 mM oxidized glutathione with varying urea concentrations of 8 M, 6 M, 3 M, 1 M and no urea for wash buffers 1- 5, respectively. Protein was eluted with 50 mM Tris-HCl pH 8.0, 100 mM NaCl, 250 mM imidazole, 5% glycerol and dialyzed against 50 mM Tris pH 8.0 (Buffer A) using 10 kDa molecular cutoff dialysis tubing. The dialyzed protein was loaded onto a MonoQ column with Buffer A and eluted using a gradient of Buffer B (50

mM Tris, pH 8.0, 1M NaCl). The MonoQ elution spectrum showed multiple peaks corresponding to differently refolded species. Protein fractions corresponding to each peak were tested for activity and for subsequent experiments only the fraction that showed highest level of activity was used. Glycerol was added to a final concentration of 10%, the protein was aliquoted and stored at -80ºC. The expressed proteins were each present as single bands on SDS-PAGE.

GroEL2: The plasmid, pACYCDuet-1 GroEL2 was transformed into *E. coli* BL21 Star (DE3) (Invitrogen, Carlsbad, CA) for protein expression. LB broth (1L) containing 34 µg/mL chloramphenicol was inoculated with 5 mL of overnight culture and incubated at 37ºC to an OD_{600} of 0.6 to 0.8. The cells were cooled to room temperature for 15-30 minutes after which 1 mM IPTG was added and the cells were incubated overnight at 28°C. The cells were then centrifuged at 10,000 rpm for 1 hour. The cell pellet containing GroEL2 was resuspended in 50 mM $NaPO_4$ pH 8.0, 300 mM NaCl, 10 mM imidazole, plus protease inhibitor cocktail (Roche Diagnostics, Indianapolis, IN), sonicated and centrifuged at 10,000 rpm for 1 hour to remove cell debris. The soluble fraction was incubated with Ni^{2+}-charged beads for 1 hour at 4°C and then applied to a gravity column. The cell lysate in the gravity column was first washed with Buffer C (50 mM $NaPO_4$ pH 8.0, 300 mM NaCl) containing 20 mM imidazole and then with Buffer C plus 50 mM imidazole. The protein was eluted with 250 mM imidazole in Buffer C and dialyzed overnight in Buffer A (50 mM Tris-HCl pH 8.0). The dialyzed protein was loaded onto a MonoQ column equilibrated with Buffer A and eluted using a gradient of Buffer B (50 mM Tris, pH 8.0, 1M NaCl). The protein was further purified by size

exclusion S200 column equilibrated with Buffer D (50 mM Tris pH 8.0, 150 mM NaCl). The purified protein was concentrated, aliquoted and stored at -80°C.

Proteins were subjected to SDS-PAGE and visualized as a single band by staining with 0.05% Coomassie blue R-250. The concentrations of purified proteins were determined by Bradford method using bovine serum albumin (BSA) as the standard.

Preparation of recombinant GroEL2 and GroEL2(cl) for macrophage stimulation

GroEL2 and GroEL2(cl) (minus the first 12 amino acids), each bearing an in-frame N-terminal 6XHis-tag were expressed in *E.coli* BL21 star (DE3) (as described above). The cell pellet containing GroEL2 or GroEL2(cl) was resuspended in binding buffer (20 mM Tris-HCl, 500 mM NaCl, 5 mM Imidazole, pH 7.9, 200 μg/ml lysozyme, 1.8 μg/μl DNase) plus protease inhibitor cocktail (Santa Cruz Biotechnology, Dallas, TX), sonicated and centrifuged at 16, 000 x g for 90 min to remove cellular debris and clarify. The soluble fraction was added to Ni^{2+}- charged beads in a gravity column. The cell lysate in the gravity column was first washed with wash buffer 1 (20 mM Tris-HCl, 500 mM NaCl, 60 mM imidazole, pH 7.9) and then wash buffer 2 (10 mM Tris-HCl) to remove residual salts from the column. To remove endotoxin, the cell lysate was washed with 0.5% ASB-14 (Millipore, Billerica, MA) in 10 mM Tris-HCl. Finally, the lysate was washed with 10 mM Tris-HCl to remove any excess detergent. The protein was eluted with 1M imidazole in 10 mM Tris-HCl and dialyzed overnight in 1× PBS buffer. The protein was further purified by size exclusion chromatography on GE Superdex 75 10/300 GL column. The purified protein was then concentrated. The endotoxin levels for

each protein were <10 ng^{-1} ml^{-1} mg^{-1} as determined using LAL Chromogenic endotoxin quantitation kit (Thermo Scientific, Rockford, IL).

Circular Dichroism (CD)

CD data was acquired using a Jasco J-810 Spectropolarimeter. The spectra was recorded from 200 to 280 nm at room temperature with a scan rate of 20 nm/min and a bandwidth of 1.0 mn Each spectra was the average of five scans. Protein concentration was 5 μM for both Hip1 and Hip1(S228A) in buffer containing 50 mM phosphate pH 7.0 plus 150 mM NaCl. The spectra of the buffer was recorded under the same conditions and subtracted from the sample spectra. The data was then converted to molar ellipticity and plotted using Prism 6.0. The plot for the molar ellipticity between 200 to 250 nm is reported.

Bacterial strains and media

Mycobacterium smegmatis (mc^2 122) strain expressing GroEL2-FLAG was grown at 37°C in Middlebrook 7H9 broth or 7H10 (Becton Dickinson, Franklin Lakes, NJ) supplemented with 10% acid-albumin-dextrose-catalase (ADC), 0.02 % glycerol, and 0.05% Tween 80 (for broth), with the addition of 10 μg/ml streptomycin (Sigma-Aldrich, St. Louis, MO) (Roche Diagnostics, Indianapolis, IN). *M. tuberculosis* H37Rv, the *hip1* mutant strain (described previously) [80,81] and *M. tuberculosis* strains expressing GroEL2-FLAG were grown at 37°C in Middlebrook 7H9 broth or 7H10 supplemented with 10% oleic acid-albumin-dextrose-catalase (OADC) (Becton Dickinson, Franklin Lakes, NJ), 0.02 % glycerol, and 0.05% Tween 80 (for broth), with the addition of 25

μg/ml kan (Sigma-Aldrich, St. Louis, MO) for the *hip1* mutant, and, for complemented strains, 10 μg/ml streptomycin (Sigma-Aldrich, St. Louis, MO) or 50 μg/ml hygromycin (Roche Diagnostics, Indianapolis, IN) was added.

Construction of mycobacterial plasmids and strains

GroEL2-FLAG: To construct FLAG-tagged GroEL2 driven by its own promoter, the *groEL2* gene was amplified from *M. tuberculosis* H37Rv genomic DNA using forward primer 5'-ACGTCTAGATGGTAGCCGATGCCGGTGTTG-3' and reverse primer 5'-AGTAAGCTTTCACTTGTCGTCGTCGTCCTTGTAGTCCGAGCCGCCCGAGCCGCCGAAATCCATGCCACCCATGTC-3' to clone GroEL2 into the *Xba*I and *Hin*dIII sites of pTC (kindly provided by Dr. Sabine Ehrt) with a C-terminal FLAG tag. Forward primer 5'-ACGAGATCTATGGCCAAGACAATTGCGTAC-3' and reverse primer 5'-AGTAAGCTTTCACTTGTCGTCGTCGTCCTTGTAGTCCGAGCCGCCCGAGCCGCCGAAATCCATGCCACCCATGTC-3' were used to clone GroEL2 into *Bam*HI and *Hin*dIII sites of pMV762 with C-terminal FLAG tag.

GroEL2 (R12)-FLAG*:* The R12 mutation was introduced into the pTC GroEL2-FLAG construct by site-directed mutagenesis using primers 5'-GAGGCCCGTCCAGGCCTCGAGCGGGGC-3' AND 5'-GCCCCGCTCGAGGCCTGGACGGGCCTC-3'.

GroEL2 (R12P G13P)-FLAG: The R12P and G13P mutations were introduced into the pTC GroEL2-FLAG construct by site-directed mutagenesis using primers 5'-GAGGCCCGTCCACCACTCGAGCGGGGC-3' and 5'-

GCCCCGCTCGAGTGGTGGACGGGCCTC-3'. All mutations were confirmed by sequencing.

Secreted GroEL2(cl)-myc: To express the cleaved form of GroEL2, GroEL2 (cl), the *groEL2* gene (minus the first 12 amino acids) was amplified from the *M. tuberculosis* genome using forward primer 5'-ACGCAGCTGGGCCTCGAGCGGGGCTTGAACGCC-3' and reverse primer 5'-AGTAAGCTTTCACAGATCTTCTTCAGAAATAAGTTTTTGTTCGAAATCCATGCCACC-3' and cloned into the *Pvu*II and *Hin*dIII sites of pMV762, downstream of the predicted N-terminal signal sequence from *M. tuberculosis* antigen 85 complex B NH_2-MTDVSRKIRAWGRRLMIGTAAAVVLPGLVGLAGGAATAGA-OH and an in-frame C-terminal Myc tag.

Preparation of protein extracts from *M. smegmatis* and *M. tuberculosis* strains

Each *M. smegmatis* and *M. tuberculosis* strain was grown to an OD_{600} of 0.6-0.8 in Sautons' medium plus 0.05% Tween 80, then pelleted, washed, resuspended into Sautons' medium minus Tween 80 and grown for 22 hours at 37°C. Supernatants were concentrated by using Centricon Plus-70 (Millipore, Billerica, MA). Each pellet was resuspended in 50 mM Tris, 10 mM NaCl, 34.3 mM BME (Sigma-Aldrich, St. Louis, MO), protease inhibitor cocktail (Santa Cruz Biotechnology, Dallas, TX), and lysing matrix B beads (MP Biomedicals, Solon, OH) and processed by bead beating for 3 cycles of 20 seconds. The lysate was then centrifuged at 12,000 rpm for 20 min at 4°C, and 100 µl was removed for protein estimation by Bradford method using BSA as the standard.

Enzyme assays

Protease activity assays against a general protease substrate, azocasein, was performed with 1%- 5% azocasein (Sigma-Aldrich, St. Louis, MO) in 1× TBS buffer pH 7.4 (Boston BioProducts, Ashland, MA). Azocasein was incubated with 1 ug each of purified recombinant Hip1, Hip1(S228A), BSA (Thermo Scientific, Rockford, IL) or the protease Subtilisin Carlsberg (Sigma-Aldrich, St. Louis, MO) at 37°C for 30 min in a total volume of 200 µL. The reactions were terminated with 200 µL of 10% trichloroacetic acid and incubated for 30 min on ice. The reactions were then centrifuged at 13, 200 rpm at 4°C for 10 min after which 200 µL of the supernatant was transferred to a 96 well plate. Next, 50 µL of 1.8 N NaOH was added to each reaction mixture and the absorbance was read at 440 nm. The enzyme activities are expressed as units of enzyme/mg protein (one enzyme unit is the quantity of enzyme required to increase absorbance by 0.01 units at 440 nm). Endpoint assays showing Hip1 peptidase activity were conducted as follows. Hip1 (7.5 µM) was incubated with 1.5 mM of each of the following peptide substrates in separate reactions: APA-*p*Na, GPL-*p*Na, Ac-APAR-*p*NA, APAR-*p*NA (AnaSpec, Fremont, CA) in 50 mM Tris, pH 8.0 for 18 hours at 25°C. Elastase (4 µM) was used in a positive control reaction. Cleavage of the peptide substrates was detected by monitoring the increase in absorbance at 410 nm using a Cary 50 Bio UV-Vis spectrophotometer.

To test for esterase activity, Hip1 (7.5 µM) or PreScission Protease (0.6 µM) (GE Healthcare) was incubated with 100 µM *p*-nitrophenylbutyrate (Sigma-Aldrich, St. Louis, MO) in 50 mM Tris, pH 8.0 at 25°C. Hydrolysis of the ester substrate was detected in a continuous assay by monitoring an increase in absorbance at 410 nm.

Visualizing GroEL2 cleavage and Western blotting

Purified recombinant GroEL2 (6.6 μM) was incubated with either Hip1 or Hip1(S228A) (19.8 μM) in 1× TBS buffer (Boston BioProducts, Ashland, MA) for 24 hours. Protein samples were added to 4× SDS-PAGE loading dye, boiled for 10 min, separated on NuPAGE 10% Bis-Tris gels (Invitrogen, Carslbad, CA), and transferred onto nitrocellulose membranes (Bio-Rad, Berkeley, CA). Membranes were blocked in TBST (150 mM NaCl, 25 mM Tris-HCl pH 7.0, 0.1% Tween 20) containing 5% Blotto (Santa Cruz Biotechnology, Dallas, TX) for 1 hour at room temperature or 1% BSA (anti-sigma 70) for 2 hours at 4°C, and probed with antisera overnight at 4°C. Antisera included rabbit polyclonal anti-Myc (1:10 000 dilution in 3% Blotto; Novus Biologicals, Littleton, CO), anti-FLAG (1:1000 dilution in 5% Blotto, Sigma-Aldrich, St. Louis, MO), anti-S-tag (1:5000 dilution in 5% Blotto, Novagen, Darmstadt, Germany), anti-sigma 70 (1:2000 dilution in 1% BSA, NeoClone, Madison, WI), and anti-His tag (1:2000 dilution in 5% Milk, Abcam, Cambridge, MA). Membranes were washed in TBST and incubated for 1 hour at room temperature with Immunopure goat anti-mouse IgG peroxidase conjugated secondary antibody (Thermo Fisher Scientific, Waltham, MA) (for anti-S-tag and anti-sigma 70) or Immunopure goat anti-rabbit IgG peroxidase conjugated secondary antibody (Thermo Fisher Scientific, Waltham, MA) (for anti-Myc). Blots were developed using the SuperSignal West Pico Chemiluminescent Substrate kit or NBT/BCIP kit (Thermo Fisher Scientific, Waltham, MA) and visualized using UVP Biospectrum imaging system (Upland, CA).

To determine the optimal pH of Hip1 cleavage of GroEL2, a series of reactions were set up in buffers containing 50 mM sodium phosphate with 150 mM NaCl at a pH range of 4.26, 4.85, 5.37, 5.65, 5.96, 6.14, 6.69, 6.86, 6.93, 7.16, 7.39, 7.67, 8.05, and 8.64. Initially the buffer for both GroEL2 and Hip1 was switched to 50 mM sodium phosphate pH 7.0 plus 150 mM NaCl. The samples were then concentrated and diluted 1:100 in the appropriate buffer. The samples were incubated for 24 hours at 37°C. Aliquots of the samples were taken and analyzed by Western blotting using mouse anti-S-tag antibody.

Inhibitor profiling of Hip1

Peptide substrate: The effect of protease inhibitors on Hip1 activity was determined by measuring the proteolytic cleavage of Ala-Pro-Ala-*p*Na. Hip1 (4 μM) was pre-incubated with inhibitor for 30 min in 50 mM Tris, pH 8, 25^{o}C and protease activity was measured by the addition of 1.5 mM Ala-Pro-Ala-*p*Na. The final concentrations of the inhibitors were AEBSF (2 mM), PMSF (1 mM), Chymostatin (0.2 mM), Leupeptin (0.4 mM), Antipain (1.0 mM), E-64 (1 mM), Pepstatin (0.3 mM), and EDTA (10 mM) (Sigma-Aldrich, St. Louis, MI)

GroEL2 substrate: Hip1 or Hip1(S228A) (19.8 μM) was added to 6.6 μM of purified recombinant GroEL2 protein and incubated for 24 hours at 37 °C in the presence or absence of the protease inhibitors as follows. Bestatin hydrochloride (Sigma-Aldrich, St. Louis, MI) was resuspended in H_2O to a final concentration 0.3 mM. AEBSF (Sigma-Aldrich, St. Louis, MI) was resuspended in H_2O to a final concentration 1 mM. PMSF (Thermo Scientific, Rockford, IL) was resuspended in methanol to a final concentration of 1 mM. PMSF (Sigma), Bestatin (Sigma) and AEBSF (Fisher) at 1 μM were added to

reaction mixtures containing 1 microgram of recombinant GroEL2 and Hip1. Following the 24 hour incubation at 37°C, one fifth of the reaction was taken for Western blot analysis.

GroEL2 cleavage site identification and LC/MS/MS analysis

To prepare protein samples of GroEL2 and GroEL2(cl) for LC/MS analysis, we made pellet and supernatant fractions (as described above) from wild type *M. tuberculosis.* For dialysis, the protein samples were injected in dialysis cassette with a 2 kDa molecular weight cut-off (Thermo Scientific, Rockford, IL) using 21 gauge 1 inch beveled needle and dialyzed against 400 ml 50 mM ammonium bicarbonate, pH 7.0. After overnight dialysis, the samples were taken out and concentrated using Millipore Amicon ultra 0.5 ml 3 kDa centrifugal filters (Millipore, Billerica, MA). The dialyzed protein samples (20-25 μg) were separated on 10% SDS-PAGE gel. The bands of interest, a blank spot and a BSA band were cut out of the gel and stored in 50 mM ammonium bicarbonate until LC/MS analysis. A synthetic peptide corresponding to the first 19 N-terminal amino acids of GroEL2 (NH_2-AKTIAYDEEARRGLERGLN-OH) was synthesized (Biosynthesis). 1mM of this peptide was incubated either alone, with Hip1 (5 μM), or with Hip1 and the serine protease inhibitor AEBSF in 500 mM Tris, pH 8, 18 hrs, 25^{o}C. Samples were analyzed by LC/MS/MS on an Agilent 1100 binary pump HPLC and Thermo Fisher LTQ XL ion trap mass spectrometer (Stanford University). Samples were diluted with water and the injection volume was 10 uL. The column was a 100 x 2.1 mm Thermo Hypersil Gold C18. The elution profile consisted of initial conditions of 95% A (0.1% formic acid in water)/5% B (0.1% formic acid in acetonitrile) for 1 minute, then a

continuous gradient to 100% B over 17min, then remained at 100% B for 3 minutes at a flow rate of 250 uL/min. Ionization was in positive ESI with mass range 150-1000 m/z. To determine the location of the enzymatic cleavage sites within the 19 amino acid peptide, the program FindPept on the ExPASy server was utilized. FindPept identifies peptides that result from unspecific cleavages of polypeptides from their experimental masses.

Mycobacterial-Protein Fragment Complementation (M-PFC)

The M-PFC plasmids pUAB100 (hyg) and pUAB200 (kan) were a kind gift of Dr. Adrie Steyn, University of Alabama Birmingham and have been previously described [122]. The bait plasmid was constructed by PCR-amplifying *groEL2* from H37Rv genomic DNA using primers 5'- GAT CCGAGATCTGAATCACTTCGCAATGG-3' and 5'-GAAGCCATCGATGAAATCCATGCC ACCCATG-3' and subsequent ligation to *Cla*I/*Bam*HI linearized pUAB100. The prey plasmid was constructed by PCR-amplifying *hip1* and *hip1(S228A)* 5'-AGCCTTGAATTCCGGGTC TGCTCTGGCAGC-3' and 5'-AGCCTTATCGATGCACTTGGCGCCGCTGG-3' and subsequent ligation to *Mun*I/*Cla*I linearized pUAB200. Control plasmids carrying *inhA*, *sigA* or *kdpE* were kindly provided by Dr. Adrie Steyn. The M-PFC bait and prey plasmid constructs were transformed into *M. smegmatis*. Protein-protein interaction between gene products were analyzed by subculturing kan/hyg transformants on 7H11 plates supplemented with 10% ADC glycerol, and 1% Difco yeast extract tryptone medium (Becton Dickenson, Sparks, MD), with the addition of 25 μg/ml kan (Sigma-Aldrich, St. Louis, MO), 50 μg/ml hyg

(Roche Diagnostics, Indianapolis, IN) and 20 μg/ml trimethoprim (Sigma-Aldrich, St. Louis, MO).

Size exclusion chromatography

GroEL2 and Hip1 proteins were concentrated to 30-100 μM and loaded onto a Superdex 200 5/150 GL column (GE Healthcare Life Sciences) equilibrated with 50 mM sodium phosphate pH 7.0 plus 150 mM NaCl. The fractions containing the GroEL2 and Hip1 proteins were collected, concentrated, and incubated together overnight at 37°C to ensure complete cleavage. The reaction mixture was then incubated with Ni^{2+} beads for 1-2 hours at 4°C to allow for binding of the GroEL2 cleaved N-terminal peptide and Hip1 to the beads. The reaction mixture supernatant was then concentrated and injected on the size exclusion column. Elution times of proteins with known molecular weights were used to obtain a standard curve by plotting log of the molecular weight verses K_{av} (partition coefficient). The K_{av} is determined by the equation:

$$K_{av} = (V_e - V_o)/ (V_c - V_o)$$

The elution volume of blue dextran is the value used for the void volume (V_0), V_e is the elution volume of the proteins, and V_c is the geometric column volume, which is determined by the equation:

$$V_c = r^2 \times \pi \times l$$

where r is the radius of the column and l is the column length.

The proteins used to determine the standard curve are Ovalbumin (44 kDa), Conalbumin (75 kDa), Aldolase (158 kDa), Ferritin (440 kDa) and Thyroglobulin (669 kDa),

Carbonic Anhydrase (29 kDa), Ribonuclease A (13.7 kDa), Aprotinin (6.5 kDa). The standard curve was plotted using GraphPad Prism 6.0.

Macrophage infection and cytokine assays

Murine bone marrow derived macrophages (BMM) were generated as previously described [81] Briefly, bone marrow cells from C57BL/6 mice were grown in DMEM/F-12 medium (Lonza) with 10% FBS (HyClone), 2 mM glutamine, 10% L-cell conditioned medium (LCM) for 7 days of differentiation at 37°C with 5% CO_2. For infection, macrophages were plated onto 24-well plates ($3x10^5$ per well). Bacteria were resuspended in DMEM/F-12 medium containing 5% LCM and sonicated twice for 5 seconds each before addition to adherent monolayers. Each bacterial strain was used for infection in triplicate at an MOI=10 and infection of macrophages was carried out for 4 hours as previously described [81]. To determine intracellular CFU, one set of infected macrophages was lysed in PBS containing 0.5% Triton X, and plated onto 7H10 agar plates containing the appropriate antibiotics. For stimulation of macrophages with recombinant proteins, endotoxin-free GroEL2 and GroEL2(cl) in 5% LCM were added to C57BL/6 or $TLR2^{-/-}$ BMM for 24 hours. Cell-free supernatants from macrophage monolayers were isolated at various time points and assayed for cytokines by ELISA kits for IL-6, IL1-β, and TNF-α (R&D Systems, Minneapolis, MN). Assays were carried out according to manufacturer's instructions. Uninfected macrophages were used as controls for each experiment.

Statistical analysis

The statistical significance of data was analyzed using the Student's unpaired t-test (GraphPad Prism 5.0a). Data are shown as mean ± S.D. of one representative experiment from three independent experiments.

Accession numbers

The following GenBank accession numbers correspond to the genes mentioned in this work: H37Rv GroEL2 Gene ID 886354; H37Rv Hip1 Gene ID 887857; H37Rv Ag85B Gene ID 885785; H37Rv KdpE Gene ID 886084; H37Rv InhA Gene ID 886523; H37Rv SigA Gene ID 887477. The following UniProtKB accession number corresponds to H37Rv GroEL2 - P0A520.

Acknowledgements

We gratefully acknowledge Adrie Steyn for providing us with the M-PFC plasmids; Vasanthi Govindu for help with purification of recombinant GroEL2 proteins used for macrophage assays; Shekar Mande for providing us with the GroEL2 plasmid; Sabine Ehrt for providing us with the pTC plasmid. We would like to thank Iva Perovic and Thomas C. Pochapsky for their help with NMR. We thank David Weiss and members of the Rengarajan, Petsko and Ringe labs for helpful discussions and insights.

Author contributions

Conceived and designed the experiments: JR JLNO MG NG RML BMD DR GAP. Performed the experiments: JLNO MG NG JR RML LD EV EB GSB SY DES. Analyzed

the data: JR JLNO MG NG RML. Contributed reagents/materials/analysis tools: JR GAP BMD. Wrote the paper: JR JLNO NG MG.

Figure 1. Purification of Hip1 and Hip1(S228A) by ion exchange chromatography. (A) and (B) Hip1 and Hip1(S228A) proteins were purified by gravity column chromatography and anion exchange chromatography. Top and bottom panels show the anion exchange column elution peak profiles of recombinant Hip1 and Hip1(S228A) respectively. The purity of the eluted protein was checked by SDS-PAGE analysis after each purification procedure. The arrows indicate the elution fractions used in subsequent assays: B6 for Hip1 and A12 for Hip1(S228A). (C) CD spectra of Hip1 and Hip1(S228A) mutant.

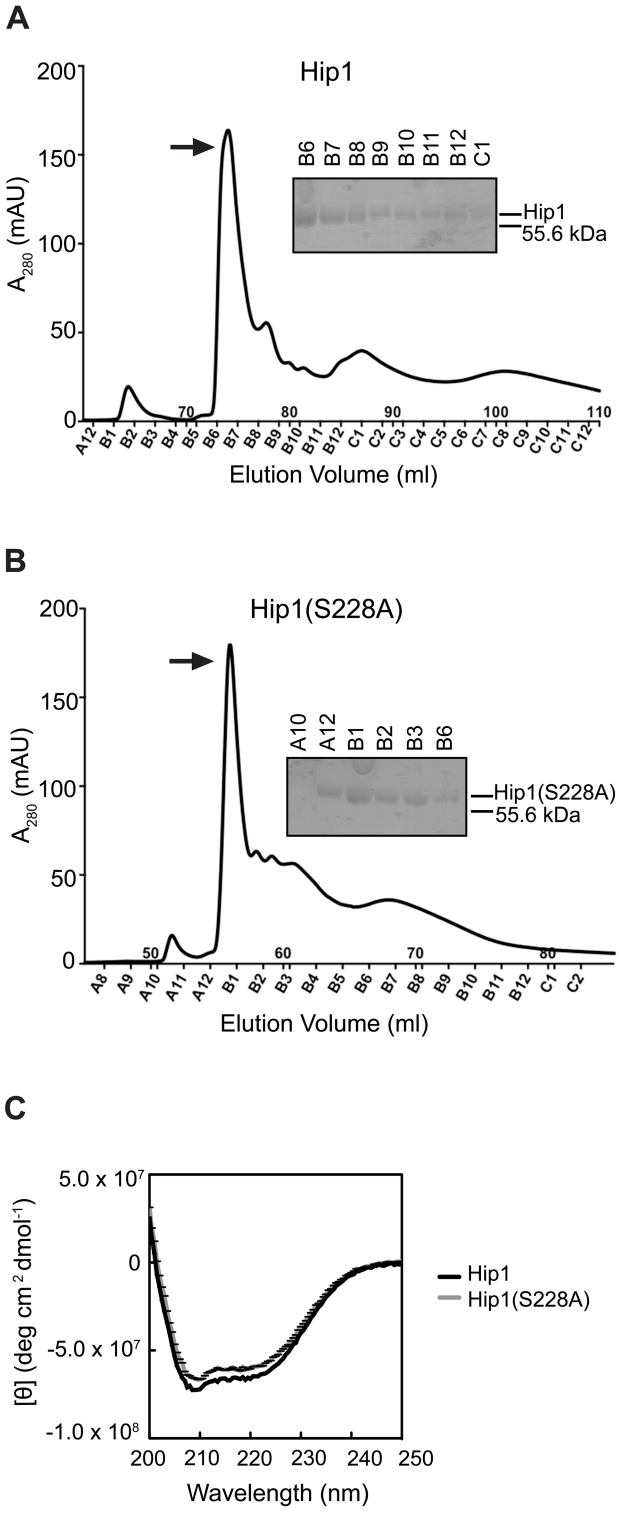
A
Hip1
200
150
100
50
0
A280 (mAU)
B6 B7 B8 B9 B10 B11 B12 C1
Hip1
55.6 kDa
70
80
90
100
110
A12 B1 B2 B3 B4 B5 B6 B7 B8 B9 B10 B11 B12 C1 C2 C3 C4 C5 C6 C7 C8 C9 C10 C11 C12
Elution Volume (ml)
B
Hip1(S228A)
200
150
100
50
0
A280 (mAU)
A10 A12 B1 B2 B3 B6
Hip1(S228A)
55.6 kDa
50
60
70
80
A8 A9 A10 A11 A12 B1 B2 B3 B4 B5 B6 B7 B8 B9 B10 B11 B12 C1 C2
Elution Volume (ml)
C
5.0 x 10^7
0
-5.0 x 10^7
-1.0 x 10^8
[θ] (deg cm^2 dmol^-1)
200 210 220 230 240 250
Wavelength (nm)
Hip1
Hip1(S228A)

Figure 2. Analysis of the enzymatic activity of Hip1. (A) Hip1 esterase activity with *p*-nitrophenylbutyrate. *P*-nitrophenylbutyrate was incubated alone for a negative control reaction (-control). PreScission protease was used in a positive control reaction (+ control). (B) Azocasein proteolysis assay showing that Hip1 is a protease. Azocasein was incubated alone (- control), with the protease subtilisin (+control), with Hip1 (0.05 mg/ml), or Hip1(S228A) (0.05 mg/ml) in 25 mM Tris pH 7.4, 150 mM NaCl. The enzyme activities are expressed as units of enzyme/mg protein (one enzyme unit is the quantity of enzyme required to increase absorbance by 0.01 units at 440 nm). (C) Endpoint assay showing proteolytic activity of Hip1. Hip1 (7.5 μM) was incubated with each peptide substrate (1.5 mM) or alone (-control) in 50 mM Tris pH 8.0 for 18 hr at 25°C. Elastase was used as a positive control (+ control). Hydrolysis of the peptide substrates was detected by monitoring an increase in absorbance at 410 nm. (D) Inhibition of Hip1 with various classes of protease inhibitors. Hip1 (4 μM) was pre-incubated with inhibitor for 30 min in 50 mM Tris, pH 8.0 at 25°C. Then, protease activity was measured by the addition of 1.5 mM Ala-Pro-Ala-*p*Na. The specific activity of Hip1 against Ala-Pro-Ala-*p*Na was defined as 100% (no inhibitor). Data are shown as one representative experiment from three independent experiments.

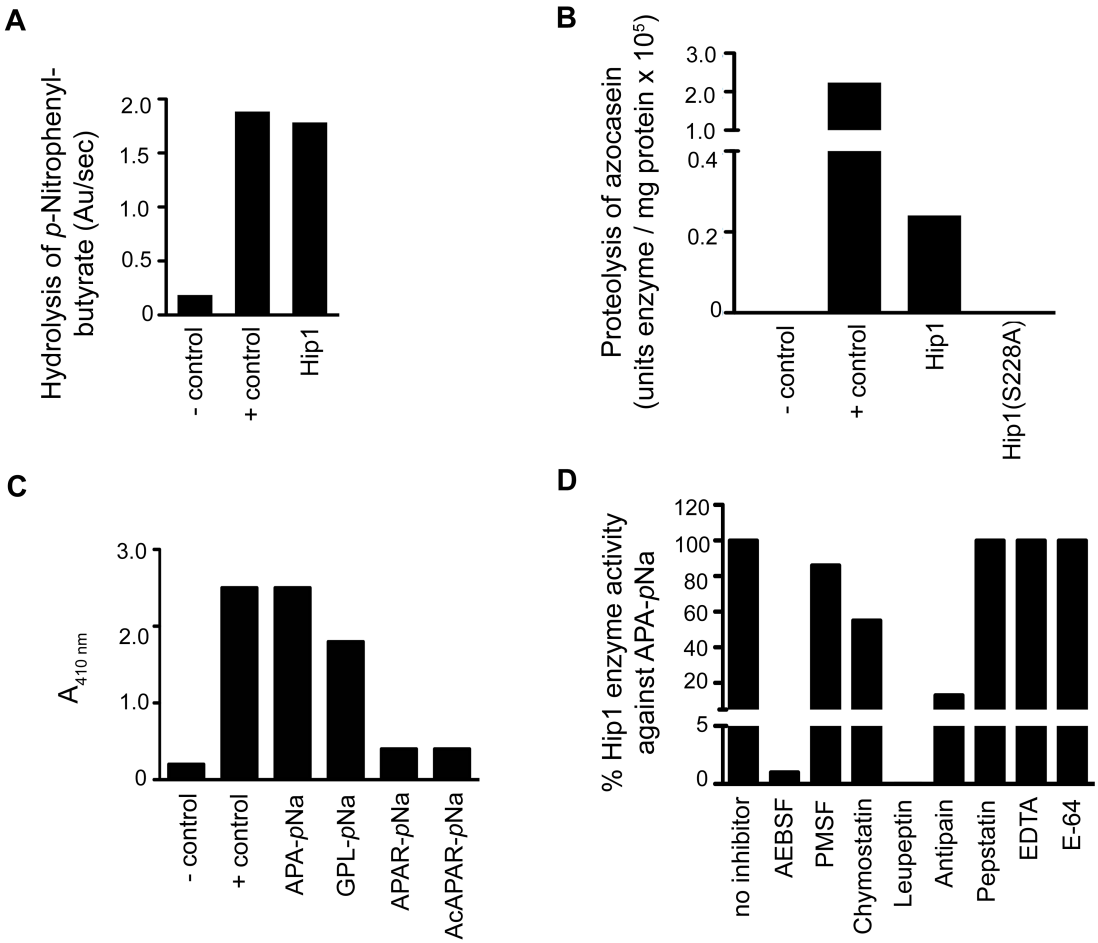
A
Hydrolysis of p-Nitrophenyl-butyrate (Au/sec)
2.0
1.5
1.0
0.5
0
- control
+ control
Hip1
B
Proteolysis of azocasein (units enzyme / mg protein x 10^5)
3.0
2.0
1.0
0.4
0.2
0
- control
+ control
Hip1
Hip1(S228A)
C
A410 nm
3.0
2.0
1.0
0
- control
+ control
APA-pNa
GPL-pNa
APAR-pNa
AcAPAR-pNa
D
% Hip1 enzyme activity against APA-pNa
120
100
80
60
40
20
5
0
no inhibitor
AEBSF
PMSF
Chymostatin
Leupeptin
Antipain
Pepstatin
EDTA
E-64

Figure 3. *M. tuberculosis* GroEL2 is a physiological substrate of Hip1 protease activity. (A) Recombinant GroEL2 is cleaved by recombinant Hip1 but not by Hip1(S228A). Samples from the cleavage reactions were taken at 0 hours and 24 hours, separated by 10% SDS-PAGE gel and analyzed by Western blot with anti-S-tag antibody to detect GroEL2 and GroEL2(cl). (B) Hip1 mediated cleavage of GroEL2 is inhibited by the serine protease inhibitor AEBSF. Recombinant GroEL2 was incubated with recombinant Hip1 for 24 hours at 37°C either alone or in the presence of inhibitors AEBSF, PMSF, or bestatin. Samples were taken after 24 hours, separated by 10% SDS-PAGE gel and analyzed by Western blot with anti-S-tag antibody to detect GroEL2 and GroEL2(cl). (C) Optimal pH range for GroEL2 cleavage. Recombinant GroEL2 was incubated with recombinant Hip1 for 24 hours at 37°C under varying pH conditions. (D) Protein-protein interaction between GroEL2 and Hip1. Mycobacterium protein fragment complementation (M-PFC) assay demonstrates interaction between *M. tuberculosis* GroEL2 and Hip1 expressed in *M. smegmatis* as shown by growth on plates containing trimethoprim. *M. smegmatis* strain expressed either GCN4 homo-dimerization domains of *Saccharomyces cerevisiae* (positive control); GroEL2 and Hip1; GroEL2 and Hip1(S228A) or negative controls: vector and Hip1; vector and Hip1(S228A); GroEL2 alone; GroEL2 and KdpE; GroEL2 and SigA; GroEL2 and InhA. Data (A-D) are shown as one representative experiment from three to five independent experiments.

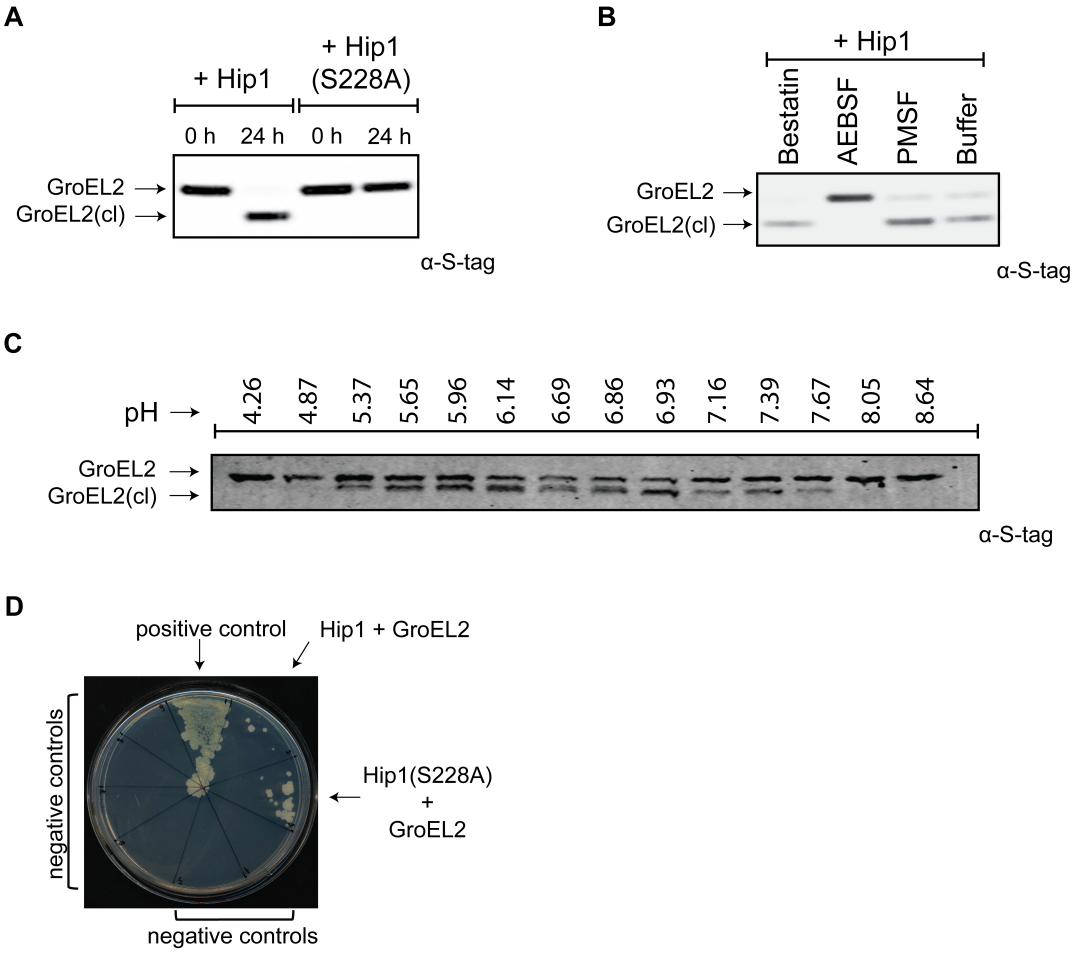
A
+ Hip1
+ Hip1
(S228A)
0 h
24 h
0 h
24 h
GroEL2
GroEL2(cl)
α-S-tag
B
+ Hip1
Bestatin
AEBSF
PMSF
Buffer
GroEL2
GroEL2(cl)
α-S-tag
C
pH
4.26
4.87
5.37
5.65
5.96
6.14
6.69
6.86
6.93
7.16
7.39
7.67
8.05
8.64
GroEL2
GroEL2(cl)
α-S-tag
D
positive control
Hip1 + GroEL2
negative controls
Hip1(S228A)
+
GroEL2
negative controls

Figure 4. GroEL2 is cleaved *in vitro* and *in vivo* by Hip1. (A) LC/MS/MS showing elution of the uncleaved GroEL2 N-terminal peptide (*m/z* = 2163). (B) LC peak profile of GroEL2 N-terminal peptide incubated with Hip1 for 18 hours at 25°C. Two abundant product fragments with *m/z* = 1122 and 757 indicate cleavages between $Thre_3$ and Ile_4, as well as between Arg_{12} and Gly_{13}. (C) AEBSF inhibits Hip1 cleavage of the GroEL2 peptide. (D) Mass spectrometry analysis of the 7.3 min peak in (C) indicates the predominant species is uncleaved GroEL2. The second peak corresponds to substrate sulfonated by AEBSF at threonine. (E) Determining cleavage site of *M. tuberculosis* GroEL2 using *M. smegmatis*. Culture supernatants from *M. smegmatis* strains expressing *M. tuberculosis* GroEL2-FLAG, GroEL2 (R12P)-FLAG or GroEL2 (R12P G13P)-FLAG were subjected to cleavage by recombinant Hip1 for 24 hours at 37°C and analyzed by Western blot. (F) Cleavage site of GroEL2 in *M. tuberculosis*. GroEL2-FLAG or GroEL2 (R12P G13P)-FLAG mutant were expressed in *M. tuberculosis* H37Rv. Protein extracts corresponding to the pellet (P) and supernatant (S) fractions of those strains were prepared, and analyzed by Western blot with anti-FLAG antibody (to detect GroEL2) and anti-SigA antibody (to detect the sigma 70 subunit of RNA polymerase). Data (A-F) are shown as one representative experiment from three independent experiments.

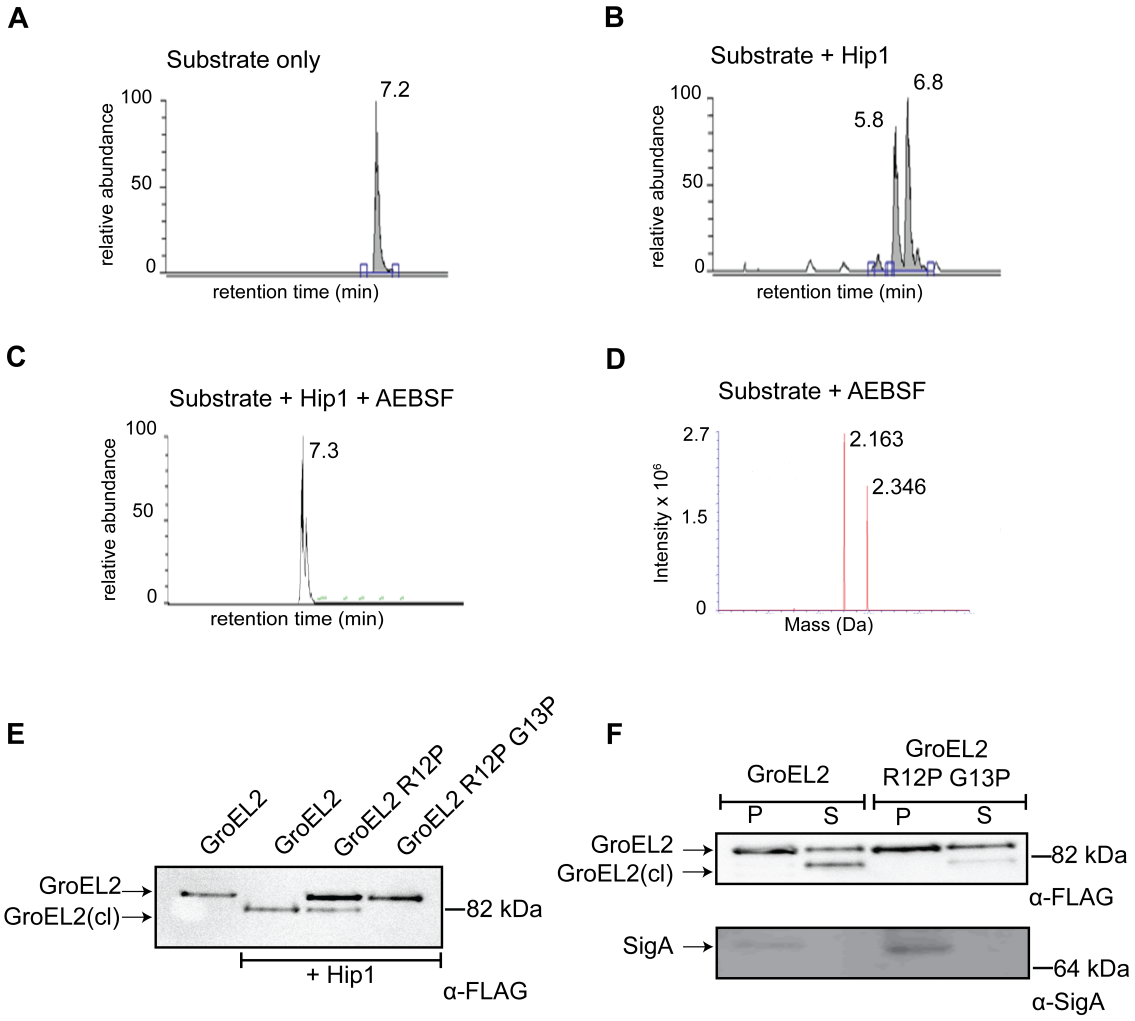
A
Substrate only
7.2
100
50
0
relative abundance
retention time (min)
B
Substrate + Hip1
6.8
5.8
100
50
0
relative abundance
retention time (min)
C
Substrate + Hip1 + AEBSF
7.3
100
50
0
relative abundance
retention time (min)
D
Substrate + AEBSF
2.163
2.346
2.7
1.5
0
Intensity x 10^6
Mass (Da)
E
GroEL2
GroEL2
GroEL2 R12P
GroEL2 R12P G13P
GroEL2
GroEL2(cl)
82 kDa
+ Hip1
α-FLAG
F
GroEL2
GroEL2 R12P G13P
P
S
P
S
GroEL2
GroEL2(cl)
82 kDa
α-FLAG
SigA
64 kDa
α-SigA

Figure 5. GroEL2 is a multimer *in vitro* and is converted to a monomer following cleavage by Hip1. (A) Size exclusion chromatograms of recombinant full length GroEL2, cleaved GroEL2 and Hip1. (B) Standard curve based on the elution profiles of a set of standard molecular weight marker proteins. The logarithms of the molecular weights (log M_r) were plotted as a function of K_{av}. Data are shown as one representative experiment from three independent experiments.

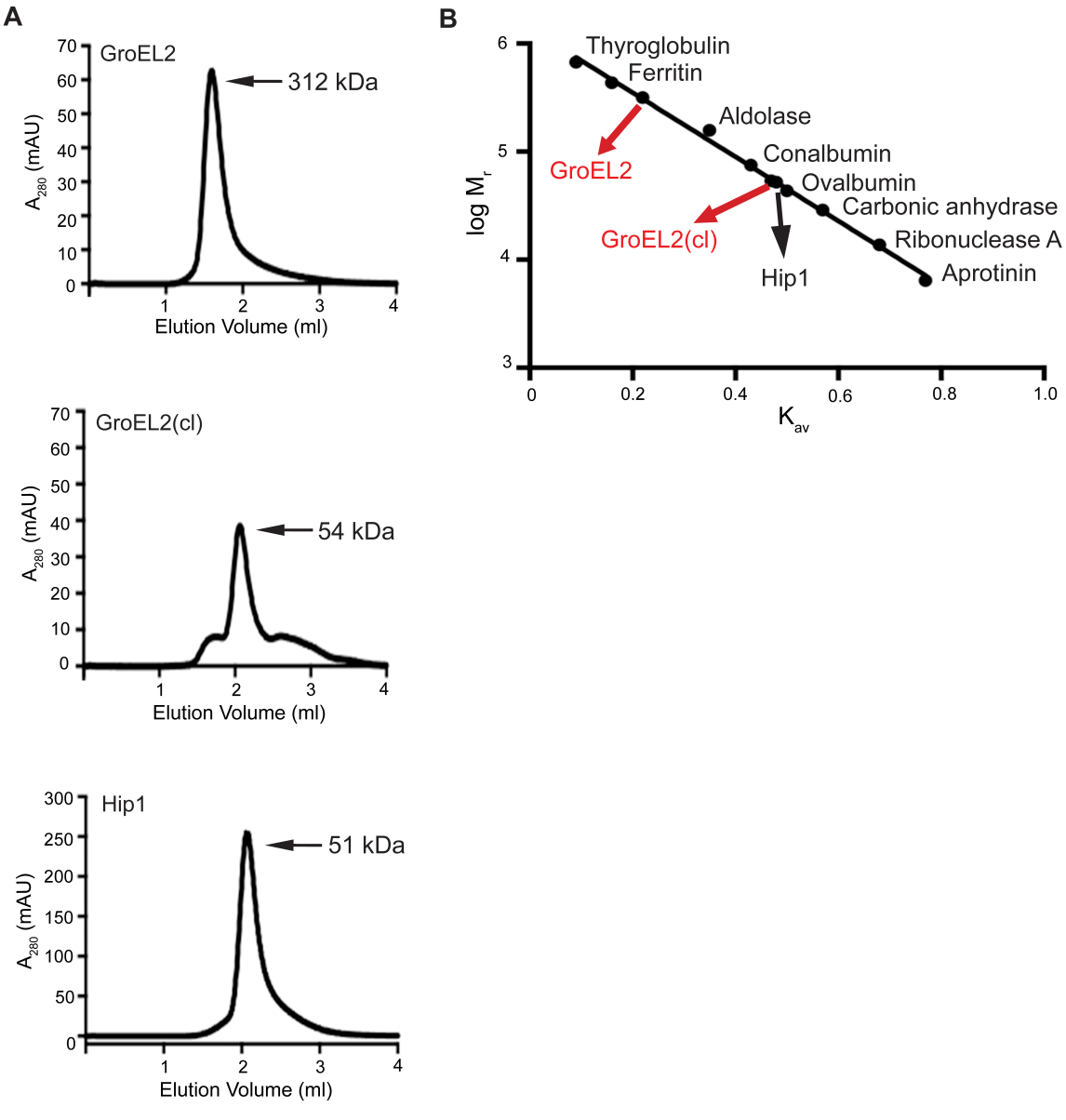

Figure 6. Expression of secreted GroEL2(cl) in *hip1* mutant restores wild type levels of proinflammatory cytokine responses in macrophages. Production of IL-6, IL-1β, and TNF-α by C57BL/6 bone marrow derived macrophages (BMM) 24 hours after infection with wild type, *hip1* mutant, and *hip1* mutant complemented with either Hip1 (comp) or GroEL2(cl). Data are shown as mean ± S.D. of one representative experiment from three independent experiments.

**, $P < 0.05$; **, $P < 0.01$.*

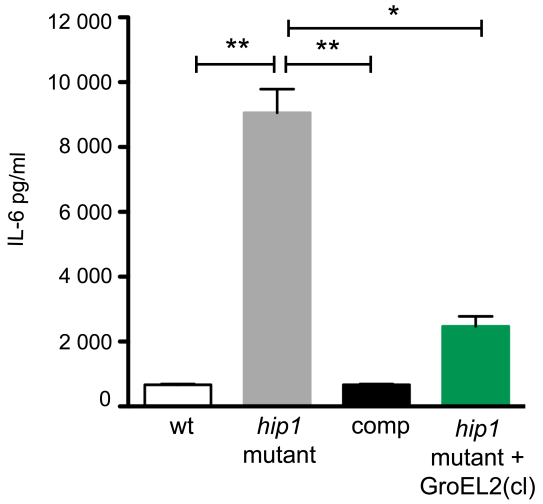
12 000
10 000
8 000
6 000
4 000
2 000
0
IL-6 pg/ml
**
**
*
wt
hip1 mutant
comp
hip1 mutant + GroEL2(cl)

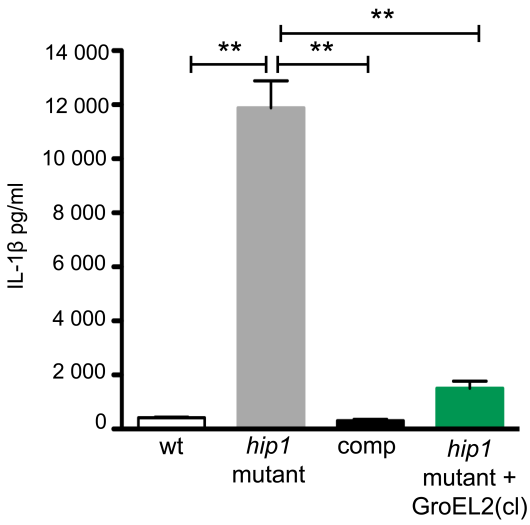
14 000
12 000
10 000
8 000
6 000
4 000
2 000
0
IL-1β pg/ml
**
**
**
wt
hip1 mutant
comp
hip1 mutant + GroEL2(cl)

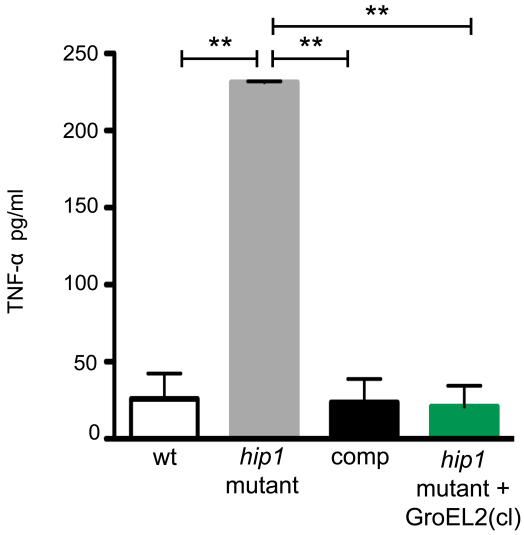
250
200
150
100
50
0
TNF-α pg/ml
**
**
**
wt
hip1 mutant
comp
hip1 mutant + GroEL2(cl)

Figure 7. Differential stimulation of proinflammatory cytokine production from macrophages by GroEL2 and GroEL2(cl). (A) Production of IL-6 and IL-1β by C57BL/6 bone marrow derived macrophages (BMM) 24 hours after stimulation with GroEL2 or GroEL2(cl). (B) Production of IL-6 and IL-1β in response to GroEL2 and GroEL2(cl) occurs in a partially TLR2-dependent manner. (C) Presence of GroEL2(cl) leads to diminished stimulatory capacity of GroEL2. Each form of GroEL2 was added to C57BL/6 BMM either alone (5 μM) or together (5 μM each) for 24 hours. The expected additive effect of GroEL2 and GroEL2(cl) is represented as a sum of the cytokine levels for each protein alone. Data are shown as mean ±S.D. of one representative experiment from three independent experiments. **, $P < 0.05$; **, $P < 0.01$.*

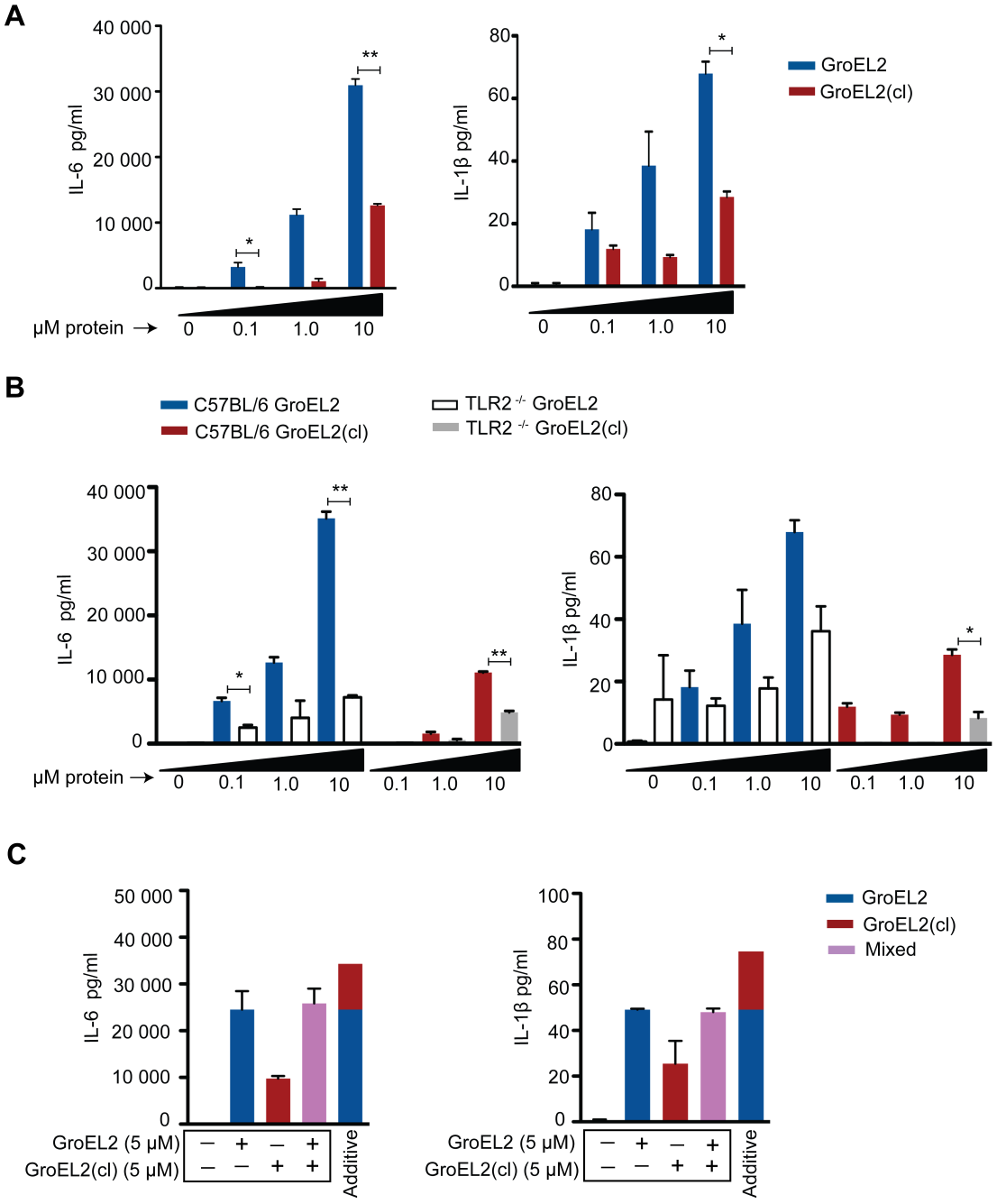
A
IL-6 pg/ml
40 000
30 000
20 000
10 000
0
IL-1β pg/ml
80
60
40
20
0
GroEL2
GroEL2(cl)
μM protein →
0
0.1
1.0
10
B
C57BL/6 GroEL2
C57BL/6 GroEL2(cl)
TLR2 -/- GroEL2
TLR2 -/- GroEL2(cl)
C
50 000
40 000
30 000
20 000
10 000
100
80
60
40
Mixed
GroEL2 (5 μM)
GroEL2(cl) (5 μM)
Additive

Figure 8. Model of Hip1-GroEL2 interactions. Proteolysis of full length GroEL2 by Hip1 converts multimeric GroEL2 to monomers. In the cell wall of wild type *M. tuberculosis*, GroEL2 multimer interacts with the Hip1 protease, which cleaves GroEL2 and leads to release of GroEL2 monomers extracellularly. In contrast, in the *hip1* mutant, GroEL2 remains in its multimeric form and is released extracellularly as a multimer.

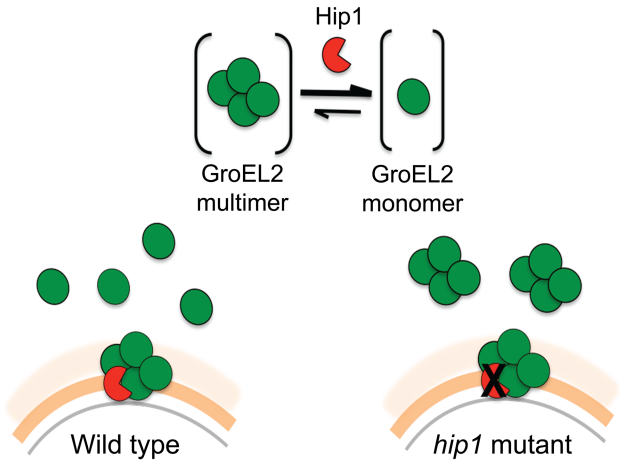

Supporting Figure S1.

Western blots of cleavage reaction samples indicating separation of Hip1 protein (via Ni^{2+} beads) from cleaved GroEL2 for analysis by size exclusion chromatography. (A) Western blot using anti-S-tag antibody detects the presence of GroEL2(cl) in the cleavage reaction sample (Lane 2), and shows that GroEL2(cl) is absent in the protein fraction bound to Ni^{2+} beads (Lane1). (B) Western blot using anti-His antibody shows the presence of Hip1 protein in the Ni^{2+} bead-bound fraction (Lane 1), and its absence in the cleavage reaction following Ni^{2+} beads depletion (Lane 2).

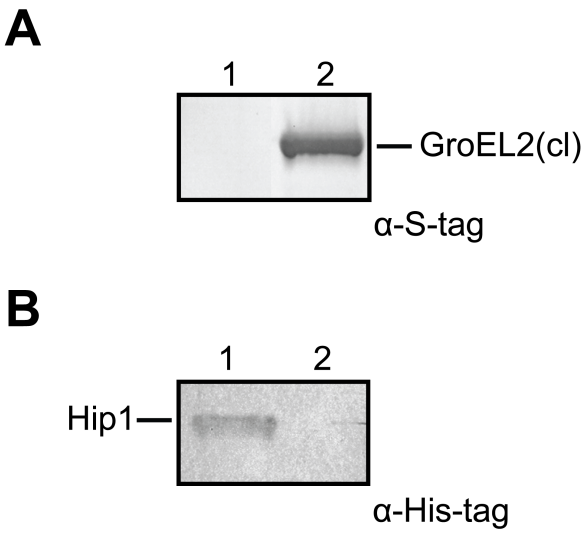

Supporting Figure S2.

(A) Western blot demonstrating presence of GroEL2(cl) in the pellet (P) and supernatant (S) fractions of a *hip1* mutant strain complemented with GroEL2(cl) with a C-terminal Myc tag.

(B) Western blot demonstrating levels of endogenous GroEL2 and GroEL2(cl) in supernatant fractions of wild type, *hip1* mutant, and *hip1* mutant complemented with either Hip1 (comp) or GroEL2(cl).

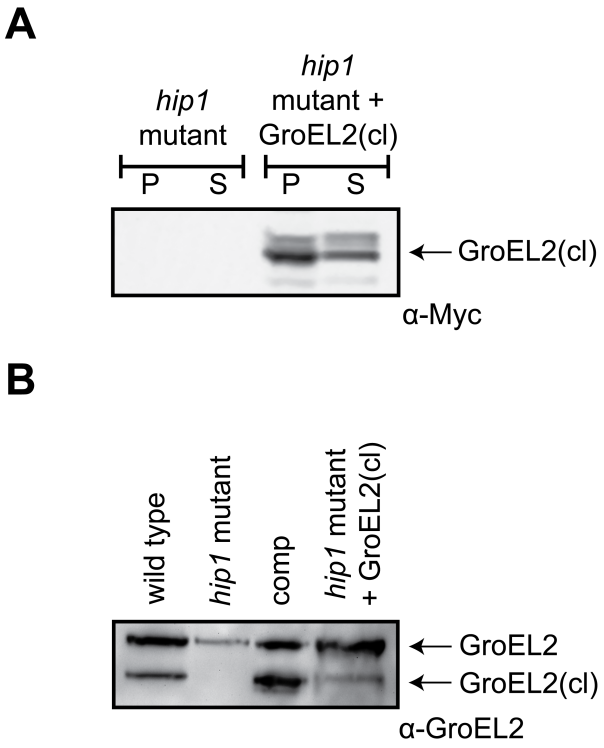

Chapter 3

Modulation of dendritic cell responses through cleavage of *Mycobacterium tuberculosis* GroEL2

Note: Chapter 3 is adapted from a manuscript currently under preparation with the following authorship:

Georgieva M, Sia JK, Madan-Lala R, Rengarajan J.

Abstract

Mycobacterium tuberculosis successfully subverts the host immune response to promote disease progression. In addition to its known intracellular niche in macrophages, recent studies have demonstrated the ability of *Mycobacterium tuberculosis* to interfere with the functions of dendritic cells (DCs), which are the primary antigen presenting cells in the immune system. A recent report from our lab showed that *M. tuberculosis* impairs DC maturation and prevents antigen presentation through the envelope-associated serine protease, Hip1. Here we present data showing that Hip1-mediated proteolysis of the *M. tuberculosis* GroEL2 protein modulates DC functions. While full-length GroEL2 protein induced robust DC responses *in vitro*, the cleaved form of GroEL2 led to attenuated production of proinflammatory cytokines from DCs and was unable to promote DC maturation and antigen presentation to T cells. Our studies suggest that cleavage of GroEL2 is an immunoregulatory mechanism that allows *M. tuberculosis* to fine-tune and moderate the host immune response during infection.

Introduction

Mycobacterium tuberculosis has evolved multiple mechanisms to manipulate its cellular niche within the host. While this pathogen primarily resides in host macrophages, there is increasing evidence that *M. tuberculosis* interferes with the ability of dendritic cells (DCs) to initiate antigen-specific T cell responses to infection [9,47]. DCs are the primary antigen presenting cells (APCs) in the immune system and play a central role in activation and differentiation of T cells by presenting antigenic peptides. DCs secrete specific cytokines that are important for T helper (Th) cell differentiation and polarization into Th subsets, and chemokines that direct their migration from tissue sites to lymph nodes [47]. Uptake of microbes by DCs results in their maturation as characterized by high surface expression of major histocompatibility class II (MHC II), co-stimulatory markers such as CD40, CD86, CD80, and secretion of Th1 polarizing cytokines such as IL-12. Recent studies have demonstrated that *M. tuberculosis* infects human and mouse DCs at high frequencies, interferes with DC migration from lungs to the draining lymph nodes and inhibits antigen presentation to T cells [3,9,45,123,124]. However, the *M. tuberculosis* factors that impair DC functions are not well understood.

Recently, our laboratory has shown that *M. tuberculosis* cell wall-associated protease Hip1 is involved in impairing DC functions [125]. Compared to wild type *M. tuberculosis*, a *hip1* mutant strain of *M. tuberculosis* induced enhanced levels of IL-12 and other proinflammatory cytokines in DCs, indicating that Hip1 limits optimal DC activation and inflammatory responses. Infection with the *hip1* mutant also resulted in

higher levels of the co-stimulatory molecules CD40, CD86, and MHC class II and increased antigen presentation to $CD4^+$ T cells, indicating that *M. tuberculosis* impairs DC functions through Hip1 [125]. We previously reported that the Hip1 manipulates the innate-adaptive immune axis by dampening macrophage responses [81]. Molecular and biochemical studies revealed that Hip1 dampens macrophage responses through proteolysis of a target substrate, GroEL2. While GroEL2 shares some features with chaperone proteins of the GroEL family, the true function of *M. tuberculosis* GroEL2 remains unclear. GroEL2 expression is induced by multiple stresses, including heat-shock, oxidative stress, growth in macrophages and hypoxia [117,126,127]. Importantly, multiple groups have previously demonstrated that full-length, recombinant GroEL2 induces cytokine responses in macrophages, suggesting the immunostimulatory functions of GroEL2 may play an important role in modulating host responses during *M. tuberculosis* infection [90,92,128]. Interestingly, we showed that Hip1 cleaves GroEL2 in its N-terminus and converts the full-length multimeric protein to a monomeric form. Moreover, the cleaved form of GroEL2, which we have termed GroEL2(cl), is the predominant form present in wild type *M. tuberculosis*. Further, we showed that full-length recombinant GroEL2 protein is significantly more immunostimulatory to macrophages compared to GroEL2(cl), suggesting that Hip1-mediated cleavage of the N-terminus abrogates the ability of GroEL2 to induce cytokine responses during infection.

Based on the identified role of Hip1 in impairing DC functions and in processing GroEL2, we hypothesized that Hip1-dependent proteolysis of GroEL2 contributes to the ability of *M. tuberculosis* to impair DCs and influences the development of antigen-specific Th

responses. Importantly, since the cleaved form of GroEL2(cl) is the dominant form in wild type *M. tuberculosis*, we sought to investigate the roles of full-length GroEL2 versus GroEL2(cl) in modulating DC functions during *M. tuberculosis* infection.

Results

Dendritic cells exposed to full-length GroEL2 induce higher levels of IL-12 and IL-6 compared to cleaved GroEL2

We first compared the ability of GroEL2 and GroEL2(cl) to induce the proinflammatory cytokines IL-12 and IL-6 (Figure 1). IL-12 is a major polarizing cytokine that drives the development of naïve $CD4^+$ T cells into IFN-γ producing Th1 cells, which are required for controlling *M. tuberculosis* infection. We exposed bone marrow-derived dendritic cells (BMDC) from C57BL/6 mice to varying concentrations of full-length GroEL2 and GroEL2(cl) and measured levels of IL-12p40 and IL-6 in the supernatants after 24 hours. The levels of endotoxin in the protein preparations were investigated and determined to be below detection levels (data not shown). Full-length GroEL2 induced high levels of both IL-12p40 and IL-6 in BMDCs at each time point. In contrast, GroEL2(cl) was unable to induce production of these two cytokines above background levels at all concentrations of the protein tested. We did not detect any IL-10 under the conditions tested (data not shown). These data indicate that full-length GroEL2 has the capacity to induce proinflammatory cytokine production in DCs but that cleavage of GroEL2 by Hip1 abrogates these functions. Thus, the ability of *M. tuberculosis* to modulate DC cytokine production may in part, be due to Hip1-dependent proteolysis of GroEL2.

Expression of co-stimulatory molecules on DCs in response to full-length GroEL2 and GroEL2(cl)

DCs are ideally poised to capture antigens at the site of infection, which in turn induces the maturation of DCs, a pivotal step in initiating antigen-specific immune responses. Following migration to lymph nodes, DCs prime T cells through cell surface expression of co-stimulatory molecules such as CD40 and CD86, which interact with their ligands on T cells to optimally induce T cell activation. To determine whether GroEL2 affects DC maturation, we exposed BMDCs to either full-length or GroEL2(cl), and measured the expression of CD40, CD86 and MHC class II on the cell surface by flow cytometry. Full-length GroEL2, induced robust expression of each of these markers (Figure 2), however, GroEL2(cl) induced significantly lower levels of CD40 and CD86. Under these conditions, neither form of GroEL2 induced further expression of MHC class II above baseline. Overall, these data indicate that cleavage of GroEL2 blunts its capacity to induce maturation of DCs.

***M. tuberculosis* GroEL2, but not GroEL2(cl), promotes DC antigen presentation**

DCs take up antigen to present it to naïve T cells, an essential step for the activation of antigen-specific T cell responses. Both cytokine production and the expression of cell surface co-stimulatory markers by dendritic cells are required for effective T cell activation. Based on our observation of differential production of proinflammatory cytokines and expression of co-stimulatory markers in response to GroEL2 and GroEL2(cl), we sought to test whether cleavage of GroEL2 impacted antigen presentation to naïve antigen-specific $CD4^+$ T cells. We first pulsed with $OVA_{323-339}$ peptide and then

exposed DCs to full-length or cleaved GroEL2 for 24 hours. We then co-cultured with TCR-Tg $CD4^+$ T cells isolated from OT-II mice and specific for the $OVA_{323-339}$ peptide. We collected supernatants 72 hours after co-culture and assayed for IFN-γ and IL-2 by ELISA, cytokines indicative of antigen-specific T cell proliferation (Figure 3A). While the presence of full length GroEL2 promoted presentation of $OVA_{323-339}$ peptide as evidenced by IFN-γ and IL-2 production, we found that the physiologically relevant cleaved GroEL2, was unable to promote antigen presentation by DCs (Figure 3B), suggesting that cleavage of GroEL2 attenuates the antigen presentation capacity of M. tuberculosis-infected DCs.

Hip1-mediated cleavage of *M. tuberculosis* GroEL2 modulates DC responses

We have previously shown that wild type *M. tuberculosis* induces sub-optimal DC responses while infection with the *hip1* mutant results in robust DC cytokine production, expression of co-stimulatory molecules and antigen presentation. In this study, we use purified recombinant full length and cleaved forms of GroEL2 protein and show that cleavage of GroEL2 is a potential mechanism by which *M. tuberculosis* blunts DC responses. To directly investigate whether Hip1-dependent cleavage of GroEL2 contributes to impaired DC functions during *M. tuberculosis* infection, we ectopically expressed cleaved GroEL2 in the *hip1* mutant background and analyzed DC responses following infection with this complemented strain (Figure 4). We infected BMDCs with either wild type, *hip1* mutant or the complemented *M. tuberculosis* strains and compared their ability to elicit the production of IL-12p40 and IL-6 (Figure 4). Consistent with our previous reports, the *hip1* mutant induced significantly higher levels of these

proinflammatory cytokines compared to wild type *M. tuberculosis*. Importantly, expression of GroEL2(cl) in the *hip1* mutant background restored wild type levels of these cytokines in infected DCs. Thus, these data suggest that the absence of full-length GroEL2 in wild type *M. tuberculosis* results impairs DC activation. Furthermore, we predict that GroEL2 cleavage also regulates maturation and antigen presentation of *M. tuberculosis*-infected DCs and impacts subsequent pathogenesis and disease progression *in vivo*. Studies are currently ongoing to address these questions in the context of the whole bacterium by using our engineered *hip1* mutant strain complemented with GroEL2(cl). In summary, our data highlight a novel role for Hip1-mediated proteolysis of GroEL2 in modulating DC and T cell responses in tuberculosis.

Discussion

The data here demonstrate that *M. tuberculosis* modulates DC functions via Hip1-dependent GroEL2 proteolysis. Specifically, we show that GroEL2 regulates DC functions such as production of proinflammatory cytokines, expression of co-stimulatory molecules and antigen presentation. Our findings are consistent with previously published data on the immunostimulatory capacity of full-length GroEL2 in macrophages. Importantly, we now extend these studies to include the physiologically relevant, cleaved form of GroEL2 and provide insight into the role of GroEL2 during *M. tuberculosis* infection of DCs.

Early after inhalation of *M. tuberculosis*, within the host, macrophages and dendritic cells become the primary intracellular niche for the bacilli. Although the ability of *M. tuberculosis* to interfere with macrophage responses is well established, the mechanisms that *M. tuberculosis* employs to abrogate DC functions are largely uncharacterized [123,124,129]. Our previously published studies addressed this inquiry and revealed a novel mechanism of DC modulation via the *M. tuberculosis* protease Hip1. While these studies implicated Hip1 proteolytic activity as a key contributor to immune modulation during DC infection, the molecular mechanisms driving this process remained unclear. We previously showed that the Hip1 substrate, *M. tuberculosis* GroEL2 protein, is an important component of Hip1-dependent modulation of macrophage functions. Based on these data, we hypothesized the involvement of GroEL2 in modulation of the innate-adaptive immune axis at the DC interface. In order to investigate this hypothesis, we

undertook focused studies to characterize the immunomodulatory capacity of GroEL2 in the context of DC infection and DC-T cell co-culture.

It is important to consider the GroEL2-related studies here within the framework of previously published findings about the putative biological role of GroEL2. Interestingly, GroEL2 is highly induced in response to environmental cues during infection such as heat shock, oxidative stress, growth in macrophages and hypoxia [130,131]. Furthermore, recombinant full-length GroEL2 is immunostimulatory, and induces cytokine responses from macrophages in a TLR2- and TLR4-dependent manner, suggestive of a likely meaningful biological role for GroEL2 during *M. tuberculosis* infection [93]. GroEL2 is also one of the most abundant *M. tuberculosis* proteins *in vivo* and a dominant contributor to the potent immune response elicited by *M. tuberculosis* Purified Protein Derivative (PPD) [120,132]. Some studies suggest that cell wall-associated full-length GroEL2 protein has adhesion-like properties important for the interaction between *M. tuberculosis* and macrophages. Curiously, comparative studies show that *Mycobacteria* are unusual among bacteria in possessing two GroEL proteins, the cytoplasmic protein GroEL1, which is highly homologous to the *E. coli* GroEL chaperonin, and GroEL2. GroEL2 is localized to the cell envelope and secreted extracellularly, and its functions appear to be more diverse [133,134]. While GroEL2 exhibits only weak ATPase activity *in vitro* and therefore does not behave as a canonical chaperone, the GroEL2 crystal structure suggests that it may still assist in protein folding or antigen presentation [115]. All the previous studies described here were conducted with full-length GroEL2, thereby leaving the role of the biologically relevant, cleaved form of GroEL2 completely unexplored.

Using our insight into the Hip1-dependent cleavage of GroEL2 in *M. tuberculosis*, our study is the first to investigate the importance of GroEL2 proteolysis and the biological role of cleaved GroEL2 at the DC - *M. tuberculosis* interface.

Using purified recombinant full-length and cleaved GroEL2, we show that proteolysis of GroEL2 abrogates its immunostimulatory capacity, i.e., its ability to elicit production of key cytokine mediators such as IL-12 and IL-6. These studies suggest that *M. tuberculosis* limits optimal DC activation via Hip1-dependent proteolytic cleavage of its physiological substrate GroEL2. The proinflammatory cytokines IL-12 and IL-6 are key mediators of host innate immunity and dampening these responses can significantly impact both disease pathogenesis and the critical balance of protective versus damaging immune responses [4]. This concept is illustrated by data from infections with the hypervirulent *M. tuberculosis* Beijing clinical isolates. These highly virulent strains induce significantly less IL-6 and IFN-γ compared to the H37Rv reference strain [135]. Such findings imply that blunting proinflammatory cytokine production is a probable mechanism for promoting impaired anti-mycobacterial immunity. Thus, it is likely that during DC infection, *M. tuberculosis* has also evolved to restrict the magnitude of inflammatory responses via GroEL2 proteolysis as a way to delay or subvert adaptive immunity and thereby gain selective advantage within the host. Within this conceptual framework, we speculate that GroEL2 proteolysis has evolved as a modulator of anti-mycobacterial host immunity.

In response to proinflammatory cytokines, DCs undergo maturation and rapidly upregulate cell surface-associated co-stimulatory molecules such as CD40 and CD86 [46]. In our study, we report significantly reduced expression of both CD40 and CD86 in the presence of cleaved GroEL2 compared to full-length protein. Moreover, the antigen presentation capacity of DCs to TCR-Tg $CD4^+$ T cells was enhanced in the presence of the full-length but not cleaved GroEL2, suggesting that in the context of DC interactions with *M. tuberculosis,* secreted GroEL2(cl) blunts the magnitude of antigen-specific T cell responses and promotes an overall subdued early immune response. Utilizing a wild type, *hip1* mutant and a complemented *hip1* mutant *M. tuberculosis* strains, previously well characterized in our lab, we found that ectopic expression of cleaved GroEL2 in the *hip1* mutant background strain restored its hyperinflammatory phenotype back to wild type levels. These results support our previous reports about the physiological relevance of GroEL2 cleavage for innate immunity and extend our appreciation for the importance of this process for DC-T cell responses. We are currently performing live infections using these same strains to analyze how DC maturation and antigen presentation are affected *in vitro* and *in vivo* in the mouse model. Overall, our current findings linking GroEL2 proteolysis to poor *M. tuberculosis* induction of IL-12, IL-6, low CD40, CD86 expression and sub-optimal antigen presentation, suggest a novel strategy of *M. tuberculosis* interference with the initiation of a robust adaptive immune response.

Although this would certainly be a novel function for GroEL2 itself, the idea of suppression of the immune response is an emerging concept in the tuberculosis field. Various *M. tuberculosis*-derived components have been directly linked to this process.

For example, recombinant early secreted antigenic target 6 (ESAT-6) was shown to markedly inhibit the production of IFN-γ by T cells stimulated with *M. tuberculosis*. Specifically, direct binding of ESAT-6 to TLR2 inhibited activation of the transcription factor NF-κB, thereby restricting TLR signaling. Moreover, culture filtrate protein 10 (CFP10), the physiological partner of ESAT-6, did not have the same inhibitory effect and the presence of CFP10 did not affect the inhibitory function of ESAT-6, setting a precedent for striking functional differences between closely-associated partner proteins [136]. In another example, the *M. tuberculosis* cell wall component Man-LAM binds to the C-type lectin DC-SIGN to interfere with DC maturation [124]. Despite growing evidence for the role of *M. tuberculosis*-derived factors in immune modulation, we still do not fully understand the contribution of these factors in the context of the whole bacterium infecting DCs. There are a few studies within this experimental framework, strongly suggesting that *M. tuberculosis* antigens specifically shape the immune response *in vivo*. For example, *M. tuberculosis* lacking the well-characterized antigen 85A induces higher expression of MHC class II on dendritic cells as well as higher levels of IL-12 in comparison to the reference strain [129]. Overall, our studies add significance to a small but growing body of data showing that various *M. tuberculosis* components modulate DC responses.

Although we do not conclude from our data that GroEL2(cl) is directly suppressing host receptor signaling pathways, we speculate that this is certainly one plausible mechanism to achieve the GroEL2-mediated immune modulation. In light of our findings, it is tempting to speculate that the cleaved form of GroEL2(cl) actively suppresses DC

functions. We are very intrigued by the possibility that cleaved GroEL2 acts directly to interfere with and inhibit the host immune response. To elucidate this question, we propose competition experiments using purified full-length and cleaved GroEL2. We plan to investigate the inflammatory responses after stimulation with various molar ratios of GroEL2 and GroEL2(cl) in combination. If the function of cleaved GroEL2 is to inhibit immune activation, we expect to observe a decrease in full-length GroEL2-induced cytokine levels in the presence of GroEL2(cl). Similarly, we expect that addition of recombinant purified GroEL2(cl) to *hip1* mutant cultures during infection would alleviate the *hip1* mutant hyperinflammatory phenotype.

Several groups have characterized full-length GroEL2 as a potential TLR ligand, thereby leaving the function of GroEL2(cl) undefined [93]. Specifically, several studies have demonstrated partial TLR2- and TLR4-dependent activation of macrophages by full-length GroEL2 [90]. Besides GroEL2, another *M. tuberculosis* chaperone-like protein, DnaK has immunomodulatory functions and is known to bind TLR2, TLR4 and CD40. Curiously, endogenous *M. tuberculosis* DnaK does not stimulate IL-12 production when exposed to the THP1 monocyte line, but the C-terminal domain of the protein does, suggesting that some form of proteolysis is required to generate cytokine production [51]. Therefore, in light of these findings, it is possible that GroEL2 engages TLR receptors *in vivo*. In our own studies, we have shown that Hip1 modulates macrophage and DC responses via TLR2- and inflammasome-dependent pathways. Most recently, our published and unpublished data suggest that both GroEL2 and GroEL2(cl) stimulate cytokine production from macrophages in a partially TLR2-dependent manner. Therefore,

in light of our previous findings, it is certainly an attractive hypothesis that TLR2 is the host receptor recognizing the *M. tuberculosis* GroEL2 protein. We are actively investigating this line of inquiry as well as the likelihood of direct binding between GroEL2 and host receptors. In these efforts, we are using various TLR knockout cell lines as well as cell lines stably transfected with a single TLR receptor to look for evidence of direct binding. Yet another alternative possibility is that GroEL2 engages some unidentified receptor on host cells. This is an interesting avenue that we are also exploring.

However tempting this hypothesis of TLR-GroEL2 interaction, we realize that interaction between GroEL2 and TLR2 would be highly unusual, given that the canonical TLR2 ligands in *M. tuberculosis* and other bacterial pathogens are lipoproteins [137]. Keeping this in mind, we envision other likely scenarios about the molecular basis for immunomodulation via GroEL2. In the absence of evidence for direct interaction between GroEL2 and TLR receptors, it is plausible that GroEL2 contributes to TLR signaling indirectly. In this context, it is possible that GroEL2 acts in a chaperoning capacity to facilitate the physical association of other true TLR ligands with their TLR receptor [138]. It is especially intriguing to view this possibility within the context of our prior knowledge about the major structural differences between GroEL2 and GroEL2(cl). Our previously published data demonstrates that, at steady state, full-length GroEL2 is a multimer. Curiously, Hip1 proteolysis of this multimer protein promotes its conversion to a monomer, leading to release of cleaved monomeric GroEL2 from *M. tuberculosis*. These major structural differences likely reflect substantial functional differences.

Specifically, the binding partners of GroEL2 and GroEL2(cl) are likely to be different [139]. In this context, we propose that the cleaved form of GroEL2 but not full-length could be shuttling host ligands, which possess immunomodulatory capacity during infection.

It is also possible that each form of the GroEL2 protein could have intrinsic differences in their stimulatory capacities as true ligands for host receptors. Rather than at the sequence level, these differences could be mediated at the protein level, by posttranslational modifications such as methylation or glycosylation. In line with this hypothesis are several studies on posttranslational alterations with substantial impact on functionality. For example, the *M. tuberculosis* cell wall-associated phenolic glycolipids, characteristic of the hypervirulent Beijing strains, were recently demonstrated to have a TLR2-dependent cytokine inhibition profile determined by the methylation pattern on the glycan part of the structure [140].

Another hypothesis is differential availability of each form of GroEL2 during the course of infection. Based on the optimal pH range that we determined for cleavage of GroEL2 *in vitro* (pH 5.65 to 7.39) (Chapter 2), we speculate that GroEL2 cleavage occurs upon contact with the macrophage cell surface (pH ~7.0) and continues within the phagosome compartment (pH ~ 6.3) but is unlikely to occur within the acidic environment of the lysosome (pH ~ 4.5-5.0). Thus, proteolysis of GroEL2 by Hip1 likely allows for both temporal and spatial regulation of the availability of GroEL2 within the physiological space. During infection, under the right conditions, GroEL2(cl) is released from *M.*

tuberculosis and finds itself perfectly positioned to interact with targets within the host environment. A plausible scenario includes interaction between GroEL2 and host intracellular receptors, as well as cell surface-associated receptors, resulting in stimulation of host signaling pathways. Various published reports have provided evidence for this phenomenon by other *M. tuberculosis*-derived factors. For example, *M. tuberculosis* CpG DNA, muramyl dipeptide, lipoproteins, phosphatidylinositol mannoside, and ESAT-6 are readily recognized by both cytosolic and cell surface host receptors [30,57]. Therefore, it is likely that Hip1-dependent regulation of GroEL2 availability is one way to rapidly fine-tune host immunity during tuberculosis infection.

In summary, we have shown that DC maturation and functions are modulated via proteolysis of *M. tuberculosis* GroEL2, highlighting the importance of cleaved GroEL2 in the context of infection. Importantly, our findings underscore the underappreciated and understudied immunomodulatory role of the biologically relevant cleaved form of GroEL2. Our studies suggest that the presence of GroEL2(cl) during *M. tuberculosis* infection promotes manipulation of the immune response exemplified by compromised DC maturation, cytokine production and antigen presentation. Overall, these data implicate GroEL2 in immune evasion and position it as an immunomodulatory component with potential use in tuberculosis vaccine design.

Material and Methods

Cloning of recombinant proteins for expression in *E.coli*

M. tuberculosis groEL2 was cloned into pACYCDuet-1 (Merck Millipore, Darmstadt, Germany) via the restriction sites *Eco*RI and *Kpn*I using the In Fusion cloning system following the manufacturer's protocol. *M. tuberculosis groEL2* was amplified using the primers 5'-GCCAGGATCCGAATTCGATGGCCAAGACAATTGCGTACGAC-3' and 5'-TTACCAGACTCGAGGGTACCGAAATCCATGCCACCCATGTCGCC-3', yielding a construct bearing an in-frame N-terminal 6XHis-tag and a C-terminal S-tag, yielding pACYCDuet-1 GroEL2. *M. tuberculosis groEL2(cl)* was amplified using the primers 5'-x-3' and 5'-TTACCAGACTCGAGGGTACCGAAATCCATGCCACCCATGTCGCC-3', yielding a construct bearing an in-frame N-terminal 6XHis-tag and a C-terminal S-tag, yielding pACYCDuet-1 GroEL2(cl).

Expression recombinant protein GroEL2 and GroEL2(cl) in *E. coli*

The plasmids, pACYCDuet-1 GroEL2 and pACYCDuet-1 GroEL2(cl) were separately transformed into *E. coli* BL21 Star (DE3) (Invitrogen, Carlsbad, CA) for protein expression. LB broth (1L) containing 34 μg/mL chloramphenicol was inoculated with 5 mL of overnight culture and incubated at 37ºC to an OD_{600} of 0.6 to 0.8. The cells were cooled to room temperature for 15-30 minutes after which 1 mM IPTG was added and the cells were incubated overnight at 28°C. The cells were then centrifuged at 10,000 rpm for 1 hour.

Preparation of recombinant GroEL2 and GroEL2(cl)

GroEL2 and GroEL2(cl) (minus the first 12 amino acids), each bearing an in-frame N-terminal 6XHis-tag were expressed in *E.coli* BL21 star (DE3). The cell pellet containing GroEL2 or GroEL2(cl) was resuspended in binding buffer (20 mM Tris-HCl, 500 mM NaCl, 5 mM Imidazole, pH 7.9, 200 μg/ml lysozyme, 1.8 μg/μl DNase) plus protease inhibitor cocktail (Santa Cruz Biotechnology, Dallas, TX), sonicated and centrifuged at 16, 000 x g for 90 min to remove cellular debris and clarify. The soluble fraction was added to Ni^{2+}- charged beads in a gravity column. The cell lysate in the gravity column was first washed with wash buffer 1 (20 mM Tris-HCl, 500 mM NaCl, 60 mM imidazole, pH 7.9) and then wash buffer 2 (10 mM Tris-HCl) to remove residual salts from the column. To remove endotoxin, the cell lysate was washed with 0.5% ASB-14 (Millipore, Billerica, MA) in 10 mM Tris-HCl. Finally, the lysate was washed with 10 mM Tris-HCl to remove any excess detergent. The protein was eluted with 1M imidazole in 10 mM Tris-HCl and dialyzed overnight in 1× PBS buffer. The protein was further purified by size exclusion chromatography on GE Superdex 75 10/300 GL column. The purified protein was then concentrated. The endotoxin levels for each protein were $<10\ ng^{-1}\ ml^{-1}\ mg^{-1}$ as determined using LAL Chromogenic endotoxin quantitation kit (Thermo Scientific, Rockford, IL).

Proteins were subjected to SDS-PAGE and visualized as a single band by staining with 0.05% Coomassie blue R-250. The concentrations of purified proteins were determined by Bradford method using bovine serum albumin (BSA) as the standard.

Bacterial strains and media

M. tuberculosis H37Rv, the *hip1* mutant strain (described previously) [80,81] and *M. tuberculosis* strain expressing GroEL2(cl) were grown at 37°C in Middlebrook 7H9 broth or 7H10 supplemented with 10% oleic acid-albumin-dextrose-catalase (OADC) (Becton Dickinson, Franklin Lakes, NJ), 0.02 % glycerol, and 0.05% Tween 80 (for broth), with the addition of 25 μg/ml kan (Sigma-Aldrich, St. Louis, MO) for the *hip1* mutant, and, for complemented strains, 10 μg/ml streptomycin (Sigma-Aldrich, St. Louis, MO) or 50 μg/ml hygromycin (Roche Diagnostics, Indianapolis, IN) was added.

Construction of mycobacterial plasmids and strains

Secreted GroEL2(cl)-myc: To express the cleaved form of GroEL2, GroEL2 (cl), the *groEL2* gene (minus the first 13 amino acids) was amplified from the *M. tuberculosis* genome using forward primer 5'-ACGCAGCTGGGCCTCGAGCGGGGCTTGAACGCC-3' and reverse primer 5'-AGTAAGCTTTCACAGATCTTCTTCAGAAATAAGTTTTTGTTCGAAATCCATGCCACC-3' and cloned into the *Pvu*II and *Hin*dIII sites of pMV762, downstream of the predicted N-terminal signal sequence from *M. tuberculosis* antigen 85 complex B NH_2-MTDVSRKIRAWGRRLMIGTAAAVVLPGLVGLAGGAATAGA-OH and an in-frame C-terminal Myc tag.

Mice

All mice were housed under specific pathogen-free conditions in filter- top cages within the vivarium at the Yerkes National Primate Center, Emory University, and provided with sterile water and food ad libitum. C57BL/6 mice were purchased from The Jackson

Laboratory. OTII-transgenic (Tg) mice specific for $OVA_{323–339}$ peptide originally generated in the laboratory of Dr. F. Carbone (University of Melbourne, Melbourne, VIC, Australia) were bred at the Yerkes animal facility.

Dendritic cells and cytokine assays

For generating murine bone marrow–derived DCs (BMDCs), bone mar- row cells from C57BL/6 mice were grown in RPMI 1640 medium (Lonza, Walkersville, MD) with 10% heat-inactivated FBS (HyClone, Logan, UT), 2 mM glutamine, 13 2-ME, 10 mM HEPES, 1 mM sodium pyruvate, 13 nonessential amino acids, and 20 ng/ml murine recombinant GM-CSF (R&D Systems, Minneapolis, MN). Incubations were carried out at 37℃ with 5% CO2. Fresh medium with GM-CSF was added on days 3 and 6, and cells were used on day 7 for all experiments. We routinely obtained ~75% $CD11c^+$ $CD11b^+$ cell purity by flow cytometry. BMDCs were further purified by using magnetic beads coupled to $CD11c^+$ mAb and passed through an AutoMACS column as per the manufacturer's instructions, where indicated (Miltenyi Biotec, Auburn, CA). For all experiments, cells were maintained throughout in medium containing GM-CSF. For infection, BMDCs were plated onto 24-well plates ($3x10^5$ per well). Bacteria were filtered through 5 micron filters, resuspended in complete medium containing 20 ng/ml GM-CSF, and sonicated twice for 5 s each before addition to the adherent monolayers. Each bacterial strain was used for infection (in duplicate or triplicate) at a multiplicity of infection (MOI) of 5 or as indicated. Infection of BMDCs was carried out for 4 h, after which monolayers were washed four times with PBS before replacing with RPMI 1640 medium containing 20 ng/ml GM-CSF. To determine intracellular CFU, one set of DCs

was lysed in PBS containing 0.5% Triton X-100 and plated on 7H10 agar plates containing the appropriate antibiotics. Alternatively, BMDCs were infected with heat-killed M. tuberculosis at an MOI of 5 or as indicated in RPMI medium containing 20 ng/ml GM- CSF. Cell-free supernatants from DC monolayers were isolated at indicated points and assayed for cytokines by ELISA using Duo Set kits for IL-12p40, IL-6, and IL-10 (BD Biosciences, San Jose, CA). Assays were carried out according to the manufacturers' instructions. Uninfected BMDCs were used as controls for each experiment.

Antigen-specific $CD4^+$ T cell antigen presentation assay

$CD4^+$ T cells were purified from single-cell suspensions of spleen and lymph nodes from 6–8 week old OTII-Tg mice using the $CD4^+$ T cell isolation kit and AutoMACS column as per the manufacturer's instructions (Miltenyi Biotec). BMDCs were incubated in 24-well plates ($3x10^5$/well) with 10 mg/ml $OVA_{323–339}$ peptide for 6 h, washed with PBS, and infected with GroEL2, GroEL2(cl) or medium alone for 24 h. Infected DCs were washed twice with PBS and co-cultured with Ag-specific $CD4^+$ T cells at a 1:4 ratio for 72 h. Supernatants collected from these cells were analyzed for IFN-γ (Mabtech, Cincinnati, OH) and IL-2 (BD Biosciences) by ELISA according to the manufacturers' instructions.

Flow cytometry

Murine anti-CD11c allophycocyanin (clone N418) and anti-CD11b FITC (clone M1/70) were obtained from BioLegend; anti-CD40 PE (clone 3//23), anti-CD86 PE (clone GL1),

and anti–MHC II PE (clone M5/ 114.15.2) were purchased from BD Biosciences. Staining for cell-surface markers was done by resuspending ~1x10^6 cells in 200 ml PBS with 2% FBS containing the antibody mixture. Cells were incubated at 4℃ for 30 min and then washed with PBS containing 2% FBS. Data were immediately acquired using an LSR flow cytometer (BD Biosciences). Data were analyzed with FlowJo software (Tree Star, San Carlos, CA).

Statistical analysis

The statistical significance of data was analyzed using the Student's unpaired t-test (GraphPad Prism 5.0a). Data are shown as mean ±S.D. of one representative experiment from three independent experiments.

Author contributions

Conceived and designed the experiments: JR MG KS RML. Performed the experiments: MG KS RML. Analyzed the data: JR MG KS RML. Contributed reagents/materials/analysis tools: JR. Wrote the manuscript: JR MG.

Figure 1. Differential stimulation of proinflammatory cytokine production from dendritic cells by GroEL2 and GroEL2(cl). Production of IL-6 and IL-12 by C57BL/6 bone marrow derived dendritic cells (BMDCs) 24 hours after stimulation with GroEL2 or GroEL2(cl). Data are shown as mean ±S.D. of one representative experiment from three independent experiments. **, $P < 0.05$; **, $P < 0.01$.*

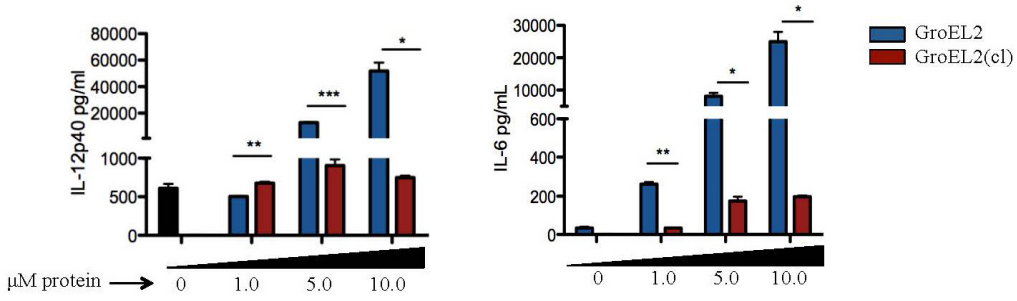

Figure 2. Enhanced surface expression of CD40 and CD86 in the presence of full-length GroEL2. C57BL/6 bone marrow-derived dendritic cells (BMDCs) were stimulated with GroEL2 or GroEL2(cl) for 24 hours and analyzed for cell surface expression of each surface marker. Data are shown as mean ±S.D. of one representative experiment from three independent experiments. **, $P < 0.05$; **, $P < 0.01$*

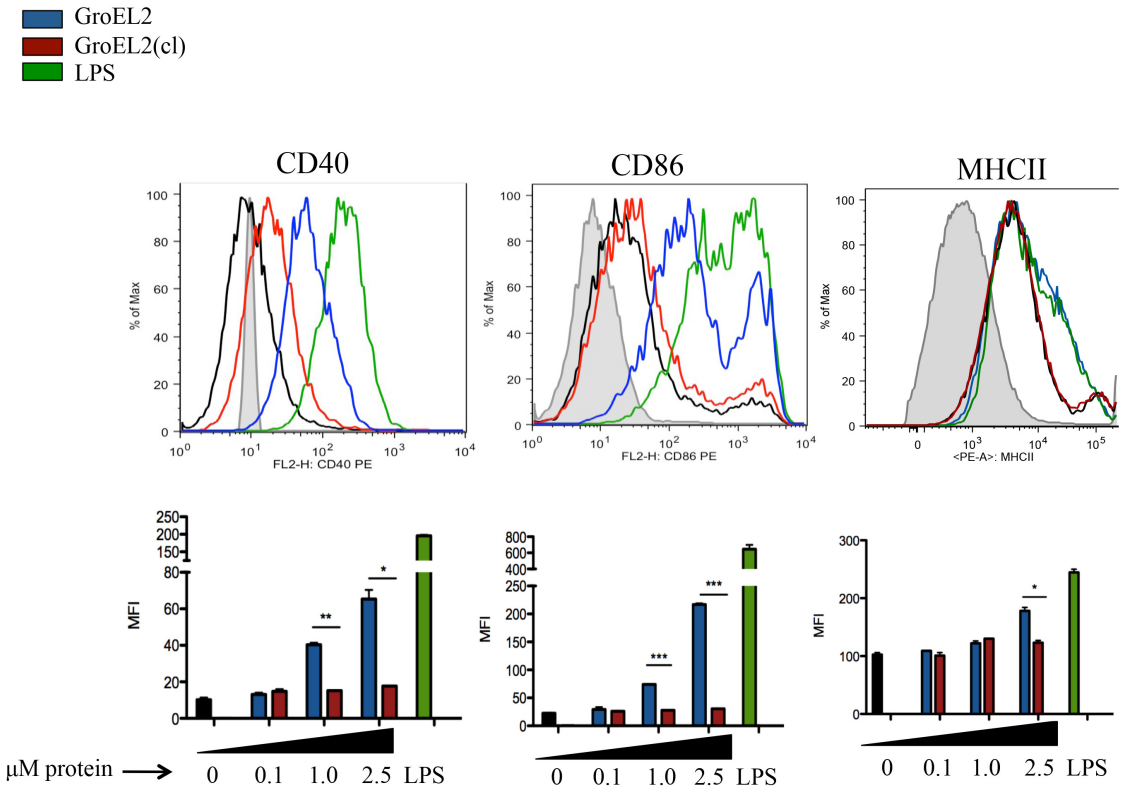

Figure 3. Proteolysis of GroEL2 modulates the antigen presentation capacity of dendritic cells. (A) Overview of the experimental setup. Bone marrow-derived dendritic cells (BMDCs) were pulsed with $OVA_{323-339}$ peptide for 6 hours and then stimulated with either GroEL2 or GroEL2(cl) for 24 hours. Then, these DCs were co-cultured with antigen-specific TCR-Tg $CD4^+$ T cells and assayed for antigen presentation by IL-2 and IFN-γ ELISA. (B) Cell-free supernatants were collected after 72 hours and assayed for IL-2 and IFN-γ by ELISA. Data are shown as mean ±S.D. of one representative experiment from three independent experiments. **, $P < 0.05$; **, $P < 0.01$.*

A.

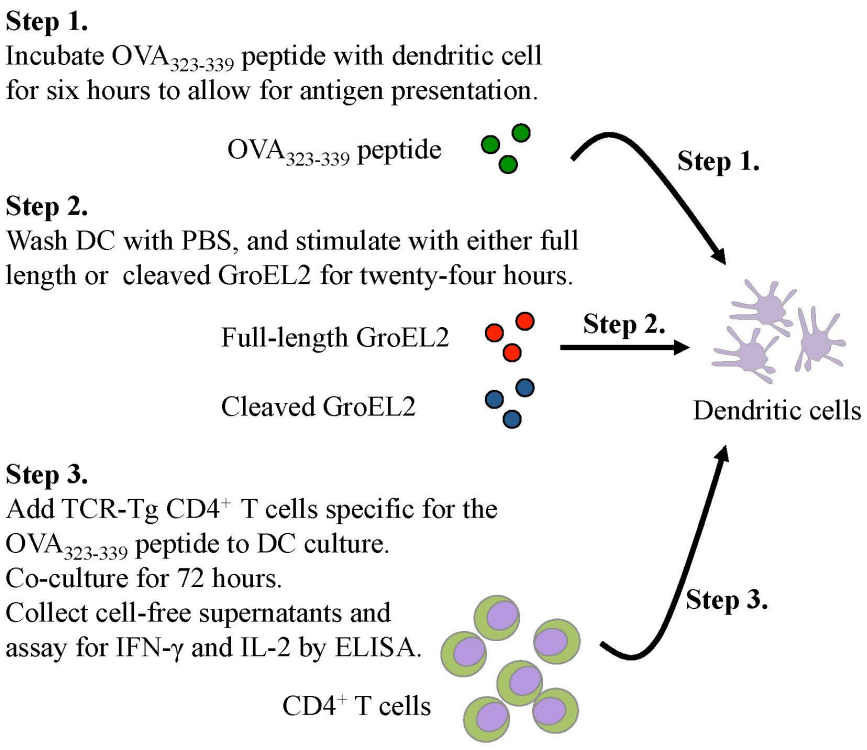

B.

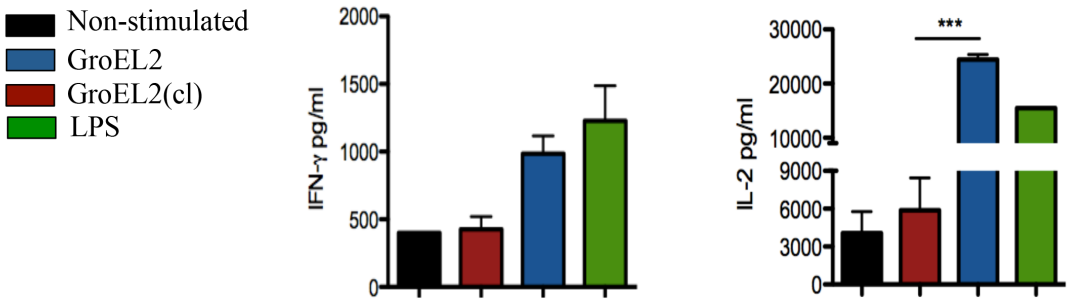
Non-stimulated
GroEL2
GroEL2(cl)
LPS
IFN-γ pg/ml
2000
1500
1000
500
0
IL-2 pg/ml
30000
20000
10000
9000
6000
3000
0
***

Figure 4. Expression of secreted GroEL2(cl) in *hip1* mutant restores wild type levels of proinflammatory cytokine responses in dendritic cells. Production of IL-6 and IL-12 by C57BL/6 bone marrow derived dendritic cells (BMDCs) 24 hours after infection with wild type, *hip1* mutant, and *hip1* mutant complemented with GroEL2(cl). Data are shown as mean ±S.D. of one representative experiment from three independent experiments. **, P < 0.05; **, P < 0.01.*

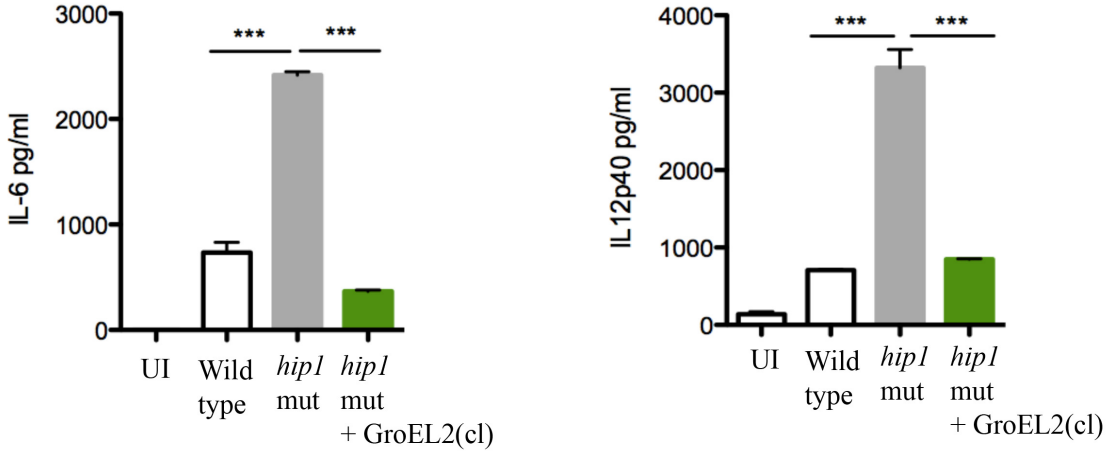

Chapter 4

Discussion

Mycobacterium tuberculosis is a highly infectious human pathogen that has evolved multiple strategies to evade host immune defenses and promote disease. Current efforts to combat tuberculosis disease include the development of new, more effective therapeutics and vaccines. Conceptually, these largely depend on a better understanding of the mechanisms driving *M. tuberculosis* evasion of host defenses and immune response modulation. Therefore, the last few years have seen a definite increase in efforts to gather insights about the mechanisms driving *M. tuberculosis* modulation of host immunity.

The huge success of *M. tuberculosis* as a pathogen can be largely attributed to its ability to subvert host innate and adaptive immune responses. The introduction of this dissertation work reviewed some of the mechanisms employed by *M. tuberculosis* to evade host immunity. We specifically outlined the importance of *M. tuberculosis*-derived cell surface-associated and extracellularly released components in immune modulation. While a substantial body of published work demonstrates the involvement of these bacterial factors in pathogenesis, the molecular basis for their activity is largely unknown.

In this dissertation work, we outlined our insights about the involvement of the *M. tuberculosis* protease Hip1 and one of its physiological substrates in immune modulation. In Chapter 2, we provided key mechanistic insight into the molecular and biochemical basis for Hip1 function. We showed that Hip1 is a serine protease with activity against protein and peptide substrates. Importantly, we also showed that the *M. tuberculosis* protein GroEL2 is a direct substrate of Hip1 protease activity. Further, we identified a specific serine protease inhibitor capable of inhibiting GroEL2 cleavage by Hip1. We

also showed that Hip1 cleaves GroEL2 within the N-terminus of the protein (Arg_{12} and Gly_{13}), releasing a peptide fragment. Currently, specific cleavage site preferences of Hip1 remain unclear. This is a question we propose to explore in our future investigations as it might provide valuable insight about the identity of additional Hip1 binding partners and substrates.

Interestingly, our findings contributed a previously unappreciated outcome of GroEL2 proteolysis. Specifically, we showed that, at steady state, GroEL2 is a multimer, and Hip1 cleaves GroEL2 multimer to release GroEL2 monomer. Building upon these mechanistic insights, we subsequently discovered a role for GroEL2 in modulating the host macrophage response during infection with *M. tuberculosis*. Further, we report that GroEL2 also modulates the innate-adaptive axis at the DC-T cell interface. In summary, our dissertation work identifies and provides insight on a novel and mechanistically intriguing approach to immune modulation by *M. tuberculosis.*

It is important to place our findings in the broader context of bacterial pathogenesis and note that chaperone-like proteins from multiple pathogens have been shown to be important for virulence [119,141-143]. For instance, in *Plasmodium falciparum,* the heat shock protein 70 is thought to play an essential role in parasite survival and virulence inside the host. Interestingly, Hsp70 is being investigated as a target for designing potential anti-malarial drugs. Also, the Hsp60 protein from *Histoplasma capsularum*, the causative agent of histoplasmosis in humans, is an immunodominant antigen important for the adaptation to temperature stress. In *Staphylococcus aureus (S. aureus),* the heat

shock cognate protein 70 plays a role in the internalization mechanism of *S. aureus*, thereby promoting successful infection. Further, virulence of *Enterococcus faecalis* is linked to ClpB, a chaperone-like protein. Members of the Clp family of family of proteins have also been linked to the tight regulation of virulence genes in *Listeria monocytogenes [119]*. Overall, these findings underscore the increasingly appreciated role of chaperone-like proteins as immunomodulatory bacterial effectors and their role in survival and virulence of multiple bacterial pathogens.

In *Mycobacterium tuberculosis*, the findings that GroEL2 can rapidly modulate host immunity via cytokine production intriguingly lend promise to GroEL2 as a target in immunotherapeutic anti-tuberculosis vaccines. So far, one line of investigation pursued by some groups involves the use of full-length GroEL2 in a subunit vaccine which generated a strong proliferative T-cell response during infection [144]. In other efforts, a DNA vaccine expressing full-length GroEL2 was developed for delivery via the liposome route [145,146]. Intriguingly, the vaccine provided protection in mice, comparable to that granted by the BCG vaccine, demonstrating the potential use of GroEL2 in vaccine development [145]. Importantly, all of these studies involve use of the full-length GroEL2 protein and never the cleaved form of GroEL2. Our studies suggest that GroEL2 cleaved is a yet unexplored, important, biologically relevant *M. tuberculosis* effector molecule, certainly worthy of investigation along the same lines. We are very interested in pursuing this line of investigation ourselves and very curious about our future findings. We propose to begin by teasing out and clarifying the biological role of the cleaved GroEL2 protein during infection *in vivo*, in the mouse model of infection.

Previously published data from our group showed that mice infected with the *hip1* mutant of *M. tuberculosis* have enhanced innate and adaptive immune responses, and mild lung pathology with small and few granulomatous lesions, despite high bacterial burdens in their lungs [80]. Considering the importance of GroEL2 proteolysis in Hip1-driven immune modulation, we hypothesize that cleavage of GroEL2 is a key contributor to the pathogenic immune response *in vivo*. We propose to test this hypothesis by using the C57BL/6 mouse model of infection. We will utilize our previously obtained *hip1* mutant complemented with GroEL2(cl) strain of *M. tuberculosis* along with reference wild type and *hip1* mutant strains to investigate the effect of GroEL2 proteolysis on host immunity and pathogenesis. Deriving from our previous experience with *M. tuberculosis* infection in mice, we propose to perform our analysis at time points when disease severity and pathology between groups can be clearly compared. Furthermore, we propose to phenotypically and functionally characterize specific cell types comprising the innate and adaptive immune responses to wild type, *hip1* mutant and complemented strains in mice.

While GroEL2 is an important component of the function of Hip1, it is unlikely to be the only substrate of Hip1 activity. As outlined in Chapter 1, the scope of Hip1 activity is quite broad as evidenced by the varied phenotypes of the *hip1* mutant *M. tuberculosis* strain. While we are interested in investigating a possible involvement of GroEL2 in these phenotypes, we also envision that other, yet unidentified, Hip1 substrates may play contributing roles. Furthermore, given the close association between the Rv2223c and Hip1 proteases (unpublished data, Erica Bizzell, Jyothi Rengarajan), another likely possibility is that they share targets with important biological roles during infection. We

propose future studies to identify the larger landscape of Hip1 interacting partners and substrates via pull-down experiments as well as protein-protein association assays. Specifically, to pull down candidate targets of Hip1, we can utilize our already engineered *M. tuberculosis* strains over-expressing conveniently-tagged wild type Hip1 and catalytically inactive Hip1(S228A). Alternatively, there is value in using purified recombinant Hip1 and Hip1(S228A) as "baits" to capture substrates from *M. tuberculosis* cultures. Yet another screen we have successfully applied before and can use in these investigations is based on protein-protein associations. This *Mycobacteria*-specific protein fragment complementation assay allows us to identify candidate targets in a physiological setting, using the model organism *Mycobacterium smegmatis*. We believe a combination of such efforts will provide insight into other Hip1 binding partners and targets and can also be applied to investigations of Rv2223c to help us understand the interplay between these two important *M. tuberculosis* proteases. Moreover, given its cell envelope localization, it is possible that Hip1 may in fact cleave host-derived substrates. To explore such interactions, we can use similar biochemical approaches in infected macrophages to attempt to pull down bound host proteins.

While this dissertation work presents focused findings about Hip1 and its substrate GroEL2, it is also suggestive of the importance of the extracellular *M. tuberculosis* protease Rv2223c. Because Hip1 and Rv2223c (52% seq ID) are part of a putative operon, it is likely they experience similar regulatory mechanisms governing their expression during *M. tuberculosis* growth. In addition, both Hip1 and Rv2223c are α/β hydrolase family members and show similarity to the TPP B (SlpD) and TPP C (SlpE)

proteases from *Streptomyces lividans*. Interestingly, our preliminary data suggests that Hip1 and Rv2223c share substrates and may work in conjunction to regulate pathogenesis (unpublished data, Erica Bizzell, Jyothi Rengarajan). Therefore, Rv2223 might share Hip1 functions during infection as well as act independently to promote virulence. Interestingly, because Rv2223c is secreted extracellularly from *M. tuberculosis*, it would be perfectly positioned to target both *M. tuberculosis*-derived factors and host substrates to promote pathogenesis via its proteolytic activity. We are actively investigating the role of the extracellularly secreted Rv2223c and the interplay between Hip1 and Rv2223c during infection.

Importantly, our studies have relevance for efforts to improve treatment options for complex infectious diseases such as tuberculosis. Specifically, our findings lend credibility to a strategy involving inhibition of Hip1 as part of adjunctive immunotherapy to tuberculosis.

The current treatment of tuberculosis consists of an extremely lengthy and arduous chemotherapy regimen. This standard treatment has remained essentially unchanged for decades in the absence of any breakthroughs that could allow decreasing either the duration or the number of administered antibiotics. Patients are prescribed a cocktail of four anti-tuberculosis drugs for six to nine months and even confined if considered highly infectious. Because these drugs have very unpleasant and intolerable side effects, interrupted treatment is very common, frequently leading to the development of multi-drug resistance. At this stage, even fewer treatment options are available and the

roadblock to successful resolution is even more challenging to overcome. These unfavorable outcomes are largely attributed to the ability of *M. tuberculosis* to persist within the host even in the presence of bactericidal / bacteriostatic stress.

For these reasons, there is urgent need for the development of shorter, more efficacious treatment regimens. Adjunctive therapies administered in conjunction with existing antibiotics are an attractive approach to shortening treatment duration. Such therapies have the potential to accelerate both clearance of *M. tuberculosis* bacilli and sterilization. In their application, adjunctive therapies may consist of host-directed therapies to target specific cellular pathways required for *M. tuberculosis* survival as well as therapies that target disease-promoting pathogen-specific factors. Overall, we see huge promise in a strategy that involves manipulation of host immunity to provide more favorable *in vivo* immune milieu for antimicrobial agents, thereby leading to increased bacterial clearance after anti-tuberculosis treatment. We propose a conceptually novel approach to tuberculosis treatment - inhibition of the immunomodulatory *M. tuberculosis* Hip1 protease as a way to enhance treatment response and improve anti-tuberculosis chemotherapy.

In pursuing this hypothesis, we want to establish the characteristics of the Hip1 three-dimensional structure, as it will provide crucial information about the design of small molecule inhibitors. We pursued this goal in close collaboration with Dr. Petsko and Dr. Ringe at Brandeis University, and we are very excited about a recent momentous breakthrough in these efforts. The Ringe and Petsko groups have crystallized the protein

and determined its three-dimensional structure (unpublished data, manuscript in preparation). The Hip1 structure is consistent with our previous predictions (outlined in Chapter 1), but also reveals several intriguing features suggesting that Hip1 constitutes a novel, yet uncharacterized family of enzymes. This key achievement constitutes a huge stride on our way to develop candidate Hip1 inhibitors. Our recent insights about Hip1 and its physiological substrate make such efforts possible and provide a focused experimental framework for their execution. Specifically, we envision that an inhibitor screen based on readout of GroEL2 proteolysis is prone to identify and select for the most promising candidates, these most likely to be successful during infection. In our efforts, we do not commit to the above avenue only, as other more general approaches involving the use of synthetic substrates hold considerable merit as well.

In order to assess the effect of Hip1 inhibition during anti-tuberculosis therapy, we propose to use the mouse model of infection with *M. tuberculosis*. To model the therapeutic situation in which adjunctive immune therapy is administered in conjunction with antibiotic therapy, we propose the following strategy. We propose to infect C57BL/6 mice and inhibit Hip1 activity at both acute and chronic stages of infection in an effort to mimic various aspects of human tuberculosis infection. In this setting, we will primarily monitor clearance rates of bacteria from lungs and spleens of mice and compare these across all experimental and control groups. However, we are also interested in and invested in pursuing more detailed analysis of the phenotypic and functional features of host immunity (both innate and adaptive) in response to infection with *M. tuberculosis* lacking Hip1 activity.

In addition to these inhibitor-oriented studies, we also envision deletion of *hip1* in BCG has potential to improve BCG vaccine efficacy. So far, the majority of efforts directed to improving the existing BCG vaccine have focused on engineering BCG to express immunodominant *M. tuberculosis* antigens, while very few studies have taken the opposite approach of deletion of specific genes in BCG. Our insights on the activity of the immunomodulatory protease Hip1 provide the basis for a novel concept to augment innate and adaptive immunity to *M. tuberculosis* by deletion of a key immune evasion gene.

In the tuberculosis field, the full range of mechanisms and strategies employed by *M. tuberculosis* to evade and subvert host immunity is a significant area of interest. Many groups, including ours, have approached this question via genome-wide studies. In most cases, the outcome of such studies is invaluably enhanced by more focused follow-up investigations centered on specific bacterial mutants and bacterial effectors. By following this sequence of efforts, our group is now providing highly important and invaluable insight into how *M. tuberculosis* modulates host immunity, thereby also informing the design of more efficacious vaccines and immunotherapies for tuberculosis.

Chapter 5

Bibliography

1. Kumar Y, Valdivia RH (2009) Leading a sheltered life: intracellular pathogens and maintenance of vacuolar compartments. Cell Host Microbe 5: 593-601.

2. Flannagan RS, Cosio G, Grinstein S (2009) Antimicrobial mechanisms of phagocytes and bacterial evasion strategies. Nat Rev Microbiol 7: 355-366.

3. Ernst JD (2012) The immunological life cycle of tuberculosis. Nat Rev Immunol 12: 581-591.

4. Monack DM, Mueller A, Falkow S (2004) Persistent bacterial infections: the interface of the pathogen and the host immune system. Nat Rev Microbiol 2: 747-765.

5. Flynn JL, Chan J (2003) Immune evasion by Mycobacterium tuberculosis: living with the enemy. Current Opinion in Immunology 15: 450-455.

6. Master SS, Rampini SK, Davis AS, Keller C, Ehlers S, et al. (2008) Mycobacterium tuberculosis prevents inflammasome activation. Cell Host Microbe 3: 224-232.

7. de Chastellier C (2009) The many niches and strategies used by pathogenic mycobacteria for survival within host macrophages. Immunobiology 214: 526-542.

8. Ehrt S, Schnappinger D (2009) Mycobacterial survival strategies in the phagosome: defence against host stresses. Cell Microbiol 11: 1170-1178.

9. Philips JA, Ernst JD (2012) Tuberculosis pathogenesis and immunity. Annu Rev Pathol 7: 353-384.

10. Russell DG (2001) Mycobacterium tuberculosis: here today, here tomorrow. Nature Reviews 2: 569-577.

11. Russell DG (2007) Who puts the tubercle in tuberculosis? Nat Rev Microbiol 5: 39-47.

12. Daniel TM (2006) The history of tuberculosis. Respir Med 100: 1862-1870.

13. Organization WH (2012) WHO: Global Tuberculosis report 2012.

14. Prevention CfDCa (2003) Treatment of tuberculosis. Morbiditiy and Mortality Weekly Report 52.

15. Almeida Da Silva PE, Palomino JC (2011) Molecular basis and mechanisms of drug resistance in Mycobacterium tuberculosis: classical and new drugs. J Antimicrob Chemother 66: 1417-1430.

16. Koul A, Arnoult E, Lounis N, Guillemont J, Andries K (2011) The challenge of new drug discovery for tuberculosis. Nature 469: 483-490.

17. Peter R. Donald PDvH (2009) The global burden of Tb, combating drug resistance in difficult times. The New England Journal of Medicine 360.

18. Ottenhoff TH, Kaufmann SH (2012) Vaccines against tuberculosis: where are we and where do we need to go? PLoS Pathog 8: e1002607.

19. Cook GM, Berney M, Gebhard S, Heinemann M, Cox RA, et al. (2009) Physiology of Mycobacteria. 55: 81-319.

20. Hett EC, Rubin EJ (2008) Bacterial growth and cell division: a mycobacterial perspective. Microbiol Mol Biol Rev 72: 126-156, table of contents.

21. Cheng VC, Yew WW, Yuen KY (2005) Molecular diagnostics in tuberculosis. Eur J Clin Microbiol Infect Dis 24: 711-720.

22. Neyrolles O, Guilhot C (2011) Recent advances in deciphering the contribution of Mycobacterium tuberculosis lipids to pathogenesis. Tuberculosis (Edinb) 91: 187-195.

23. Sinha S, Kosalai K, Arora S, Namane A, Sharma P, et al. (2005) Immunogenic membrane-associated proteins of Mycobacterium tuberculosis revealed by proteomics. Microbiology 151: 2411-2419.

24. Gordon SV, Bottai D, Simeone R, Stinear TP, Brosch R (2009) Pathogenicity in the tubercle bacillus: molecular and evolutionary determinants. Bioessays 31: 378-388.

25. Gupta UD, Katoch VM (2005) Animal models of tuberculosis. Tuberculosis (Edinb) 85: 277-293.

26. Chackerian AA, Behar SM (2003) Susceptibility to Mycobacterium tuberculosis: lessons from inbred strains of mice. Tuberculosis 83: 279-285.

27. Flynn JL (2006) Lessons from experimental Mycobacterium tuberculosis infections. Microbes Infect 8: 1179-1188.

28. Kleinnijenhuis J, Oosting M, Joosten LA, Netea MG, Van Crevel R (2011) Innate immune recognition of Mycobacterium tuberculosis. Clin Dev Immunol 2011: 405310.

29. Pieters J (2008) Mycobacterium tuberculosis and the macrophage: maintaining a balance. Cell Host Microbe 3: 399-407.

30. Saiga H, Shimada Y, Takeda K (2011) Innate immune effectors in mycobacterial infection. Clin Dev Immunol 2011: 347594.

31. Ehlers S, Schaible UE (2012) The granuloma in tuberculosis: dynamics of a host-pathogen collusion. Front Immunol 3: 411.

32. Lang R (2013) Recognition of the mycobacterial cord factor by Mincle: relevance for granuloma formation and resistance to tuberculosis. Front Immunol 4: 5.

33. Briken V, Porcelli SA, Besra GS, Kremer L (2004) Mycobacterial lipoarabinomannan and related lipoglycans: from biogenesis to modulation of the immune response. Mol Microbiol 53: 391-403.

34. Ishikawa E, Ishikawa T, Morita YS, Toyonaga K, Yamada H, et al. (2009) Direct recognition of the mycobacterial glycolipid, trehalose dimycolate, by C-type lectin Mincle. J Exp Med 206: 2879-2888.

35. Russell AB, Hood RD, Bui NK, LeRoux M, Vollmer W, et al. (2011) Type VI secretion delivers bacteriolytic effectors to target cells. Nature 475: 343-347.

36. Fontana MF, Banga S, Barry KC, Shen X, Tan Y, et al. (2011) Secreted bacterial effectors that inhibit host protein synthesis are critical for induction of the innate immune response to virulent Legionella pneumophila. PLoS Pathog 7: e1001289.

37. Abdallah M. Abdallah NCGvP, Patricia A. DiGiuseppe Champion, Jeffery Cox, Joen Luirink, Christina M. J. E. Vandenbroucke-Grauls, Ben J. Appelmelk and Wilbert Bitter (2007) Type VII secretion - mycobacteria show the way. Nature Reviews 5.

38. Fortune SM, Rubin EJ (2007) The complex relationship between mycobacteria and macrophages: it's not all bliss. Cell Host Microbe 2: 5-6.

39. Rohde K, Yates RM, Purdy GE, Russell DG (2007) Mycobacterium tuberculosis and the environment within the phagosome. Immunological Reviews 219: 37-54.

40. Kinchen JM, Ravichandran KS (2008) Phagosome maturation: going through the acid test. Nat Rev Mol Cell Biol 9: 781-795.

41. Cosma CL, Sherman DR, Ramakrishnan L (2003) The secret lives of the pathogenic mycobacteria. Annu Rev Microbiol 57: 641-676.

42. Yonekawa A, Saijo S, Hoshino Y, Miyake Y, Ishikawa E, et al. (2014) Dectin-2 is a direct receptor for mannose-capped lipoarabinomannan of mycobacteria. Immunity 41: 402-413.

43. Sturgill-Koszycki S, Schlesinger PH, Chakraborty P, Haddix PL, Collins HL, et al. (1994) Lack of acidification in *Mycobacterium* phagosomes produced by exclusion of the vesicular proton- ATPase. Science 263: 678-681.

44. Brodin P, Poquet Y, Levillain F, Peguillet I, Larrouy-Maumus G, et al. (2010) High content phenotypic cell-based visual screen identifies Mycobacterium tuberculosis acyltrehalose-containing glycolipids involved in phagosome remodeling. PLoS Pathog 6: e1001100.

45. Guilliams M, Lambrecht BN, Hammad H (2013) Division of labor between lung dendritic cells and macrophages in the defense against pulmonary infections. Mucosal Immunol 6: 464-473.

46. Kopf M, Schneider C, Nobs SP (2015) The development and function of lung-resident macrophages and dendritic cells. Nat Immunol 16: 36-44.

47. Mihret A (2012) The role of dendritic cells in Mycobacterium tuberculosis infection. Virulence 3: 654-659.

48. Meylan E, Tschopp J, Karin M (2006) Intracellular pattern recognition receptors in the host response. Nature 442: 39-44.

49. Mortaz E, Adcock IM, Tabarsi P, Masjedi MR, Mansouri D, et al. (2014) Interaction of Pattern Recognition Receptors with Mycobacterium Tuberculosis. J Clin Immunol.

50. Reiling N, Ehlers S, Holscher C (2008) MyDths and un-TOLLed truths: sensor, instructive and effector immunity to tuberculosis. Immunol Lett 116: 15-23.

51. Luong M, Zhang Y, Chamberlain T, Zhou T, Wright JF, et al. (2012) Stimulation of TLR4 by recombinant HSP70 requires structural integrity of the HSP70 protein itself. J Inflamm (Lond) 9: 11.

52. Drage MG, Pecora ND, Hise AG, Febbraio M, Silverstein RL, et al. (2009) TLR2 and its co-receptors determine responses of macrophages and dendritic cells to lipoproteins of Mycobacterium tuberculosis. Cell Immunol 258: 29-37.

53. Tseng TT, Tyler BM, Setubal JC (2009) Protein secretion systems in bacterial-host associations, and their description in the Gene Ontology. BMC Microbiol 9 Suppl 1: S2.

54. Yu X, Xie J (2012) Roles and underlying mechanisms of ESAT-6 in the context of Mycobacterium tuberculosis-host interaction from a systems biology perspective. Cell Signal 24: 1841-1846.

55. de Jonge MI, Pehau-Arnaudet G, Fretz MM, Romain F, Bottai D, et al. (2007) ESAT-6 from Mycobacterium tuberculosis dissociates from its putative chaperone CFP-10 under acidic conditions and exhibits membrane-lysing activity. J Bacteriol 189: 6028-6034.

56. Fransois-XavierBerthet PBR, Ida Rosenkrands, Peter Andersen and Brigitte Gicquel (1998) A Mycobacterium tuberculosis operon encoding ESAT6 and a novel low molecular mass culture filtrate protein (CFP-10). Microbiology 144.

57. Manzanillo PS, Shiloh MU, Portnoy DA, Cox JS (2012) Mycobacterium tuberculosis activates the DNA-dependent cytosolic surveillance pathway within macrophages. Cell Host Microbe 11: 469-480.

58. Kleinnijenhuis J, Joosten LA, van de Veerdonk FL, Savage N, van Crevel R, et al. (2009) Transcriptional and inflammasome-mediated pathways for the induction of IL-1beta production by Mycobacterium tuberculosis. Eur J Immunol 39: 1914-1922.

59. Feng Shao PMM, Zhaoqin Bao, Roger W. Innes, and Jack E. Dixon (2002) Yersinia Cysteine proteases functioning in Bacterial Pathogenesis. Cell 109.

60. Ingmer H, Brondsted L (2009) Proteases in bacterial pathogenesis. Res Microbiol 160: 704-710.

61. Makinoshima H, Glickman MS (2006) Site-2 proteases in prokaryotes: regulated intramembrane proteolysis expands to microbial pathogenesis. Microbes Infect 8: 1882-1888.

62. Zhong G (2011) Chlamydia trachomatis secretion of proteases for manipulating host signaling pathways. Front Microbiol 2: 14. doi: 10.3389/fmicb.2011.00014. eCollection 02011.

63. Chen AL, Johnson KA, Lee JK, Sutterlin C, Tan M (2012) CPAF: a Chlamydial protease in search of an authentic substrate. PLoS Pathog 8: e1002842.

64. Jorgensen I, Bednar MM, Amin V, Davis BK, Ting JP, et al. (2011) The Chlamydia protease CPAF regulates host and bacterial proteins to maintain pathogen vacuole integrity and promote virulence. Cell Host Microbe 10: 21-32.

65. Orth K (2000) Disruption of Signaling by Yersinia Effector YopJ, a Ubiquitin-Like Protein Protease. Science 290: 1594-1597.

66. Shao F VP, Bao Z, Bowers K, Fierke C, and Dixon J (2003) Biochemical characterization of the Yersinia YopT protease. PNAS 100: 904-909.

67. Roberts DM, Personne Y, Ollinger J, Parish T (2013) Proteases in Mycobacterium tuberculosis pathogenesis: potential as drug targets. Future Microbiol 8: 621-631.

68. Ribeiro-Guimaraes ML, Pessolani MC (2007) Comparative genomics of mycobacterial proteases. Microb Pathog 43: 173-178.

69. Makinoshima H, Glickman MS (2005) Regulation of Mycobacterium tuberculosis cell envelope composition and virulence by intramembrane proteolysis. Nature 436: 406-409.

70. Ohol YM, Goetz DH, Chan K, Shiloh MU, Craik CS, et al. (2010) Mycobacterium tuberculosis MycP1 protease plays a dual role in regulation of ESX-1 secretion and virulence. Cell Host Microbe 7: 210-220.

71. Estorninho M, Smith H, Thole J, Harders-Westerveen J, Kierzek A, et al. (2010) ClgR regulation of chaperone and protease systems is essential for Mycobacterium tuberculosis parasitism of the macrophage. Microbiology 156: 3445-3455.

72. Shui W, Petzold CJ, Redding A, Liu J, Pitcher A, et al. (2011) Organelle membrane proteomics reveals differential influence of mycobacterial lipoglycans on macrophage phagosome maturation and autophagosome accumulation. J Proteome Res 10: 339-348.

73. Di Cera E (2009) Serine proteases. IUBMB Life 61: 510-515.

74. Zhao Q, Xie J (2011) Mycobacterium tuberculosis proteases and implications for new antibiotics against tuberculosis. Critical Reviews in Eukaryotic Gene Expression 21: 347-361.

75. Vandal OH, Pierini LM, Schnappinger D, Nathan CF, Ehrt S (2008) A membrane protein preserves intrabacterial pH in intraphagosomal Mycobacterium tuberculosis. Nat Med 14: 849-854.

76. White MJ, He H, Penoske RM, Twining SS, Zahrt TC (2010) PepD participates in the mycobacterial stress response mediated through MprAB and SigE. J Bacteriol 192: 1498-1510.

77. White MJ, Savaryn JP, Bretl DJ, He H, Penoske RM, et al. (2011) The HtrA-like serine protease PepD interacts with and modulates the Mycobacterium tuberculosis 35-kDa antigen outer envelope protein. PLoS One 6: e18175.

78. Sklar JG, Makinoshima H, Schneider JS, Glickman MS (2010) M. tuberculosis intramembrane protease Rip1 controls transcription through three anti-sigma factor substrates. Mol Microbiol 77: 605-617.

79. Rengarajan J, Bloom BR, Rubin EJ (2005) Genome-wide requirements for Mycobacterium tuberculosis adaptation and survival in macrophages. Proc Natl Acad Sci U S A 102: 8327-8332.

80. Rengarajan J, Murphy E, Park A, Krone CL, Hett EC, et al. (2008) Mycobacterium tuberculosis Rv2224c modulates innate immune responses. Proc Natl Acad Sci U S A 105: 264-269.

81. Madan-Lala R, Peixoto KV, Re F, Rengarajan J (2011) Mycobacterium tuberculosis Hip1 dampens macrophage proinflammatory responses by limiting toll-like receptor 2 activation. Infect Immun 79: 4828-4838.

82. Vandal OH, Roberts JA, Odaira T, Schnappinger D, Nathan CF, et al. (2009) Acid-susceptible mutants of Mycobacterium tuberculosis share hypersusceptibility to cell wall and oxidative stress and to the host environment. J Bacteriol 191: 625-631.

83. Flores AR, Parsons LM, Pavelka MS, Jr. (2005) Characterization of novel Mycobacterium tuberculosis and Mycobacterium smegmatis mutants hypersusceptible to beta-lactam antibiotics. J Bacteriol 187: 1892-1900.

84. Rawlings ND, Barrett AJ, Bateman A (2012) MEROPS: the database of proteolytic enzymes, their substrates and inhibitors. Nucleic Acids Res 40: D343-350.

85. Georgieva M, Naffin-Olivos J, Goldfarb N Mycobacterium tuberculosis Hip1 modulates macrophage responses through proteolysis of GroEL2 .pdf. PLoS Pathog.

86. Binnie C, Butler MJ, Aphale JS, Bourgault R, DiZonno MA, et al. (1995) Isolation and characterization of two genes encoding proteases associated with the mycelium of Streptomyces lividans 66. J Bacteriol 177: 6033-6040.

87. Lun S, Bishai WR (2007) Characterization of a novel cell wall-anchored protein with carboxylesterase activity required for virulence in Mycobacterium tuberculosis. J Biol Chem 282: 18348-18356.

88. Qamra R, Srinivas V, Mande SC (2004) Mycobacterium tuberculosis GroEL homologues unusually exist as lower oligomers and retain the ability to suppress aggregation of substrate proteins. J Mol Biol 342: 605-617.

89. Hickey TB, Thorson LM, Speert DP, Daffe M, Stokes RW (2009) Mycobacterium tuberculosis Cpn60.2 and DnaK are located on the bacterial surface, where Cpn60.2 facilitates efficient bacterial association with macrophages. Infect Immun 77: 3389-3401.

90. Cehovin A, Coates AR, Hu Y, Riffo-Vasquez Y, Tormay P, et al. (2010) Comparison of the moonlighting actions of the two highly homologous chaperonin 60 proteins of Mycobacterium tuberculosis. Infect Immun 78: 3196-3206.

91. Fan M, Rao T, Zacco E, Ahmed MT, Shukla A, et al. (2012) The unusual mycobacterial chaperonins: evidence for in vivo oligomerization and specialization of function. Mol Microbiol 85: 934-944.

92. Lewthwaite JC, Clarkin CE, Coates AR, Poole S, Lawrence RA, et al. (2007) Highly homologous Mycobacterium tuberculosis chaperonin 60 proteins with differential CD14 dependencies stimulate cytokine production by human monocytes through cooperative activation of p38 and ERK1/2 mitogen-activated protein kinases. Int Immunopharmacol 7: 230-240.

93. Bulut Y, Michelsen KS, Hayrapetian L, Naiki Y, Spallek R, et al. (2005) Mycobacterium tuberculosis heat shock proteins use diverse Toll-like receptor pathways to activate pro-inflammatory signals. J Biol Chem 280: 20961-20967.

94. Lancioni C, Nyendak M, Kiguli S, Zalwango S, Mori T, et al. (2012) CD8+ T cells provide an immunologic signature of tuberculosis in young children. Am J Respir Crit Care Med 185: 206-212.

95. Ferre F, Clote P (2005) DiANNA: a web server for disulfide connectivity prediction. Nucleic Acids Res 33: W230-232.

96. Hedstrom L (2002) Serine protease mechanism and specificity. Chem Rev 102: 4501-4523.

97. Ferraris DM, Sbardella D, Petrera A, Marini S, Amstutz B, et al. (2011) Crystal structure of Mycobacterium tuberculosis zinc-dependent metalloprotease-1 (Zmp1), a metalloprotease involved in pathogenicity. J Biol Chem 286: 32475-32482.

98. Small JL, O'Donoghue AJ, Boritsch EC, Tsodikov OV, Knudsen GM, et al. (2013) Substrate specificity of MarP, a periplasmic protease required for resistance to acid and oxidative stress in Mycobacterium tuberculosis. J Biol Chem 288: 12489-12499.

99. Biswas T, Small J, Vandal O, Odaira T, Deng H, et al. (2010) Structural insight into serine protease Rv3671c that Protects M. tuberculosis from oxidative and acidic stress. Structure 18: 1353-1363.

100. Raju RM, Unnikrishnan M, Rubin DH, Krishnamoorthy V, Kandror O, et al. (2012) Mycobacterium tuberculosis ClpP1 and ClpP2 function together in protein degradation and are required for viability in vitro and during infection. PLoS Pathog 8: e1002511.

101. Personne Y, Brown AC, Schuessler DL, Parish T (2013) Mycobacterium tuberculosis ClpP proteases are co-transcribed but exhibit different substrate specificities. PLoS One 8: e60228.

102. Ollinger J, O'Malley T, Kesicki EA, Odingo J, Parish T (2012) Validation of the essential ClpP protease in Mycobacterium tuberculosis as a novel drug target. J Bacteriol 194: 663-668.

103. Powers JC, Asgian JL, Ekici OD, James KE (2002) Irreversible inhibitors of serine, cysteine, and threonine proteases. Chem Rev 102: 4639-4750.

104. Kuramochi H, Nakata H, Ishii S (1979) Mechanism of association of a specific aldehyde inhibitor, leupeptin, with bovine trypsin. J Biochem 86: 1403-1410.

105. Umezawa H (1976) Structures and activitites of protease inhibitors of microbial origin. 45: pp.678-695.

106. Kumar CM, Khare G, Srikanth CV, Tyagi AK, Sardesai AA, et al. (2009) Facilitated oligomerization of mycobacterial GroEL: evidence for phosphorylation-mediated oligomerization. J Bacteriol 191: 6525-6538.

107. Qamra R, Mande SC, Coates AR, Henderson B (2005) The unusual chaperonins of Mycobacterium tuberculosis. Tuberculosis (Edinb) 85: 385-394.

108. Lewthwaite JC, Coates AR, Tormay P, Singh M, Mascagni P, et al. (2001) Mycobacterium tuberculosis chaperonin 60.1 is a more potent cytokine stimulator than chaperonin 60.2 (Hsp 65) and contains a CD14-binding domain. Infect Immun 69: 7349-7355.

109. Fujii R, Nakagawa Y, Hiratake J, Sogabe A, Sakata K (2005) Directed evolution of Pseudomonas aeruginosa lipase for improved amide-hydrolyzing activity. Protein Eng Des Sel 18: 93-101.

110. Bachovchin DA, Cravatt BF (2012) The pharmacological landscape and therapeutic potential of serine hydrolases. Nat Rev Drug Discov 11: 52-68.

111. Madan T, Saxena S, Murthy KJ, Muralidhar K, Sarma PU (2002) Association of polymorphisms in the collagen region of human SP-A1 and SP-A2 genes with pulmonary tuberculosis in Indian population. Clin Chem Lab Med 40: 1002-1008.

112. Lalvani A, Sridhar S, von Reyn CF (2013) Tuberculosis vaccines: time to reset the paradigm? Thorax 68: 1092-1094.

113. Vandal OH, Nathan CF, Ehrt S (2009) Acid resistance in Mycobacterium tuberculosis. Journal of Bacteriology 191: 4714-4721.

114. MacCuish AC, Urbaniak SJ, Campbell CJ, Duncan LJ, Irvine WJ (1974) Phytohemagglutinin transformation and circulating lymphocyte subpopulations in insulin-dependent diabetic patients. Diabetes 23: 708-712.

115. Shahar A, Melamed-Frank M, Kashi Y, Shimon L, Adir N (2011) The dimeric structure of the Cpn60.2 chaperonin of Mycobacterium tuberculosis at 2.8 A reveals possible modes of function. J Mol Biol 412: 192-203.

116. Horovitz A, Bochkareva ES, Girshovich AS (1993) The N terminus of the molecular chaperonin GroEL is a crucial structural element for its assembly. J Biol Chem 268: 9957-9959.

117. Dosanjh NS, Rawat M, Chung JH, Av-Gay Y (2005) Thiol specific oxidative stress response in Mycobacteria. FEMS Microbiol Lett 249: 87-94.

118. Lee B, Horwitz MA (1995) Identification of macrophage and stress-induced proteins of Mycobacterium tuberculosis. J Clin Invest 96: 245-249.

119. Kaufmann S (1990) Heat shock proteins and the immune response. Immunology Today 11.

120. Yang H, Troudt J, Grover A, Arnett K, Lucas M, et al. (2011) Three protein cocktails mediate delayed-type hypersensitivity responses indistinguishable from that elicited by purified protein derivative in the guinea pig model of Mycobacterium tuberculosis infection. Infect Immun 79: 716-723.

121. Mukherjee P, Sureka K, Datta P, Hossain T, Barik S, et al. (2009) Novel role of Wag31 in protection of mycobacteria under oxidative stress. Mol Microbiol 73: 103-119.

122. Singh A, Mai D, Kumar A, Steyn AJ (2006) Dissecting virulence pathways of Mycobacterium tuberculosis through protein-protein association. Proc Natl Acad Sci U S A 103: 11346-11351.

123. Makino M, Maeda Y, Mukai T, Kaufmann SH (2006) Impaired maturation and function of dendritic cells by mycobacteria through IL-1beta. Eur J Immunol 36: 1443-1452.

124. Geijtenbeek TBH, van Vliet SJ, Koppel EA, Sanchez-Hernandez M, Vandenbroucke-Grauls CMJE, et al. (2002) Mycobacteria Target DC-SIGN to Suppress Dendritic Cell Function. Journal of Experimental Medicine 197: 7-17.

125. Madan-Lala R, Sia JK, King R, Adekambi T, Monin L, et al. (2014) Mycobacterium tuberculosis impairs dendritic cell functions through the serine hydrolase Hip1. J Immunol 192: 4263-4272.

126. Hickey TB, Ziltener HJ, Speert DP, Stokes RW (2010) Mycobacterium tuberculosis employs Cpn60.2 as an adhesin that binds CD43 on the macrophage surface. Cell Microbiol 12: 1634-1647.

127. Starck J, Kallenius G, Marklund BI, Andersson DI, Akerlund T (2004) Comparative proteome analysis of Mycobacterium tuberculosis grown under aerobic and anaerobic conditions. Microbiology 150: 3821-3829.

128. Winrow VR, Mesher J, Meghji S, Morris CJ, Maguire M, et al. (2008) The two homologous chaperonin 60 proteins of Mycobacterium tuberculosis have distinct effects on monocyte differentiation into osteoclasts. Cell Microbiol 10: 2091-2104.

129. Katti MK, Dai G, Armitige LY, Rivera Marrero C, Daniel S, et al. (2008) The Delta fbpA mutant derived from Mycobacterium tuberculosis H37Rv has an enhanced susceptibility to intracellular antimicrobial oxidative mechanisms, undergoes limited phagosome maturation and activates macrophages and dendritic cells. Cell Microbiol 10: 1286-1303.

130. Affronti MRAaLF (1994) Induction of mycobacterial proteins during phagocytosis and heat shock. Journal of Leukocyte Biology 55.

131. Khan N, Alam K, Mande SC, Valluri VL, Hasnain SE, et al. (2008) Mycobacterium tuberculosis heat shock protein 60 modulates immune response to PPD by manipulating the surface expression of TLR2 on macrophages. Cell Microbiol 10: 1711-1722.

132. Cho YS, Dobos KM, Prenni J, Yang H, Hess A, et al. (2012) Deciphering the proteome of the in vivo diagnostic reagent "purified protein derivative" from Mycobacterium tuberculosis. Proteomics 12: 979-991.

133. Goyal K, Qamra R, Mande SC (2006) Multiple gene duplication and rapid evolution in the groEL gene: functional implications. J Mol Evol 63: 781-787.

134. Dekker C, Willison KR, Taylor WR (2011) On the evolutionary origin of the chaperonins. Proteins 79: 1172-1192.

135. Wang C, Peyron P, Mestre O, Kaplan G, van Soolingen D, et al. (2010) Innate immune response to Mycobacterium tuberculosis Beijing and other genotypes. PLoS One 5: e13594.

136. Pathak SK, Basu S, Basu KK, Banerjee A, Pathak S, et al. (2007) Direct extracellular interaction between the early secreted antigen ESAT-6 of Mycobacterium tuberculosis and TLR2 inhibits TLR signaling in macrophages. Nat Immunol 8: 610-618.

137. Oliveira-Nascimento L, Massari P, Wetzler LM (2012) The Role of TLR2 in Infection and Immunity. Front Immunol 3: 79.

138. Millar DG, Garza KM, Odermatt B, Elford AR, Ono N, et al. (2003) Hsp70 promotes antigen-presenting cell function and converts T-cell tolerance to autoimmunity in vivo. Nat Med 9: 1469-1476.

139. Tapley TL, Korner JL, Barge MT, Hupfeld J, Schauerte JA, et al. (2009) Structural plasticity of an acid-activated chaperone allows promiscuous substrate binding. Proc Natl Acad Sci U S A 106: 5557-5562.

140. Lowary HRHEaTL (2014) Inhibition of Cytokine Release by Mycobacterium tuberculosis Phenolic Glycolipid Analogues. ChemBioChem doi:10.1002/cbic.201402001.

141. Lund PA (2009) Multiple chaperonins in bacteria--why so many? FEMS Microbiol Rev 33: 785-800.

142. M Galdieto GDLe, A Marcatili (1997) Cytokine and Adhesion Molecule Expression in Human Monocytes and Endothelial Cells Stimulated with Bacterial Heat Shock Proteins. Infect Immun 65.

143. Leach MD, Budge S, Walker L, Munro C, Cowen LE, et al. (2012) Hsp90 orchestrates transcriptional regulation by Hsf1 and cell wall remodelling by MAPK signalling during thermal adaptation in a pathogenic yeast. PLoS Pathog 8: e1003069.

144. Bonato VL, Lima KM, Tascon, Lowrie S (1998) Protective T cells in hsp65 DNA-vaccinated and Mtb-infected mice. Infection and Immunity 66(1).

145. Jose C. Ferraz ES, Min Yang, Steve Coade, Clara Espitia, Douglas B. Lowrie, M. Joseph Colston and Ricardo E. Tascon (2004) A Heterologous DNA Priming-Mycobacterium bovis BCG Boosting Immunization Strategy Using Mycobacterial Hsp70, Hsp65, and Apa Antigens Improves Protection against Tuberculosis in Mice. Infect Immun 72.

146. CL Silva MS, RCLR Pietro, DB Lowrie (1994) Protection against tuberculosis by passive transfer with T-celi clones recognizing mycobacterial heat-shock protein 65. Immunology 83.